Paulina Szyszka

Evaluation of the effect

of selected PI3K/Akt/mTOR and RAF/MEK/ERK pathways inhibitors

on proliferation and apoptosis

in human H295R adrenocortical cancer cell line

Doctoral Thesis

Supervisor: dr hab. med. Dorota Dworakowska

Department of Nuclear Medicine
Chair of Nuclear Medicine and Radiology Informatics
Faculty of Health Sciences with Subfaculty of Nursing
and Institute of Maritime and Tropical Medicine

Medical University of Gdansk

Head of the Department: Prof. dr hab. Piotr Lass

Gdańsk 2015

Paulina Szyszka

Ocena wpływu

wybranych inhibitorów szlaków Pl3K/Akt/mTOR oraz RAF/MEK/ERK

na proliferację i apoptozę

ludzkiej linii komórkowej raka kory nadnercza H295R

Roprawa doktorska

Promotor: dr hab. med. Dorota Dworakowska

Zakład Medycyny Nuklearnej
Katedra Medycyny Nuklearnej i Informatyki Radiologicznej
Wydział Nauk o Zdrowiu z Oddziałem Pielęgniarstwa
i Instytutem Medycyny Morskiej i Tropikalnej

Gdański Uniwersytet Medyczny

Kierownik: prof. dr hab. med. Piotr Lass

Gdańsk 2015

I would like to start by thanking
my supervisor Dr Dorota Dworakowska MD (Hons) PhD
for an opportunity to take part in the FNP-founded grant
as well as for an interesting research topic, great commitment,
fruitful cooperation and advice provided during performing my part of the project.

Thanks as well to Dr Gregory Weitsman
for providing support and a lot of valuable advice.

I would like to thank all the employees of
prof. Tony Ng's laboratory for great work atmosphere.

Special gratitude to my family and friends
for motivation and support in my endeavours, especially to my Mum, aunt Janka, Kuba,
Kamil, Jaśmina, Monika, Natalia, Ula, Tamara, Fabian, Appi, Michela and Oana.

*Na wstępie chciałabym podziękować
Pani promotor dr hab. med. Dorocie Dworakowskiej
za możliwość uczestnictwa w grancie FNP, a także za ciekawy temat badań,
wielkie zaangażowanie, owocną współpracę i przekazane wskazówki
podczas wykonywania mojej części projektu.*

*Podziękowania również dla dr Gregorego Weitsmana
za duże wsparcie i wiele nieocenionych porad.*

*Dziękuję wszystkim pracownikom laboratorium
prof. Tony'ego Ng za wspaniałą atmosferę pracy.*

*Szczególne podziękowania składam mojej rodzinie i przyjaciołom za motywację
i wsparcie w moich działaniach, a szczególnie: mojej mamie, cioci Jance, Kubie,
Kamilowi, Jaśminie, Monice, Natalii, Uli, Tamarze, Fabianowi, Appi, Micheli i Oanie.*

Table of Contents

Abbreviations

#

4EBP1 - eukaryotic translation initiation factor 4E binding protein 1 (EIF4EBP1)

A

Ac-DEVD-AMC - N-acetyl-DEVD-7-amino-4-methylcoumarin

ACA - adrenocortical adenoma

ACC - adrenocortical carcinoma

ACT - adrenocortical tumour

ACTH - adrenocorticotropic hormone, corticotropin

Akt - protein kinase B (PKB)

AKT1S1 - proline-rich Akt substrate 40 kDa, PRAS40

AMC - 7-amino-4-methylcoumarin

B

BWS - Beckwith–Wiedemann syndrome

β-ME - β-mercaptoethanol

BPB - bromophenol blue

C

CNC - Carney complex

CREB - cAMP-responsive element binding protein

CREM - cAMP responsive element modulator

CT – computed tomography

CYP11A1 - cytochrome P450scc, cholesterol side-chain-cleaving monooxygenase, cholesterol desmolase

CYP11B1/2 - P450c11B1, steroid 11-β-monooxygenase, 11β-hydroxylase

CYP17A1 - P450c17, steroid 17-α-monooxygenase, 17α-hydroxylase

CYP21A2 - P450c21, steroid 21-monooxygenase, 21-hydroxylase

D

DEVD - amino acid sequence: Aspartic acid-Glutamic acid-Valine-Aspartic acid (Asp-Glu-Val-Asp)

DHEA - dehydroepiandrosterone

DMSO - dimethylsulfoxide

DTT - dithiothreitol

E

EC_{50} - half maximal effective concentration

EGFR - epidermal growth factor receptor

EIF4EBP1 - eukaryotic translation initiation factor 4E binding protein 1 (4EBP1)

ENC1 - ectodermal-neural cortex 1

ERK1, ERK2 - extracellular signal-regulated protein kinases, mitogen-activated protein kinases, MAPKs

EVE - Everolimus (RAD001)

F

FAP - familial adenomatous polyposis coli

G

GC - glucocorticoid

GIPR - gastric inhibitory polypeptide receptor

H

HIF-1α - hypoxia-inducible factor-1α (HIF1A)

HIF1A - hypoxia-inducible factor-1α (HIF-1α)

HSD3B1/2 - hydroxy-δ-5-steroid dehydrogenase, 3 β- and steroid δ-isomerase 1/2, 3β-hydroxysteroid dehydrogenase/Δ-5 isomerase type

I

ICER - inducible cAMP early repressor

IGF2 - insulin-like growth factor

IGFBP2 - insulin-like growth factor-binding protein 2

IRS-1 - insulin receptor substrate 1

L

LFS - Li-Fraumeni syndrome

LHR - luteinizing hormone receptor

LOH - loss of heterozygosity

LY - LY294002

M

MAPK - mitogen-activated protein kinase, extracellular signal-regulated protein kinase, ERK

MAPKAP1 - mSIN1 protein (stress-activated protein kinase-interacting 1).

MAPKKs - MEK1 and MEK2, dual specificity mitogen-activated protein kinase kinases, MAPK/ERK kinases

MAS - McCune–Albright syndrome

MEK1, MEK2 - dual specificity mitogen-activated protein kinase kinases, MAPK/ERK kinases, MAPKKs

MEN1 - multiple endocrine neoplasia

MIT - Mitotane

mLST8 - also known as G protein beta subunit-like, GβL

mTOR - mammalian target of rapamycin

mTORC1 - mammalian target of rapamycin complex 1

N

NR5A1 - steroidogenic factor 1 (SF1)

NVP - NVP-BEZ235 (BEZ235)

P

p70S6K - p70 ribosomal protein S6 kinase 1 (S6K1, RPS6KB1)

pAkt - phosphorylated Akt protein

PARP - poly (ADP-ribose) polymerase

PBS - phosphate-buffered saline

PDK1 - 3-phosphoinositide-dependent protein kinase-1 (PDPK1)

PDPK1 - 3-phosphoinositide-dependent protein kinase-1 (PDK1)

PI3K - phosphoinositide 3-kinase

PIP2 - phosphatidylinositol bisphosphate

PIP3 - phosphatidylinositol triphosphate

PKA - protein kinase A

PKB - protein kinase B, Akt

PRAS40 - proline-rich Akt substrate 40 kDa, AKT1S1

PTEN (phosphatase and tensin homologue)

R

raptor - regulatory-associated protein of mTOR

rictor - rapamycin-insensitive companion of mTOR

RFU - relative fluorescence unit

RPS6KB1 - p70 ribosomal protein S6 kinase 1 (S6K1, p70S6K)

S

S6K1 - p70 ribosomal protein S6 kinase 1 (RPS6KB1, p70S6K)

SEM - standard error of the mean

SF1 - steroidogenic factor 1 (NR5A1)

STAR - steroidogenic acute regulatory protein

SV40 - Simian Virus 40

T

TSC1/2 - tuberous sclerosis complex

TKR - tyrosine kinase receptor

Figures

Tables

Abstract

Introduction: Adrenocortical carcinoma (ACC) is associated with a low cure, a high recurrence rate and poor prognosis. The current therapeutic options are limited and the results remain unsatisfactory; hence, there is a high clinical requirement for novel therapeutic options for ACC. The pathways PI3K/Akt/mTOR and Ras/Raf/MEK/ERK play a key role in regulating proliferation and tumourigenesis. Inhibitors of their elements are potential selective anti-cancer agents.

Aim of the Project: The main aim of this project was to investigate the effect of single and combination treatment with PI3K/Akt/mTOR (everolimus, NVP-BEZ235, LY294002) and Ras/Raf/MEK/ERK (U0126) inhibitors on the H295R cell proliferation, caspase-3-like activity, and protein expression. The secondary aim was to assess the combinatorial therapy of these compounds with mitotane.

Materials and methods: The model used in this study was the human adrenocortical carcinoma H295R cell line. To assess the effect of selected agents on its viability, the Resazurin assay was used. To complete the picture on more detailed mechanism of action, the caspase-3-like activity and Western Blot analyses were performed.

Results: The most promising combination tested was everolimus and NVP-BEZ235 that showed synergistic effect on cell viability inhibition. All tested agents were potent inhibitors of H295R cell viability with limited effect on caspase-3-like activity. Mitotane efficacy has been confirmed, while its combination with PI3K/mTOR or MEK inhibitors yielded at most the additive effect. U0126 showed the highest potential for further studies that may possibly bring synergism with different dosing regime.

Discussion and conclusions: The selected compounds (everolimus, NVP-BEZ235, LY294002, and U0126, and above all the combination of everolimus and NVP-BEZ235) showed high efficacy in decreasing cell proliferation in preclinical ACC model. They present high potential to be used in further *in vivo* studies. The studies on the caspase-3-like activity and protein expression provided valuable clues for the mechanisms of action of these compounds.

Streszczenie (Abstract in Polish)

Wprowadzenie: Rak kory nadnercza (RKN) charakteryzuje się niską wyleczalnością, wysokim ryzykiem nawrotu i złym rokowaniem. Obecnie dostępne opcje terapeutyczne są ograniczone, a ich wyniki są mało satysfakcjonujące. W związku z tym istnieje wysokie kliniczne zapotrzebowanie na nowe opcje leczenia RKN. Szlaki sygnalizacyjne PI3K/Akt/mTOR oraz Ras/Raf/MEK/ERK pełnią kluczową rolę w regulacji proliferacji i w nowotworzeniu. Czynniki hamujące elementy tych kaskad stanowią potencjalne środki przeciwnowotworowe, działające wybiórczo.

Cel projektu: Głównym celem projektu było określenie wpływu pojedynczej i kombinowanej terapii inhibitorami szlaków PI3K/Akt/mTOR (everolimus, NVP-BEZ235, LY294002) oraz Ras/Raf/MEK/ERK (U0126) na proliferację, aktywację kaspazy 3 i ekspresję białek w komórkach H295R. Drugorzędowym celem była ocena skuteczności terapii kombinowanej tych inhibitorów z mitotanem.

Materiały i metody: W projekcie użyto ludzkiej linii komórkowej raka kory nadnercza H295R. Aby określić wpływ wybranych czynników na żywotność tych komórek, zastosowano test oparty na resazurynie. W celu określenia dokładniejszych mechanizmów działania wykonano test aktywności kaspazy 3 i Western blot.

Wyniki: Najbardziej obiecującą terapią kombinowaną było połączenie everolimusa i NVP-BEZ235, które wykazało efekt synergistyczny w hamowaniu żywotności komórek. Wszystkie badane środki okazały się silnie działającymi czynnikami hamującymi żywotność komórek H295R, a wywierającymi ograniczony wpływ na aktywność kaspazy 3. Skuteczność mitotanu została potwierdzona, a jego połączenie z inhibitorami PI3K/mTOR albo MEK nie doprowadziło do uzyskania znamiennego efektu synergistycznego. Najbardziej obiecujący w tym połączeniu jest U0126 - dalsze badania nad doborem sposobu dawkowania mogą przynieść pozytywne wyniki.

Wnioski i dyskusja: Wybrane związki (everolimus, NVP-BEZ235, LY294002 i U0126, a przede wszystkim kombinacja everolimusa i NVP-BEZ235) wykazały dużą skuteczność obniżania proliferacji w przedklinicznym modelu RKN. Dzięki temu mają duży potencjał wykorzystania w dalszych badaniach *in vivo*. Badania aktywności kaspazy 3 i ekspresji białek dostarczyły cennych wskazówek dotyczących mechanizmów działania tych związków.

1. Introduction

1.1. Adrenocortical cancer

1.1.1. Epidemiology, diagnosis and treatment

Adrenocortical tumours (ACTs) are relatively common tumours whose prevalence tends to increase with patient's age. Adrenal incidentalomas are found in approximately 4% of CT scans and 6% of autopsies, but this is probably still an underestimate. Although the majority of ACTs are non-functional adrenocortical adenomas (ACAs), there are cases of functional adenomas associated with hypercortisolaemia and/or hyperaldosteronism [1, 2]. On the other hand, the malignant form, adrenocortical carcinoma (ACC), occurs rarely with an annual incidence of 0.5–2 per million population [3] and 0.3 per million for children younger than 15 years [4]. ACC generally presents either during childhood (prior to the age of 5) or during the fourth and fifth decade, being more common in women than in men [1, 5].

The histopathologic diagnosis of ACC has been controversial and several scoring systems have been proposed to establish a reliable diagnosis [6-9]. The Weiss system is the most frequently used one since 1984 [10]. It is based on histological analysis and is valued for its simplicity and high reliability. Still, there arises a clinical requisite for proper classification of a tumour case either to the benign or malignant group in order to discern the possible metastatic conditions as soon as possible. Promise lies in molecular studies, which elucidate the differences between benign and malignant lesions on the molecular level [11, 12].

The prognosis of adrenocortical cancer is very poor with an overall 5-year survival rate of less than 35%. Majority of patients at the diagnosis present advanced, but localized disease, which is limited to adrenal glands and qualify for a surgical removal. Still, about 30-40% of them have clear evidence of metastasis at

the clinical presentation of neoplasm and the available systematic treatment rarely yields a complete remission [13, 14].

The first-line therapeutic approach for ACC is a complete surgical resection of the tumour; however, it does not grant full recovery, as the post-surgery recurrence occurs in around 70-80% of cases [15]. In order to improve the prognosis, the administration of mitotane is recommended, alone or in combination with cytotoxic chemotherapy. Mitotane is considered first-line adjuvant therapy, improving recurrence-free survival, but at best 24% of the patients show an objective tumour response [13, 16, 17]. As this therapeutic strategy remains unsatisfactory, there is a requirement for new therapeutic options for ACC that would improve survival rates and decrease recurrence cases.

1.1.2. Mitotane

Mitotane (o,p'-DDD; 1-chloro-2-[2,2-dichloro-1-(4-chlorophenyl)-ethyl]-benzene), commercially known as Lysodren, is a derivative of the insecticide DDT (1,1,1-Trichloro-2,2-bis(4-chlorophenyl)ethane) with the adrenocorticolytic activity. Being in clinical use to treat the advanced adrenocortical carcinoma since the 1960s, mitotane causes highly specific growth inhibition of the adrenal cortex cells and reduces adrenal steroids production [18].

The main locations of mitotane-induced degeneration are the zona fasciculata and reticularis in the adrenal grands, while the effect on the zona glomerulosa is minimal. Mitotane activity is contingent on its metabolic conversion, which takes place in the adrenal mitochondria and produces the active metabolites: o,p'-DDE (1-chloro-2-[2,2-dichloro-1-(4-chlorophenyl)ethenyl]benzene) and p,p'-DDA (2,2-bis(4-chlorophenyl)acetic acid) [18]. Such requirement for its activation may contribute to this agent selectiveness.

Mitotane characterises with a narrow therapeutic range and causes, beside hypocortisolism, a range of clinically relevant side effects in the gastrointestinal tract, central nervous system, cardiovascular system, and bone marrow toxicity. A

significant group of patients experience severe adverse effects at therapeutic doses with the necessity to withdraw the treatment [19]. As well, mitotane adrenocorticolytic activity requires introducing glucocorticoid replacement therapy, usually along with mineralocorticoid and androgen supplementation [20].

The exact biochemical mechanism of action of mitotane has not been established yet. A number of studies in adrenocortical cancer H295R and H295 cell lines provide some clues (**Tab. 1**). Most of the analyses on H295R cells demonstrated that mitotane significantly decreases the cell proliferation/viability in dose-dependent manner [21-27], two studies reporting concurrent induction of apoptosis via caspase-3 and -7 activation [24, 27].

Tab. 1 Review of literature reporting mitotane effects in H295R and H295 cell lines.

Reported effects	Ref.
H295R cell line	
• decreased cell proliferation	[21]
• decreased cell viability • no effect on early and late apoptotic cell ratios	[22]
• decreased cell viability • reduced cortisol and aldosterone secretion • increased *CYP11B1* mRNA levels • decreased *HSD3B2* mRNA levels • no effect on mRNA levels of *STAR*, *CYP11B2*, *CYP11A*, *CYP17*, and *CYP21*	[23]
• decreased cell viability • increased caspase-3 and -7 activities • decreased cortisol and DHEAS concentration in the culture media • decreased mRNA levels of two cytochromes P450 (*CYP11A1* and *CYP17A1*) • no effect on mRNA levels of cyclin dependent kinase inhibitor 1A (encoding p21) and MYC (encoding cMyc) • inhibited expression of transforming growth factor β1 gene	[24]
• inhibited cell growth • reversible delay in G_2-phase • reduced glucocorticoids, mineralocorticoids, and androgens secretion • altered expression of triose phosphate isomerase, a-enolase, D-3-phosphoglycerate	[25]

dehydrogenase, peroxiredoxin II and VI, heat shock protein 27, prohibitin, histidine triad nucleotide-binding protein, and profilin-1 (total cell extracts) • downregulated proteins: aldolase A, peroxiredoxin I, heterogenous nuclear ribonucleoprotein A2/B1, tubulin-b isoform II, heat shock cognate 71 kDa protein, and nucleotide diphosphate kinase (mitochondrial fraction) • up-regulated proteins: adrenodoxin reductase, cathepsin D, and heat shock 70 kDa protein 1A (mitochondrial fraction)	
• decreased cell viability • reduced cortisol and androstenedione secretion • underexpressed genes: *HSD3B1*, *HSD3B2*, *CYP21A2* • overexpressed genes: *GDF15*, *ALDH1L2*, *TRIB3*, *SERPINE2*	[26]
• cytostatic and cytotoxic effects through an apoptotic mechanism involving caspase 3/7 • alterations in the mitochondria morphology (marked swelling and decrease in the number of respiratory cristae), significant depolarization of the mitochondrial membrane potential, drastic reduction of oxygen consumption, decrease in the levels of VDAC1 integral membrane channel	[27]
• reduced cortisol and 17-hydroxyprogesterone secretion • decreased expression of genes encoding mt proteins involved in steroidogenesis (*STAR*, *CYP11B1*, and *CYP11B2*) • inhibited maximum velocity of the activity of the respiratory chain complex IV (cytochrome c oxidase (COX)) • reduced steady-state levels of the whole COX complex • reduced mRNA expression of both mtDNA-encoded COX2 (MT-CO2) and nuclear DNA-encoded COX4 (COX4I1) subunits • no effect on activity and expression of respiratory chain complexes II and III • enhanced mt biogenesis (increase in mtDNA content and PGC1a (*PPARGC1A*) expression) and triggered fragmentation of the mt network	[28]
H295 cell line	
• reduced cortisol secretion in H295 cells • not inducing cell death of H295 cells • inhibited basal expression of StAR and P450scc proteins • inhibited *STAR*, *CYP11A1* and *CYP21* mRNA expression • no effect on *HSD3B2* and *CYP17* mRNA expression • stimulated *CYP11B1* mRNA expression	[29]
• suppressed cell growth of H295 cells • reduced cortisol concentration in H295 cells	[30]

Known inhibitory effect of mitotane on glucocorticoids, mineralocorticoids, and androgens production in H295R cells was studied in detail, combining the results of hormone secretion with the expression analyses, showing alterations in the expression of genes and proteins involved in the process of steroidogenesis. Altered expression was observed for genes encoding enzymes belonging to the cytochrome P450 family, such as: *CYP11A1* (encoding the cholesterol side-chain-cleaving monooxygenase, P450scc), *CYP11B1* and *CYP11B2* (steroid 11-β-monooxygenase), *CYP21A2* (steroid 21-monooxygenase), *CYP17A1* (steroid 17-α-monooxygenase) as well as P450-independent enzymes, such as: *HSD3B1* and *HSD3B2* (hydroxy-δ-5-steroid dehydrogenase, 3-β- and steroid δ-isomerase 1 and 2) and *STAR* (steroidogenic acute regulatory protein) [23-26, 28]. The effect on mitochondria has been reported as well, revealing alterations in morphology of this organelle and defects of the mitochondrial respiratory chain upon mitotane treatment, along with the expression alterations [27, 28].

Two studies on H295 cell line confirm similar inhibitory effect on cortisol production both in non-cytotoxic [29] and cytotoxic conditions [30]. The alterations in expression of some of the above mentioned genes were confirmed as well [29].

1.1.3. Molecular basis of adrenocortical cancer

Adrenocortical carcinoma has been intensively studied from the molecular perspective over the recent years with the knowledge on its underlying molecular events improving. A range of susceptibility genes, found in affected individuals with a family history, were the initial candidates for determining tumour malignancy and its differentiation from benign neoplasms. Genome-wide studies such as transcriptome analysis allow us to cluster tumours that follow similar molecular and prognostic profile. It may represent a real turning point in the adrenocortical tumours diagnosis and treatment. The methods enabling these analyses include: microsatellite analysis, conventional and array-based comparative genomic hybridisation (CGH), cDNA, oligonucleotide, SNP, miRNA microarrays, and PCR arrays. A number of research groups have carried out experiments on the

expression of a large number of genes in adrenocortical tumours. While studies using microsatellite markers identify genomic regions of high concentration of loss of heterozygosity (LOH) [31, 32], conventional comparative genomic hybridisation assesses copy number alterations across the entire genome [33-39]. However, the main disadvantage of conventional CGH is its limited resolution (2 Mbp for amplifications and 10–20 Mbp for single-copy deletions), making it an unreliable method to detect changes at the locus level. This has been addressed by CGH arrays, which allow the detection of DNA copy number aberrations at the gene level, locus by locus [40]. A number of recent studies have reported the results of the CGH array-based experiments for adrenocortical tumours [41-44]. Other types of DNA microarrays used in ACT research are cDNA, oligonucleotide, and SNP microarrays. The first two are the basis of expression profiling studies, differing slightly in precision and reliability. The volume of research reports based on microarrays 'spotted' with cDNA probes [45-51] is comparable to the number of studies using Affymetrix GeneChips (high-density oligonucleotide microarrays) [52-62]. A few recent reports have focused on single nucleotide polymorphism (SNP) analysis of adrenocortical tumours employing SNP arrays [63-65]. SNP microarrays enable the detection of copy number variations and LOH in the samples. Another type of specifically-designed chip is microRNA microarray, allowing the genome-wide investigation of miRNA populations [66-70]. Microarray technology also allows methylation profiling studies, suggesting that it may be another means of differentiating malignant from benign neoplasms [71-73]. As for PCR arrays, they are a method of choice for studies oriented on a specific group of genes, for example implicated in a specific cell-signalling cascade [50, 74, 75]. The techniques used to validate the results of a genome-wide study for chosen samples include immunohistochemistry, Western blotting, qPCR, and fluorescence *in situ* hybridisation (FISH). Apart from transcriptome analyses, one of the most common methods to screen a large number of samples is tissue microarray: it has been widely used for immunohistochemistry studies on adrenocortical tumours [52, 53, 76-81].

The high-throughput gene expression assays based on transcriptomes, which enable studying a large number of genes in a single experiment, have revealed the

distinct profiles for benign and malignant adrenocortical tumours, offering a new diagnostic tool and consequently optimal treatment [11, 12, 41, 53, 56, 82-84]. The mean number of genetic alterations was reported to be considerably higher for carcinomas than for adenomas [11, 12, 34, 41]. The alterations occurring in ACCs include change in expression, mutations, copy-number variations, and loss of heterozygosity; they span across the whole genome (**Fig. 1**) and are associated with multiple cellular processes.

Among the most frequent molecular events playing crucial role in formation of malignant adrenocortical lesions are: *IGF2* (insulin-like growth factor) overexpression, *TP53*-inactivating mutations (p53 protein), constitutive activation of Wnt/β-catenin signalling pathway via activating mutations of the β-catenin gene (*CTNNB1*). Alterations in protein kinase A (PKA) and steroidogenic factor 1 (SF1) are as well involved in adrenocortical carcinogenesis. Recent studies reveal that these cannot be treated as the only drivers of malignant adrenocortical tumourigenesis, but as mild contributors, and other accompanying factors also play role [85, 86]. The types of mutations observed in sporadic ACCs are very similar to that of inherited tumours (see section **1.1.4 Familial syndromes associated with adrenocortical cancer**), with missense changes being the most common.

1.1.3.1. Insulin-like growth factor II pathway

IGF-II exerts its function through binding to the membrane tyrosine kinase receptor, IGF1R. After the ligand is bound, the receptor autophoshorylates and the insulin receptor substrate 1 (IRS-1) is also recruited [87]. Tyrosine phosphorylation of IRS-1 releases the downstream signalling of pathways, such as PI3K/Akt/mTOR and Ras/Raf/MEK/ERK (see section **1.3.1** and **1.4.1**, respectively).

The genetic alterations at the 11p15.5 locus in sporadic ACCs primarily include: rearrangements, loss of heterozygosity (LOH), paternal isodisomy, rearrangements, and abnormal imprinting. These events result in a decrease in p57^{kip2} and H19, and an increase in *IGF2* mRNA levels, which have been correlated with a worse prognosis and higher risk for ACC recurrence [88, 89]. However, the most frequent

transcriptional change in ACC, occurring in over 80% cases, is over-expression of the *IGF2* gene [31, 46, 53, 55, 59, 80, 84]. Later referred to as "the adrenal-specific malignancy signature", as it is characteristic of ACC, but not ACA or the normal adrenal gland, this molecular alteration was initially studied in association with the Beckwith-Wiedemann syndrome (see section **1.1.4 Familial syndromes associated with adrenocortical cancer**). The IGF-II cluster is a group of related genes that also show elevated expression in ACC and includes predominantly genes for growth factors and their receptors [12, 45]. The IGF-II cluster contains as well a gene for insulin-like growth factor-binding protein 2 (IGFBP2), acting as a carrier protein for IGF-II; its expression and plasma level have been correlated with tumour mass in ACC [90]. For paediatric tumours, IGF-II levels are similar in adenomas and carcinomas. However, the difference lies in *IGF1R* gene expression, which seems to be the prime indicator for malignant adrenocortical tumour in children [91, 92].

1.1.3.2. TP53 signalling pathway

The alterations within *TP53* gene in ACCs occur mainly within the exon 5, the 'hot spot', but exons 6, 7, 8, and 10 are also affected [93, 94]. *TP53* mutations occur side by side with p53 accumulation, as revealed by immunohistochemistry [95]. Somatic inactivating *TP53* mutations are among the most frequently reported in ACC, estimated to occur in 15-70% cases [43, 56, 96, 97] and correlating with larger size, more advanced stage, higher metastatic rate, and shorter disease-free survival [95, 98].

1.1.3.3. Wnt/β-catenin signalling pathway

This Wnt/β-catenin cascade regulates proliferation, differentiation, survival, and apoptosis, with overlapping actions in a range of pathways, such as: TP53, TGFβ, PI3K/Akt/mTOR, or Ras/Raf/MEK/ERK. In the adrenal cortex, the Wnt/β-catenin cascade is involved in adrenal development and differentiation [99, 100].

Abnormal functioning of this system may lead to adrenal tumourigenesis. The most pronounced underlying molecular implications include the abnormal cytoplasmic and nuclear accumulation of β-catenin as well as somatic activating mutations of the β-catenin gene (*CTNNB1*). These events occur almost exclusively in ACCs with poor prognosis [43, 56, 81, 101]. Another target for Wnt/β-catenin pathway, ectodermal-neural cortex 1 (*ENC1*), is as well up-regulated in adrenocortical carcinomas [52]. Recently, in ACA and ACC samples an in-frame 12-bp deletion has been found in the *AXIN2* gene, a negative regulator of Wnt/β-catenin signalling [102].

1.1.3.4. cAMP/PKA pathway

Modifications in the protein kinase A (PKA) R1A subunit, the core of cAMP pathway, occur repeatedly among Carney complex patients (see section **1.1.4 Familial syndromes associated with adrenocortical cancer**). Bertherat et al. have shown that losses of 17q23-q24 loci are frequent in adrenocortical tumours with higher frequency in carcinomas than in adenomas. However, *PRKAR1A* gene mutations were detected in ACAs, but not ACCs, suggesting different role of PKA in tumourigenesis in benign and malignant lesions [103]. Consistently, defective R2B subunit (*PRKAR2B* gene, 7q22.3) expression is present in secreting adenomas with no change in secreting carcinomas and non-secreting adenomas [104]. Loss of the R1A subunit was reported to increase mTOR signalling [105]. The cAMP-dependent ACTH/G_s/PKA cascade plays a key role in regulating glucocorticoid and androgen production. Genetic modifications or expression changes of cAMP pathway genes associated with altered secretion and formation of adrenocortical carcinomas include:

— decreased expression and LOH of the ACTH receptor [106];

— genetic defects in *PDE8B* gene (phosphodiesterase 8B) [107];

— decreased expression of cAMP-responsive element binding protein (CREB) [108, 109];

— higher telomerase activity [109];
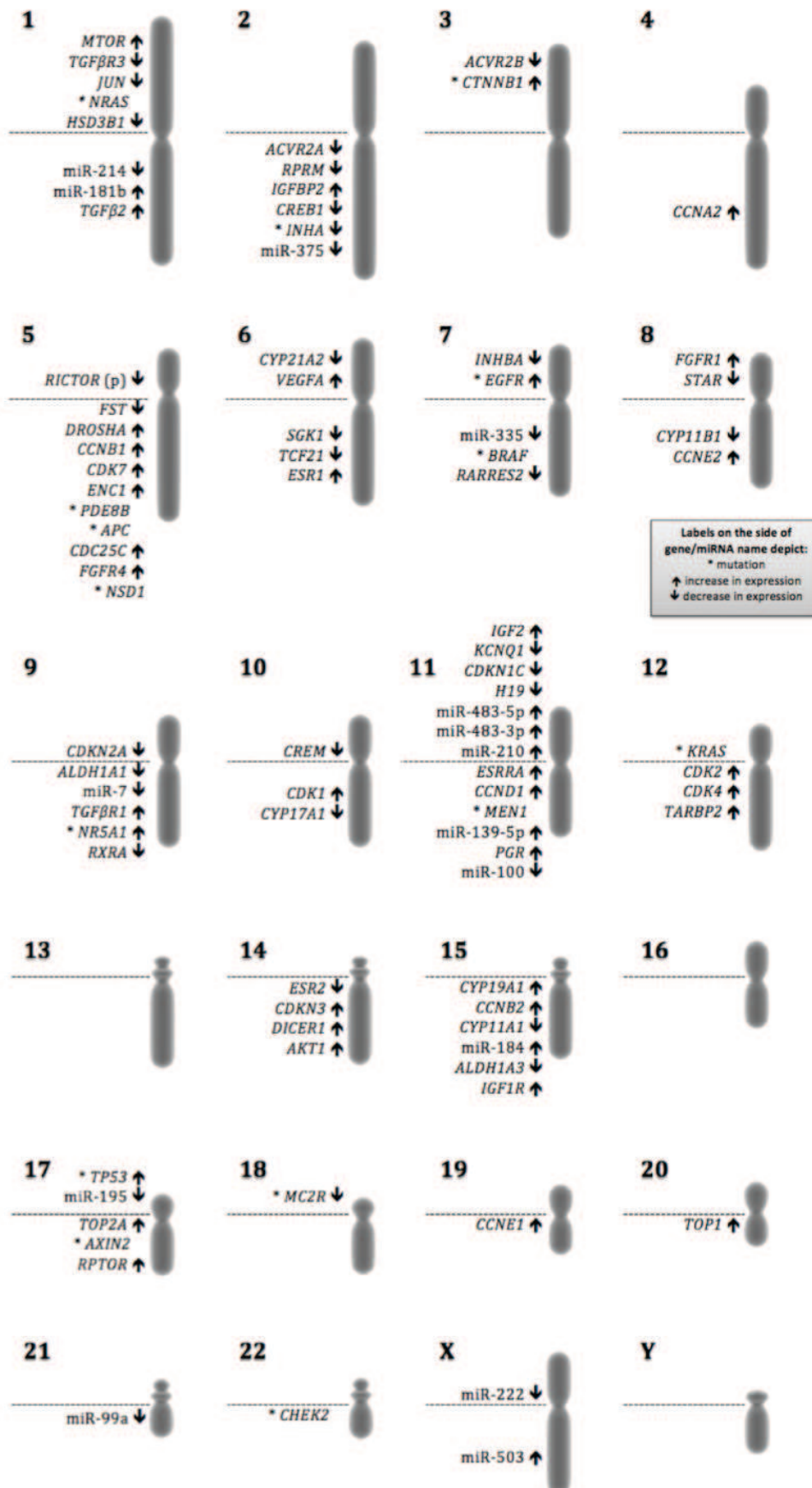
Fig. 1 Molecular alterations characteristic for adrenocortical carcinoma.
It is indicated within which arm of the respective chromosomes (upper p or lower q) the genes/miRNAs are located. Labels on the side of gene/miRNA name depict: asterisk – mutation, up arrow – increase in expression, down arrow – decrease in expression. Chromosome illustrations sourced from Somersault 18:24 – Library of Science Illustrations (www.somersault1824.com).

− decreased expression of ICER (inducible cAMP early repressor) isoforms, deriving from an internal promoter of *CREM* gene (for cAMP responsive element modulator) [109].

Opposite changes are reported in ACA, suggesting that they may be indicators of malignancy. However, most of these alterations are associated with Cushing's syndrome, which suggests that altered functioning of cAMP signalling is strongly correlated with that type of tumour of the adrenal cortex.

1.1.3.5. Steroidogenic pathway

Nuclear receptor steroidogenic factor 1 (SF-1, NR5A1) acts as a master regulator of adrenocortical differentiation and steroidogenesis by controlling the expression of cytochrome P450 steroidogenic enzymes. SF-1 is involved in the proliferation, apoptosis, angiogenesis, adhesion, and cytoskeleton dynamics of adrenocortical cells [110, 111]. High levels of SF-1 were reported to increase the proliferation rate of adrenocortical cells and to decrease the secretion of cortisol and aldosterone with no effect on dehydroepiandrosterone (DHEA). Multiple copies of *SF-1* (*NR5A1*) gene stimulate tumour development [112]. A study focusing on the SF-1 inhibitor, Pod-1 (capsulin, epicardin, Tcf21), established that the *TCF21* gene is down-regulated in ACCs, comparing with ACAs and normal tissue [113]. SF-1 over-expression is much more significant in childhood than adult ACTs. In the majority of paediatric tumours, the number of *SF-1* gene copies is increased as a result of chromosome gain or amplification at 9q33 [79, 114, 115]. SF-1 also shows prognostic information: higher expression correlates with more advanced tumour stage, poorer clinical outcome and shorter overall 5-year survival [76, 116].

Another factor involved in steroidogenesis is ACTH (adrenocorticotropic hormone, corticotropin); it plays key role in the maximal cell-specific expression of steroidogenic enzymes needed for the synthesis of glucocorticoids and androgens in the zona reticularis and zona fasciculata. It acts through receptors coupled to G_s protein, increasing the levels of cAMP and thus inducing PKA, which targets in turn stimulate the expression of P450 steroidogenic enzymes. Generally, the

ACTH/G$_s$/PKA cascade is crucial for maintaining a highly differentiated adrenal phenotype, but is only of moderate importance for cell proliferation [117, 118]. Adrenocortical carcinomas show decreased expression levels and LOH of *ACTH-R* gene, encoding the corticotropin receptor [106, 109].

A cluster of steroidogenesis genes also differentiates ACC from ACA and contains: *CYP11A1* (cytochrome P450scc, cholesterol desmolase), *CYP11B1* (P450c11B1, 11β-hydroxylase), *CYP17A1* (P450c17, 17α-hydroxylase), *CYP21A2* (P450c21, 21-hydroxylase), *HSD3B1* (3β-hydroxysteroid dehydrogenase/Δ-5 isomerase type), and *STAR* (StAR, steroidogenic acute regulatory protein). In contrast to IGF-II cluster expression, this steroidogenesis cluster shows low expression in adrenocortical carcinomas and is high in adenomas. That is in line with glucocorticoid overproduction in ACAs [45]. The link between IGF-II and steroidogenesis pathways is observed particularly during adrenal development and differentiation. IGF-II stimulates expression of ACTH-regulated steroidogenic enzymes, such as P450scc, P450c17, and HSD3B1 [88]. Recent studies also indicate connections with TGFβ and Wnt/β-catenin signalling. However, the precise mechanisms of that interrelation are yet to be identified [111, 119]. The suggested explanation indicates the involvement of a downstream target for Wnt/β-catenin signalling pathways, SGK1, serum glucocorticoid (GC) kinase 1, which have been reported to show lower expression in adrenocortical carcinomas. SGK1 is a serine/threonine kinase that may be regulated by a number of factors, including corticosteroid hormones, growth factors, p53, and mTORC2 [63].

1.1.4. Familial syndromes associated with adrenocortical cancer

Most adrenocortical carcinoma cases are sporadic; however, the literature provides numerous reports of familial syndromes associated with an increased prevalence of adrenocortical tumours, which was the groundwork for the research on their molecular basis. Examples of such hereditary syndromes include: Li-Fraumeni (LFS) and Beckwith–Wiedemann syndromes (BWS), and Carney complex (CNC), which highlighted the specific susceptibility genes: *TP53*, *IGF2*, and *PRKAR1A*,

respectively [120]. Other ACT-associated syndromes are: multiple endocrine neoplasia (MEN1), McCune–Albright syndrome (MAS), and familial adenomatous polyposis coli (FAP) with its variant Gardner syndrome (familial colorectal polyposis), all summarised in **Tab. 2** [120-124].

In the majority of cases these conditions originate from a specific underlying molecular profile with germline mutations, which may be as simple as a point mutation, but more often are complex alterations, concerning multiple genes and molecular pathways [90]. The focus of this research project was the adrenocortical carcinoma and consequently the syndromes characterizing with increased prevalence of this kind of cancer are below described in detail.

Tab. 2 Genes involved in genetic/familial syndromes associated with adrenocortical tumours. Abbreviations: ACA – adrenocortical adenoma, ACC – adrenocortical carcinoma. Prepared based on [120-124].

Familial Syndrome	ACA / ACC	Location	Gene/Locus	Protein
Li-Fraumeni Syndrome 1 (LFS1)	ACC	17p13.1	*TP53*	Tumour protein p53
Li-Fraumeni Syndrome 2 (LFS2)	-	22q12.1	*CHEK2*	Checkpoint kinase 2
Li-Fraumeni Syndrome 3 (LFS3)	-	1q23	(not known yet)	
Beckwith–Wiedemann Syndrome (BWS)	ACA, ACC	5q35.2-q35.3	*NSD1*	Nuclear receptor binding SET domain protein 1
		11p15.5	*H19*	H19, imprinted maternally expressed transcript (non-protein coding)
		11p15.5	*IGF2*	Insulin-like growth factor II
		11p15.5	*KCNQ1OT1*	KCNQ1 opposite strand/antisense transcript 1 (non-protein coding)
		11p15.4	*CDKN1C*	Cyclin-dependent kinase inhibitor 1C (p57, Kip2)
Multiple Endocrine Neoplasia, Type 1 (MEN1)	ACA / (rare ACC)	11q13.1	*MEN1*	Menin
Familial Adenomatous Polyposis-1 (FAP1) and its variant Gardner Syndrome	ACA / (rare ACC)	5q22.2	*APC*	APC
Carney complex, Type 1 (CNC1)	ACA	17q24.2	*PRKAR1A*	Protein kinase, cAMP-dependent, regulatory, type I, alpha
Carney complex, Type 2 (CNC2)	ACA	2p16	(not known yet)	
McCune–Albright Syndrome (MAS)	ACA	20q13.32	*GNAS*	G_s-alpha (the alpha subunit of the guanine nucleotide-binding protein (G protein))

Inherited in autosomal dominant manner, the Li-Fraumeni syndrome (OMIM 151623) is characterised by multiple types of early onset non-site specific neoplasms, occurring in patients younger than 45 years. The most prevalent are pre-menopausal breast cancer, soft-tissue sarcoma, brain tumours, osteosarcoma, adrenocortical carcinoma, lung carcinoma, and leukaemia as the least frequent of this group (data obtained from IARC TP53 Database) [94, 125, 126]. ACC develops in less than 10% of LFS-patients and, compared with the other neoplasms mentioned, is diagnosed in the youngest patients in early childhood [93, 94, 127]. Most patients with Li-Fraumeni or Li-Fraumeni-like (LFL) syndromes carry heterozygous mutations in the *TP53* gene (17p13.1), encoding p53 tumour suppressor protein, also called the 'guardian of the genome'. The p53 transcription factor acts by activating the expression of genes involved in: cell cycle control, arrest in G_1 phase in case of DNA damage (maintenance of genomic stability), and apoptosis [128]. There is much variation in the reported incidence of mutations in the *TP53* gene in LFS/LFL patients – being around 80% and 40%, respectively [129] or almost 30% as a combined value for both syndromes [130]. For all familial tumour cases in general, up to 17% are reported to be the effect of alterations in the *TP53* gene [127]. It is worth noting that, in line with the Chompret criteria for LFS, every single patient with ACC, regardless of their age at diagnosis or family history, demonstrates a high probability (usually between 50-80%) of having a germline mutation in *TP53* [127, 131]. According to the International Agency for Research on Cancer (IARC), LFS-related mutations concentrate in *TP53* in exons 5 – 8 (around 80–90%) and then in exons 4 and 10 (below 10% altogether), most of them being missense (almost 70%), followed by splicing (10%), nonsense (9%), and frame-shift (7%) changes [94]. Two main functions of p53 are ameliorated by alterations in those regions: the DNA contact via DNA binding domain (DBD) and the support of the structure of protein-DNA contact surface, obtained by two large loops (L2 and L3), stabilised by zinc binding and a loop–sheet–helix motif (loop L1). Consequently, the mutant proteins are divided into two groups: "contact" (results of mutations, such as S241F, R248W, and C277F) and "structural" (R175H, C176F, H179R, and C242F). Other suggested mechanisms for altered p53 functioning include: gain-of-function (GOF) and dominant–negative effects (DNE) over the wild-type protein,

when no selective pressure is exerted for the loss of the wild-type allele [131, 132]. Studies of the individuals from Southern Brazil with family history compliant with the clinical definitions of LFS or LFL syndrome have shown that around 13% of them are carriers of the c.1010G>A (p.R337H) mutation in exon 10 of *TP53* gene [130]. Despite the previous alternative theories, a recent study confirms that the high prevalence of this mutation, around 0.3% in the dense population of this region, results from the occurrence of a founder effect in the Brazilian population. In Southern Brazil the incidence of childhood ACC is 10-15 higher compared with other parts of the world, being strongly associated with the p.R337H mutation [133-135]. A small number of the families afflicted with LFS carry a mutation in another gene – *CHEK2* (22q12.1); this has led to its renaming as Li-Fraumeni Syndrome 2 (LFS2) (OMIM 609265) [93, 121]. There is also the LFS3 (OMIM 609266), associated with the region 1q23, which requires further investigation [121, 136].

The Beckwith-Wiedemann syndrome (OMIM 130650) is a rare imprinting disorder, mostly sporadic with familial cases representing less than 15% of cases. This paediatric syndrome is predominantly characterised by anterior abdominal wall defects, macroglossia and overgrowth. Around 10% of Beckwith-Wiedemann cases are associated with an increased risk of tumour development, the most frequent being Wilms tumours, hepatoblastomas, rhabdomyosarcomas, and adrenocortical tumours [123, 137]. Genetically, Beckwith-Wiedemann syndrome is caused by altered expression of imprinted genes in the region 11p15.4-p15.5. The telomeric domain (called imprinting centre 1, IC1 or differentially methylated region 1, DMR1) contains *IGF2* (insulin-like growth factor II) and *H19* genes. The centromeric domain 2 (IC2, DMR2) comprises around 10 imprinted genes, encoding the cyclin-dependent kinase inhibitor p57^{KIP2} (cyclin-dependent kinase inhibitor 1C gene, *CDKN1C* or *p57kip2*), a subunit of a potassium voltage-gated channel (*KCNQ1*), and its overlapping transcript (*KCNQ1OT1* or *LIT1*) [137, 138]. The majority of BWS-related genetic defects are due to the loss of imprinting, caused by abnormal methylation in the IC2, whilst most familial cases are associated with alterations in *CDKN1C* gene or microdeletions along IC1, presenting an autosomal dominant pattern of inheritance [123, 139]. Another gene implicated in the development of Beckwith-Wiedemann syndrome is *NSD1* (5q35.2-q35.3). Baujat et al. described its

mutations in a small number of BWS patients and suggested the possible influence of the product of this gene, the nuclear receptor binding SET domain protein 1, on the imprinting in the 11p15 region. It acts also as a co-regulator of the androgen receptor [140].

The multiple endocrine neoplasia type 1 (OMIM 131100) is a highly penetrant, autosomal dominant condition, presenting with tumours of the parathyroid glands, endocrine pancreas, anterior pituitary gland, thymus (carcinoids), thyroid (adenomas), and, in up to 40% of patients, adrenocortical neoplasm or hyperplasia. ACCs occur but are extremely rare. The majority of affected families (75-95%) have a heterozygous inactivating germline mutation in the *MEN1* gene (11q13.1) [32, 141]. The menin protein is a tissue-specific tumour suppressor and has been reported to interact with a variety of proteins like: transcriptional factors (e.g. Jun D, NFκB and Smad3), or histone H3 methyltransferases (e.g. MLL, MLL2) [142]. Consequently, its field of action is the regulation of cell cycle, proliferation, and apoptosis [143]. The impact of menin on cellular growth seems to be quite complex, as it acts as a suppressor in endocrine cells and as an activator in certain types of leukaemia cells [142].

The familial adenomatous polyposis (FAP) 1 and its variant Gardner syndrome (OMIM 175100) are autosomal dominant disorders. In its typical form, FAP manifests by hundreds to thousands of colorectal adenomatous polyps and cancer [144], while Gardner syndrome reveals gastrointestinal polyposis and other lesions, such as osteomas, epidermoid cysts, hepatoblastoma, papillary or follicular thyroid cancer, and adrenal adenomas [145]. The molecular cause underlying these syndromes is found at the locus 5q22.2, containing the adenomatous polyposis coli (*APC*) gene, which acts as a tumour suppressor by decreasing the activity of β–catenin. In the absence of the regulating effect of APC, nuclear β–catenin accumulation leads to up-regulation of genes involved in the cell cycle entry and progression. The pathogenic alterations in *APC* gene are mainly frame-shift or nonsense mutations, then large gene deletions and splice site changes [144]. It was observed that FAP patients show increased risk for the ACC formation, compared with the general population. That may be explained with the fact that increased levels of β–catenin possibly play role in the ACC development, as this protein

potently activates a spectrum of genes essential for the adrenocortical tissue development and homeostasis [90, 146].

1.2. *In vitro* and *in vivo* analysis of adrenocortical cancer

1.2.1. Primary cultures and cell lines

Primary cultures of adrenocortical cells may be used in the research of adrenal physiology. Though useful, they have strictly finite life span and pose a number of issues with fresh tissue availability, isolation of adequate cells, variability of material; hence, to overcome them cell lines proved to be more convenient and accessible, allowing more straightforward planning of the experiments.

Cell culture models are the key tools in the molecular biology research, enabling studies on the cell physiology and biochemistry and assessment of the efficacy of drugs and other compounds. The main advantages of cell culture are its relative simplicity and universality as well as consistency and reproducibility of results. It provides a simple way to test the toxicity of drugs and various compounds before the tests on animals are performed.

A number of adrenocortical cell lines have been established from primary cultures maintained in various types of media for longer time and then selected for the best characteristics. The currently available adrenocortical cell model systems for adrenal studies are summarised in **Tab. 3** [147, 148]. These cell lines present various combinations of basic characteristics (such as their origin, steroid production and responsiveness), which enable researchers to choose the best model to address the research questions they plan to answer. The most commonly used adrenocortical cell lines are human NCI-H295 derived cell lines, and mouse Y-1.

In this study, the adrenocortical carcinoma NCI-H295R cell line was used. It is the best model to study the efficacy of various compounds against ACC, being easy to culture (growing as the adherent monolayer) and having retained the ability to

produce mineralocorticoids, glucocorticoids, and adrenal androgens, which allows to move the studies to the next step and investigate the effect of these compounds on adrenal steroidogenesis. The NCI-H295R cell line is described in detail in the chapter **3.1 Cell line**.

Tab. 3 Summary of adrenocortical cell lines.
Abbreviations: ACTH – adrenocorticotropic hormone, corticotropin; ACC – adrenortical carcinoma; SCC – small-cell carcinoma; AC – adrenal cortex; Mts – metastasis; PPNAD – primary pigmented nodular adrenocortical disease; CNC – Carney complex. Prepared based on [147, 148].

Cell line	Origin	Steroids produced			Responsiveness	
		Mineralo-corticoids	Gluco-corticoids	Adrenal androgens	ACTH	cAMP
NCI-H295	ACC	+	+	+	–	+
NCI-H295A	ACC	+	+	+	–	+
NCI-H295R strains	ACC	+	+	+	–/+	+
HAC15 (derived from H295R)	ACC	+	+	+	+	+
SW13	SCC (AC/Mts)	–	–	–	N/D	N/D
CAR47	PPNAD, CNC	–	–	–	–	–
ACT-1	ACC	–	–	–	N/D	N/D
RL-251	ACC	–	–	–	–	N/D
Pediatric adrenocortical adenoma derived cell line	ACT	+	+	–	N/D	N/D
SV40 transformed cell line	Fetal adrenal cells	N/D	N/D	N/D	N/D	+
Y-1 (murine)	radiation-induced tumour	+	+	–	+	+
***ras*-transformed cells lines (rat)**	Kirsten murine sarcoma virus transformed cells	–/+ (low)	–/+ (low)	N/D	+	+
SV40 transformed cell lines (murine)	ACT	+	N/D	N/D	–	+
SV40 transformed cell lines (bovine)	adrenal cells	N/D	+	N/D	N/D	+

1.2.2. Animal models

Studies on adrenocortical tumour cell lines provide clues on the molecular events that may lead to tumour formation and present good models for testing a spectrum of potential targets for novel therapies. An expected step further into the adrenocortical tumour research is transferring the results obtained from molecular studies to the animal models of this disease. Therefore, feasible animal systems are required, enabling easy transfer of molecular research to a higher level. Animal models offer enhanced insight in cancer biology studies, reflecting cell interactions and immune response occurring in a living organism. The groundwork in anti-cancer therapy research is the traditional mouse xenograft model; this method involves culturing human tumour cells over the years and then injecting them into a mouse.

The necessity for development of the animal model research in terms of adrenocortical tumour is emphasized by the fact that currently the only specific pharmacological treatment for carcinomas is mitotane [13]. Gaining the deeper knowledge on etiology and pathology of ACTs will be a basis for novel therapies targeting specific molecules.

Three most promising model organisms in the adrenocortical tumour research are mouse, ferret, and dog. In mice and ferrets the functional tumour formation may be induced by gonadectomy; such neoplasms tend to be benign. This method proved to be successful also in other animals, such as goats and hamsters. Higher susceptibility to adrenal tumour development in mice is observed also in strains with a polymorphism in the steroidogenic factor 1 (SF-1). ACT mouse models are obtained as well through transplantation of adrenocortical tumour cells or through specific genetic modifications (by transgenesis or knock-out). The most common cells transplanted to stimulate tumour formation are: bovine adrenal cells transduced with the gastric inhibitory polypeptide receptor (GIPR) or LH receptor (LHR) as well as human ACC cell line NCI-H295. Transgenic mouse models developing adrenocortical tumours were reported in animals with Simian Virus 40 (SV40) large T-antigen expressed under the control of promotors for *CYP11A* gene,

the aldose reductase-like (*AKR1B7*) gene or the inhibin-α. As well, mice with multiple copies of *SF1* gene have been more prone to develop ACC.

Natural occurrence of adrenocortical tumours is found in 20% of gonadectomised ferrets, but also may be stimulated by inbreeding at commercial facilities or unnatural photoperiodic stimulation. The protein expression evaluated for ferret ACTs shows high concentration of: luteinizing hormone receptor (LHR), inhibin-α, AMH, GATA4, CYP19, cytochrome b_5. In dogs, spontaneous Cushing's syndrome occurs in 1–2 per 1000 individuals per year. Like in human treatment, the excision of adrenal glands is a method of choice. In case of inoperable or metastatic tumours, the mitotane treatment is applied. Canine therapeutic adrenalectomy may serve as a source for primary canine ACT tissue to use in *in vitro* research [149, 150].

All three of described animal models for adrenocortical tumours – mouse, ferret, and dog – demonstrate the high incidence of this neoplasm. The main advantages of mouse ACT models include easy access to the genotype and epigenetic information for that species, facilitating tumour genetics studies. Tumour latency is quite short, spanning over weeks or months. Mouse models may also be used for xenograft studies that are essential for preclinical screening of novel drugs [151]. On the other side, the anatomy and functionality of adrenal glands is quite different than that of human. Another disadvantage, applicable to ferrets as well, is the fact that adrenocortical tumours in that species tend to produce sex hormones and not gluco- or mineralocorticoids. When it comes to the benefits of using ferret models, the close to human overall physiology proved to be useful in studying reproductive endocrinology and airway diseases. The difficulties may arise along the fact that the information on genotype and epigenetics is not sufficient for this species and the tumour latency lasts years. Dogs are very promising model for adrenocortical tumours, especially for their similarities in adrenal glands anatomy and functionality, biological behaviour of ACTs (usually cortisol-producing), and treatment options [150].

1.3. PI3K/Akt/mTOR pathway and its inhibitors

1.3.1. PI3K/Akt/mTOR pathway description

Being most frequently altered in human tumours, PI3K/Akt/mTOR signalling pathway has recently been in the spotlight of pursuit for targeted therapies for cancer [152]. It is as well a promising target for ACC therapy with recent studies showing the anti-proliferative activity of PI3K/mTOR inhibitors in adrenocortical cancer cells [153-159].

The initiation of this pathway is based on the recruitment phosphoinositide 3-kinase (PI3K) to the membrane by IRS-1, bound to the IGF-II-activated membrane receptor (**Fig. 2**). In this way PI3K is activated and facilitate conversion of phosphatidylinositol bisphosphate (PIP2) to phosphatidylinositol triphosphate (PIP3). This association provides docking sites for serine-threonine kinases: 3-phosphoinositide-dependent protein kinase-1 (PDK1, PDPK1) and Akt (protein kinase B, PKB). PTEN (phosphatase and tensin homologue) counteracts PI3K by dephosphorylating PIP3. PDK1 phosphorylates Akt, thus activating it. Subsequently, Akt inhibits TSC2 from the tuberous sclerosis complex (TSC1/2) through adding a phosphate group. As TSC2 acts as an indirect inhibitor for mammalian target of rapamycin complex 1 (mTORC1), the above event causes its release from inactive state [160, 161]. The mTORC1 complex comprises a serine/threonine-protein kinase mTOR (mammalian target of rapamycin), regulatory-associated protein of mTOR (raptor), and mLST8 (also known as G protein beta subunit-like, GβL), and PRAS40 (proline-rich Akt substrate 40 kDa, AKT1S1). PRAS40 is as well a direct target for Akt kinase and is an inhibitor of the mTORC1 complex. Phosphorylated PRAS40 negatively regulates mTORC1. Akt may also directly activate mTOR, generating phospho-mTOR (p-mTOR).
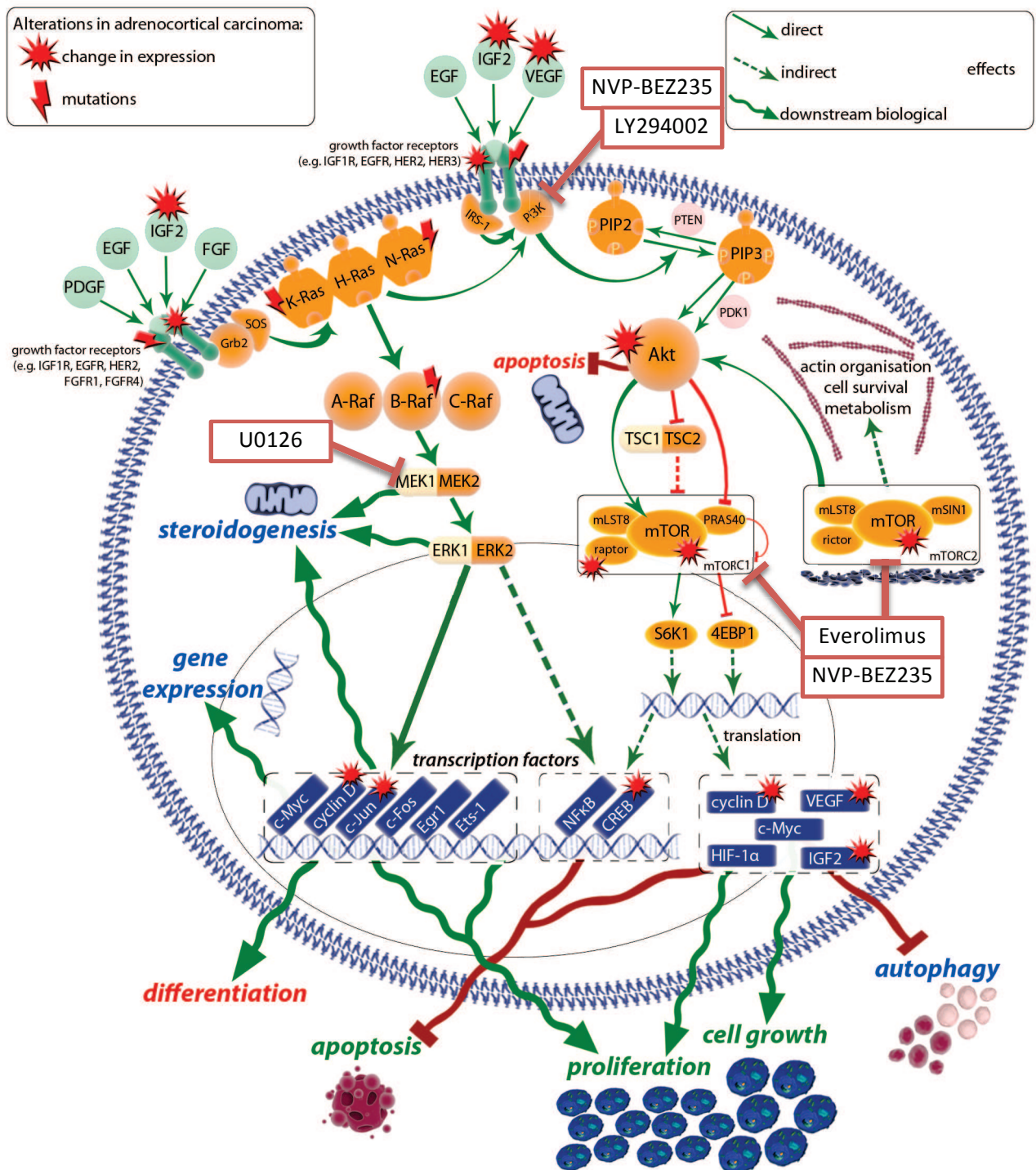
Fig. 2 PI3K/Akt/mTOR and Ras/Raf/MEK/ERK signalling pathways.
The alterations of the signalling components observed in adrenocortical carcinoma are indicated with the red star for changes in expression, the red lightning for mutations. Green arrows indicate stimulatory effect and red - inhibitory. The downstream biological effects are grouped in three categories: favourable for cancer cell growth and survival (marked in green), unfavourable (red) and of ambivalent impact (blue). Selected PI3K/mTOR and MEK inhibitors are indicated with red boxes (everolimus, NVP-BEZ235, LY294002, U0126). Shapes and illustrations sourced from Somersault 18:24 – Library of Science Illustrations (www.somersault1824.com).

The downstream mTORC1 effectors are, among others, p70 ribosomal protein S6 kinase 1 (p70S6K, S6K1, RPS6KB1) and eukaryotic translation initiation factor 4E binding protein 1 (4EBP1, EIF4EBP1) [162, 163]. S6K1 and 4EBP1 stimulate mRNA translation of oncogenic proteins, such as c-Myc, hypoxia-inducible factor-1α (HIF-1α, HIF1A), VEGF, IGF-II and cyclin D [160]. The main downstream effects of the mTORC1 complex include stimulating cell growth and proliferation, as a reaction to growth factors, nutrient availability, stress, cellular energy, and oxygen levels. It also regulates autophagy as a part of the response to nutrient starvation [3, 163-165].

The mTORC2 complex contains mTOR, mLST8 protein (as in mTORC1), rictor (rapamycin-insensitive companion of mTOR), and mSIN1 protein (stress-activated protein kinase-interacting 1, MAPKAP1). The role of mTORC2 is primarily the regulation of the actin cytoskeletal organisation, but it also seems to be involved in cell survival and metabolism. Furthermore, while mTORC1 acts downstream to Akt, mTORC2 – upstream and activates this protein kinase [161-163].

1.3.2. PI3K/Akt/mTOR pathway alterations in ACC

The alterations in the PI3K/Akt/mTOR pathway that are associated with the development of adrenocortical tumours affect a number of its components. Several growth factors that initiate this signalling cascade, such as IGF-II, VEGF, and EGF, are altered. Moreover, Fassnacht et al. described elevated total Akt protein expression in ACCs, but not in ACAs and normal tissue. This research group also assessed the level of phosphorylated Akt (pAkt) and showed that in fact the pAkt/Akt ratio was not altered in carcinomas [166]. However, another study reported that expression of pAkt was higher in ACCs [80]. Additionally, mTOR, phospho-mTOR, and raptor protein levels were markedly increased in adrenocortical tumours. Accordingly, mTOR activity was higher in ACTs than in controls. On the other hand, rictor was not detectable in tumour or normal adrenal tissue [154].

1.3.3. Inhibitors of PI3K/Akt/mTOR pathway – everolimus, NVP-BEZ235, LY294002

Examples of the PI3K/Akt/mTOR pathway inhibitors include: everolimus (RAD001), NVP-BEZ235, and LY294002 (as indicated in **Fig. 2**). Everolimus (RAD001, 40-*O*-(2-hydroxyethyl)-rapamycin) is a derivative of rapamicyn (rapalog), commercially known as Afinitor, and is currently used in treatment of renal cell carcinoma [167, 168]. The mechanism of mTOR inhibition is based on the formation of the complex between everolimus and cyclophilin FKBP-12, which then binds to the mTORC1 and mTORC2 complex, inhibiting downstream signaling. The cellular level effects of everolimus include growth and proliferation inhibition as well as reduction of HIF-1α and VEGF expression [167].

An imidazo[4,5-*c*]quinoline derivative, NVP-BEZ235, is a dual pan-class I PI3K and mTOR kinase inhibitor. The mechanism of its action is through binding to the ATP-binding cleft of PI3K and mTOR kinases, thus acting as an ATP competitor. It decreases the activity of both mTORC1 and mTORC2 complexes. NVP-BEZ235 shows antineoplastic properties with strong antiproliferative activity trough growth arrest in the G_1 phase, but no apoptosis induction in prostate tumour cells [169].

LY294002 (2-(4-Morpholinyl)-8-phenyl-chromone) is a potent selective and reversible PI3K inhibitor, binding competitively to its ATP-binding site. *In vitro* effects of LY294002 include proliferation and cell growth decrease as well as apoptosis induction [170, 171].

1.4. Ras/Raf/MEK/ERK pathway and its inhibitors

1.4.1. Ras/Raf/MEK/ERK pathway description

The Ras/Raf/MEK/ERK pathway, also called the mitogen-activated protein kinase (MAPK) cascade, is another downstream cascade initiated by tyrosine kinase

receptor (TKR) activation. This cascade, activated by ligands and stress, is initiated with recruitment of the Ras GTPases (HRas, KRasA, KRasB, and NRas) to the cell surface receptor via spectrum of adapter proteins and exchange factors (**Fig. 2**). The Ras proteins in their active, GTP-bound state exert their downstream action by activating Raf, a serine/threonine-protein kinase [172]. The Raf family includes three types of kinases: A-Raf, B-Raf, and C-Raf (Raf-1). Raf kinases phosphorylate specifically MEK1 and MEK2 (dual specificity mitogen-activated protein kinase kinases, MAPKKs, MAPK/ERK kinases). MEK1/2 shows strict phosphorylation specificity for its substrates, ERK1 and ERK2 (extracellular signal-regulated protein kinases, mitogen-activated protein kinases, MAPKs).

Protein serine/threonine kinases ERK1/2 act on over 160 substrates [173]. ERKs may directly phosphorylate transcription factors such as Fos, Jun, Myc, Ets-1, Egr1, and cyclin D1. Indirectly, ERK may activate CREB and NFκB. Generally, the Ras/Raf/MEK/ERK cascade regulates gene expression, proliferation, differentiation and apoptosis, overlapping to some extent with PI3K/Akt/mTOR signalling effects [174-176].

1.4.2. Ras/Raf/MEK/ERK pathway alterations in ACC

A few reports regarding Ras proteins describe overexpression of *KRAS* mRNA and mutations in *KRAS* gene in benign adrenal alterations [177], carcinomas [178] as well as mutations in *NRAS* gene in both ACCs and ACAs [178, 179]. However, some other studies have reported a lack of mutation of those genes and *HRAS* (HRas) in adrenal neoplasms [179-181]. Moreover, Kotoula et al. found activating mutations in the *BRAF* gene (B-Raf) in almost 6% of carcinomas tested [178]. These observations suggest that alterations in genes encoding elements of Ras and Raf families may occur in adrenal lesions, but are not common events.

1.4.3. Inhibitor of Ras/Raf/MEK/ERK pathway – U0126

A direct and selective inhibitor of MEK1/2, U0126 (1,4-diamino-2,3-dicyano-1,4-*bis*(2aminophenylthio)butadiene), blocks phosphorylation and activation of ERK, thus causing decrease in downstream MAPK cascade activation (as indicated in **Fig. 2**). It acts via non-competitive mechanism to both MEK substrates, ATP and ERK [182, 183]. MEK inhibitors are very promising components of combined therapy, because of observed synthetic lethality, for instance with inhibitors of tyrosine kinases [184] or PI3K/Akt/mTOR pathway [185].

2. Aim of the Project

This research project aimed to test the hypothesis that selective and combinatorial inhibition of the cell signalling pathways: PI3K/Akt/mTOR (everolimus (RAD001), NVP-BEZ235, LY294002) and Ras/Raf/MEK/ERK (U0126) can decrease proliferation and induce apoptosis in human H295R adrenocortical carcinoma cells, potentially having synergistic effect. The combination therapy is seen as a possibility to overcome the resistant cells that often appear after treatment with single agent [186]. Aiming at two 'targets' at once seems to be a promising approach to avoid potential drug escape mechanisms.

The cytotoxic potential of these compounds has been reported in other types of cancer cells [167-171, 182, 183]; however, it has not been extensively tested for adrenocortical cancer H295R cell line with only a small number of research groups exploring this field [154-156, 158, 159, 169, 187-190].

Therefore, we investigated the effect of everolimus (RAD001), NVP-BEZ235, LY294002 and U0126 on the cell proliferation, apoptosis and modulation of signalling pathways in the H295R adrenocortical carcinoma cells. In addition to various combinations of treatment with these compounds, we also assessed co-treatment with mitotane, which is used as a standard therapy in clinical practice.

The long-term aim of this project was to assess the potential of treatment with these selected compounds and find the most effective and promising combination, which may be estimated by further animal studies and, potentially, in clinical trials.

3. Materials and methods

3.1. Cell line

The NCI-H295R [H295R] (ATCC® CRL-2128™) cell line (human adrenocortical carcinoma) was a generous gift from Dr Peter J. King (Molecular Endocrinology Department, William Harvey Research Institute, Barts and The London School of Medicine and Dentistry, Queen Mary University of London). The origin of the cell line was confirmed with PCR tests.

The NCI-H295R cell line was derived from the continuous pluripotent NCI-H295 adrenocortical carcinoma cell line (ATCC® CRL-10296), established and characterized in 1990 by A.F. Gazdar et al. [191]. The H295 cells originate from an invasive primary adrenocortical carcinoma culture and grow in suspension culture. It is the first established cell line which maintains the ability to produce adrenocortical steroids, being a good model for studies of mechanisms underlying adrenal steroidogenesis [192]. The H295 cells were adapted to grow as an adherent culture in a monolayer, thus establishing H295R cell line, which retains the ability to produce mineralocorticoids, glucocorticoids, and adrenal androgens.

The H295R cells characterise with epithelial-like morphology: they are polygonal in shape, having multiple projections and tend to form groups when growing attached to the surface in relatively high density. Some cells present fibroblast-like morphology, being elongated in shape with two or more projections (see **Fig. 3**).

The studies carried out during this research project were approved by the Independent Bioethics Commission for Research at the Medical University of Gdańsk (permission number: NKBBN/342/2012).
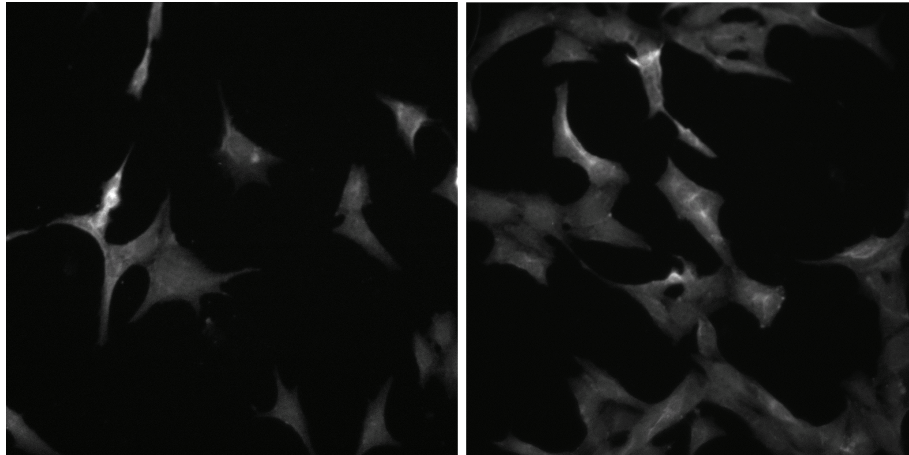
Fig. 3 Morphology of the H295R cells.
Fluorescent images were acquired with fluorescence lifetime imaging microscopy (FLIM) in open microscope systems using anti-EGFR antibody labelled with Alexa546 [193].

3.2. Cell culture

3.2.1. Cell culture conditions

H295R cells were cultured according to previously described protocol [148] (complying with ATCC recommendations). The cell culture was initiated with thawing the cryopreserved cells and adding the cell suspension into the medium in culture flask. H295R cells were cultured in DMEM/F-12 medium (HyClone) supplemented with:

- 2.5% NuSerum (BD BioSciences),

- 2mM L-glutamine (L-Glutamine 200 mM (100x), PAA),

- 100 U/ml penicillin and 100 µg/ml streptomycin (Penicillin-Streptomycin 100x Solution, HyClone), and

- 10 mg/L insulin, 5.5 mg/L transferrin, and 67 µg/ml sodium selenite (Insulin-Transferrin-Selenium (ITS-G) 100x, Gibco).

Cell culture was maintained in the culture vessels (e.g. flasks, Petri dishes, multi-well plates) at 37°C in a humidified 5% CO_2 atmosphere. Cells were used for experiments between the passage 3 and 8. Cells handling was performed inside the class II laminar flow cabinet.

3.2.2. Sub-culturing

The medium was renewed every 3-4 days. Every 5-8 days (depending on confluence level), cells were harvested, counted and sub-cultured, following the protocol:

1) Remove and discard conditioned medium;

2) Rinse the cell layer with PBS to remove remains of serum (which contains trypsin inhibitor);

3) Add trypsin solution (1x) (Gibco) in amount sufficient to cover the culture surface (i.e. 3 ml for 75cm^2 culture flask);

4) Place cell culture vessel in incubator for 5-15 min. (checking visually with light microscope to see if the cells are detached from the surface);

5) Aspirate cells by gently pipetting fresh medium and transfer the cell suspension to conical tube;

6) Centrifuge – 1200 rpm, 4 min.;

7) Discard supernatant and resuspend cell pellet in fresh medium;

8) Count cells in a FastRead disposable counting slide (Immune Systems);

9) Seed accordingly in cell culture vessels for the experiments and to keep up the cell culture (at the subculture ratio between 1:4 and 1:6).

3.2.3. Cryopreservation

To obtain the cryovial with cells that can be stored for longer period in cryogenic storage, the following protocol was carried on:

1) Harvest cells (see: **3.2.2 Sub-culturing 1-6**);

2) Discard supernatant and resuspend cell pellet in the ice-cold cryopreservation medium (complete medium with 30% Nu-Serum);

3) Distribute cell solution to labelled cryogenic vials (900 µl each);

4) Add 100µL of DMSO (dimethylsulfoxide) to each cryovial (10% DMSO) and shake off each of them;

5) Place cryovials in the cooled isopropanol chamber, Mr. Frosty Freezing Container (Thermo Scientific);

6) Store cryovials in Mr. Frosty for at least 3 hours in -80°C;

7) Transfer cryovials to liquid nitrogen and store them in the gas phase above the liquid nitrogen (-196°C).

3.2.4. Cell line quality control (testing for *Mycoplasma* contamination)

Mycoplasma species are common contaminants of the laboratory-based cell cultures. *Mycoplasma* is a genus of very small-cell bacteria that lack the cell wall. The main problems caused by *Mycoplasma* contamination are their impact on cell morphology, metabolism, growth and viability as well as difficulties with detection, both with naked eye and classic light microscope. One of the techniques developed to detect *Mycoplasma* contamination is MycoAlert™ Mycoplasma Detection Kit (Lonza). It is based on a biochemical reaction specifically catalysed by mycoplasmal enzymes. The NCI-H295R cell line used was confirmed to be *Mycoplasma*-free.

3.3. Compounds

Stock solution (10 mM) of mitotane ((2,4′-Dichlorodiphenyl)dichloroethane; o,p'-DDD) (Santa Cruz Biotechnology) was made in ethanol. Everolimus (RAD001) and NVP-BEZ235 were kindly provided by Novartis, Switzerland within the grant "Bridge" (POMOST/2012-5/3) to Dr Dorota Dworakowska, entitled "Pre-clinical targeting of PI3K/Akt/mTOR and RAF/MEK/ERK signaling pathways in adrenocortical cancer: impact on steroidogenesis, cell proliferation and apoptosis", co-financed by the Foundation for Polish Science and European Union. LY294002 was obtained from Jena Bioscience, and U0126 – from Calbiochem. Stock solutions (10 mM) were made in DMSO. Stock solution of EGF (100 μg/ml, Sigma) was made in PBS (Gibco). Aliquots of stock solutions were stored at –20°C. Test dilutions for *in vitro* assays were prepared in PBS (Gibco). Final concentration of DMSO in cell cultures was kept below 0.1% to avoid the effect of DMSO on the cells.

PI3K/Akt/mTOR and Ras/Raf/MEK/ERK inhibitors characterise with relatively short half-life: everolimus (RAD001) – 30 hours, NVP-BEZ235 (BEZ235) – 3.5-13.5 hours, LY294002 – up to 15 minutes, U0126 – 2 hours (**Tab. 4**). Mitotane has relatively long half-life of 18-159 days (based on circulating plasma levels).

Tab. 4 Summary of used compounds.

Compound	Protein(s) directly inhibited	Half-life
Everolimus (RAD001)	mTOR (both mTORC1 and mTORC2)	30 h
NVP-BEZ235 (BEZ235)	PI3K, mTOR (both mTORC1 and mTORC2)	3.5 – 13.5 h
LY294002	PI3K (catalytic domain p110)	< 15 min.
U0126	MEK1/2	2 h
Mitotane	N/A	18 – 159 days

3.4. Cell viability Resazurin assay

The Resazurin cell viability assay (also known under the commercial name as the Alamar Blue assay) is based on the ability of metabolically active living cells to reduce the non-fluorescent blue dye resazurin to the strongly fluorescent pink dye resorufin (**Fig. 4**). Continued cell growth preserves a reduced environment, while growth inhibition results in an oxidized environment. The oxidized form of dye, resazurin, is an intermediate electron acceptor in the electron transport chain, not interfering with the normal electrons transfer processes. The irreversible reduction (oxygen is removed and replaced by hydrogen) of resazurin to resorufin occurs inside the cells and is probably as a result of the action of several different redox enzymes, localised in mitochodria, cytosol, and microsomes, such as mitochondrial reductases, diaphorases, NAD(P)H:quinone oxidoreductase, and flavin reductase. It has been reported that $FADH_2$, $FMNH_2$, NADH, NADPH, and cytochromes may reduce resazurin. Accepting the electrons, the dye changes from the blue, oxidized, non-fluorescent state to the pink, reduced, fluorescent one [194].

The quantity of produced resazurin may indicate various changes in cell metabolism (not only resulting from mitochondrial dysfunction) and is proportional to aerobic respiration and thus to the number of viable cells. It is captured by proportional absorbance/fluorescence output detected by spectrophotometer/ fluorometer [195]. Absorbance detection is far less sensitive than fluorescence measurement and for this reason the latter one was used in this project.

As shown in **Fig. 5**, expected correlation between cell number and fluorescence output was observed in H295R cells used in this project. The saturating effect was seen and for this reason the seeding density of $5*10^3$ cells/100µl was used, as it lies within the linear range for this correlation.

The resazurin working solution was obtained by dissolving the resazurin powder (7-Hydroxy-3H-phenoxazin-3-one 10-oxide, sodium salt, Acros Organics) in PBS at the concentration of 440 µM. The resazurin solution was then filter-sterilized using 0.2 µm filter; its aliquots were stored at −20°C.
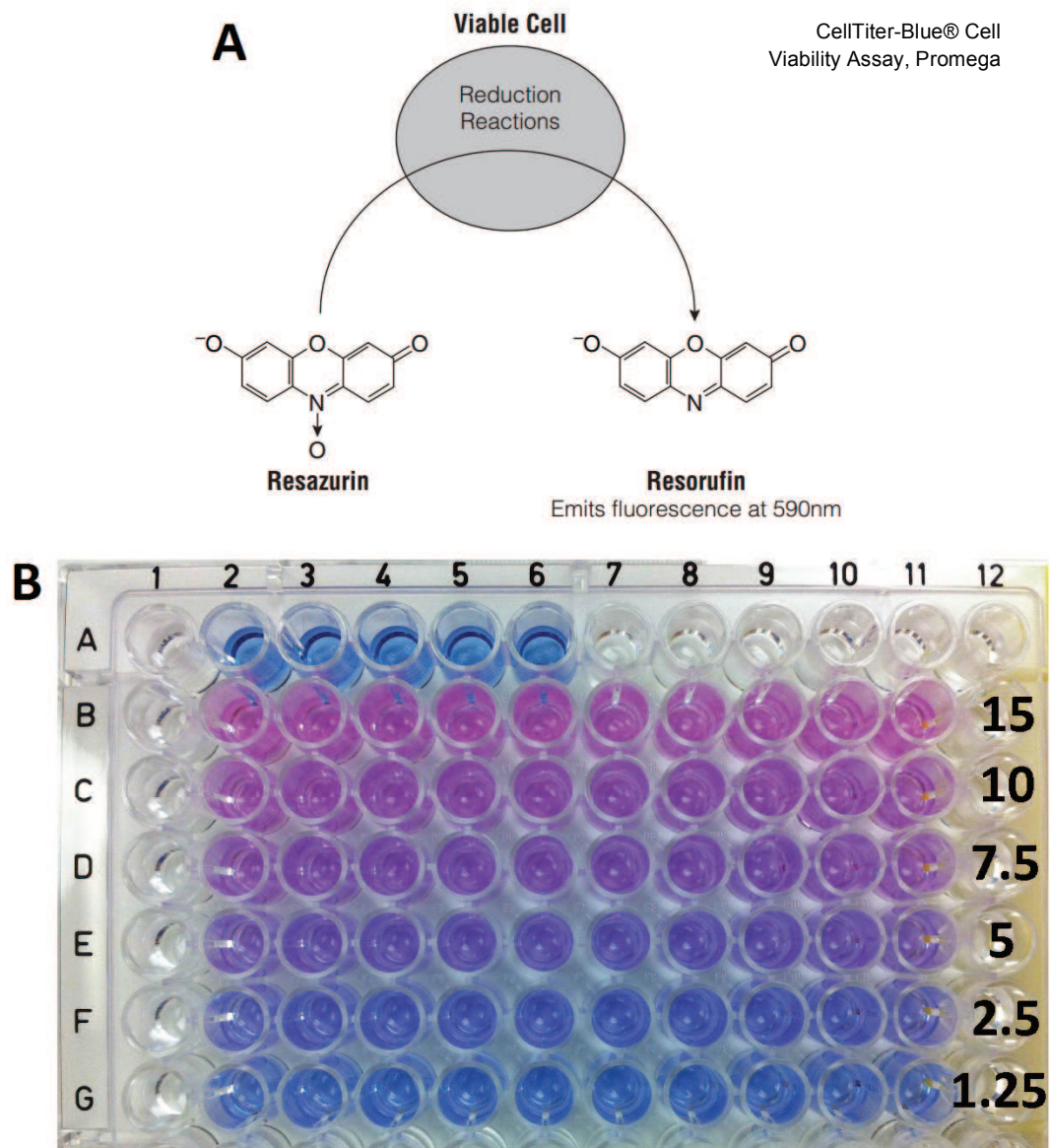
Fig. 4 Resazurin cell viability assay.
A Principle underlying the assay is the ability of viable cells to reduce the non-fluorescent blue dye resazurin to the strongly fluorescent pink dye resorufin (sourced from manufacturer's protocol, CellTiter-Blue® Cell Viability Assay, Promega). **B** Experiment presenting the change of observed solution colour after 4-hour incubation, being proportional to increasing cell numbers (from $1.25*10^3$ to $15*10^3$ seeded cells) 96 hours after seeding.
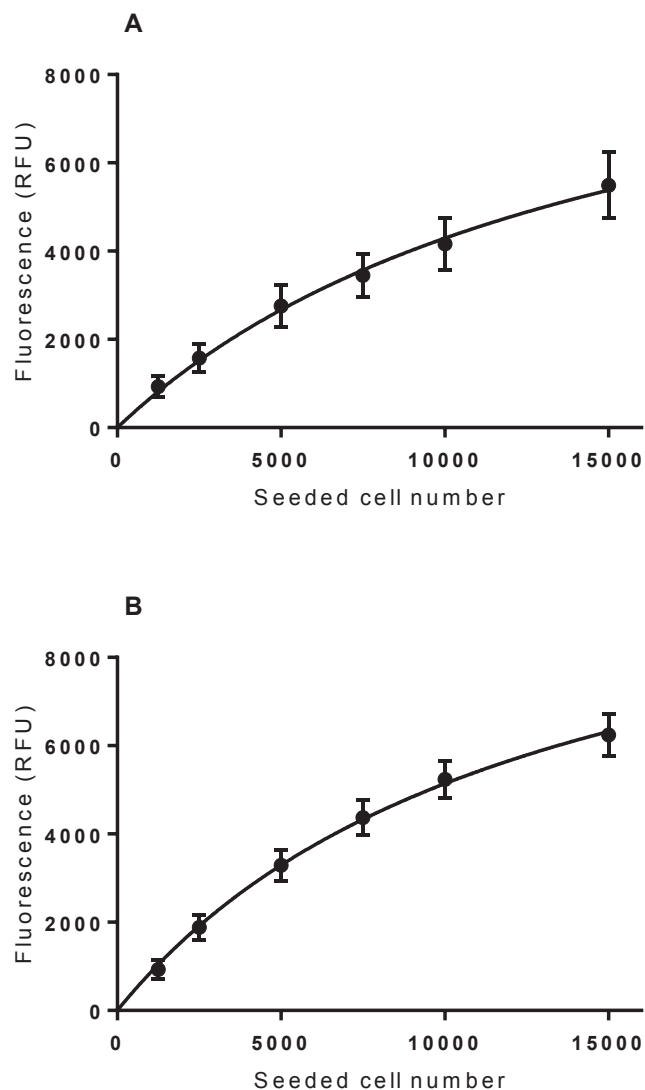
Fig. 5 Resazurin assay in H295R cells.
The fluorescence output corresponding to resazurin reduction by viable cells is proportional to the number of seeded cells in 96-well plates. The measurement was captured 48 hours (n=4) (**A**) and 96 hours (n=11) (**B**) after seeding. Fluorescence presented in relative fluorescence units (RFU). Data expressed as mean±SEM.

Cells were seeded in 96-well plates at a density of $5*10^3$ cells/100 μl/well. For cell number-response experiments, cells were seeded at a density between $1.25*10^3$ and $15*10^3$ cells/100 μl/well. They were allowed to grow for 24 hours, then were treated with vehicle (control) or test compounds and returned to the incubator. Optimum time points for dose-response experiments were: 24 hours for mitotane, 72 hours for U0126, everolimus (RAD001), NVP-BEZ235, and LY294002, repeated

every 24 hours for the latter three compounds. After the indicated time, resazurin working solution (10 μl/well) was added to each well and incubated for a further 4 hours at 37°C. The fluorescence was measured using a plate reader (POLARstar Galaxy, BMG LabTechnologies) at excitation wavelength 544 nm and emission wavelength 590 nm to obtain the relative fluorescent units (RFU). Each experimental group consisted of quintuplicates and was repeated in at least three independent experiments. The fluorescence output (in relative fluorescence units, RFU) for experimental groups was normalized to the output of blanks (medium only). Cytotoxicity (%), the opposite of viability rate, was calculated as shown on equation below:

$$Cytotoxicity\ (\%) = 1 - \frac{normalized\ mean\ RFU\ of\ treated\ sample}{normalized\ mean\ RFU\ of\ controls} * 100\%$$

3.5. Caspase-3-like activity assay

Apoptosis, caspase-dependent programmed cell death, when triggered by extracellular or intracellular death signals, is mediated by cascade of initiator-executioner caspases – cysteine peptidases, proteolytic enzymes – which cleave particular proteins located in the cytoplasm and nucleus at specific aspartic acids sites. The cascade initiators, activated by various death stimuli, include caspase-8, -9, -10 and, -12, which cleave and activate downstream caspases-3, -6, and -7.

Caspase-3 is activated by both caspase-8 and caspase-9, being a convergence point for intrinsic and extrinsic apoptosis activation, and thus serving as a perfect indicator of its initiation in cells. Activated caspase-3 cleaves PARP, poly(ADP-ribose) polymerase, a DNA repair enzyme, at a specific site with the upstream amino acid sequence of DEVD (Asp-Glu-Val-Asp).

To determine caspase activity a specific caspase-3 substrate, Ac (N-acetyl)-DEVD-AMC (7-amino-4-methylcoumarin) (Enzo Life Sciences), was used. The DEVD tetrapeptide sequence is recognized as well by caspase-1, -4, -7 and -8 and their activity will also be detected by this assay; however caspase-3 cleaves at this site

with the highest efficiency among those enzymes. The intact peptide-coumarin conjugate is non-fluorescent, but when the DEVD peptide is cleaved by an active caspase present in lysates of apoptotic cells, the resulting product is fluorescent (**Fig. 6**). The amount of AMC released in the reaction is measured by spectrofluorometer and is directly proportional to the amount of active enzyme present in cell extracts, since substrate is added in excess to the reaction, and that in turn is directly proportional to the number of apoptotic cells in the sample.
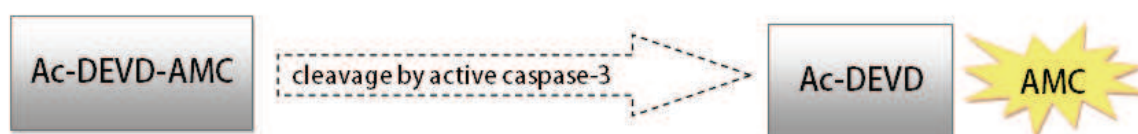
Fig. 6 Caspase-3-like activity assay.
The rationale behind the caspase-3-like activity assay, which is based on the release of fluorescent product upon the cleavage by active caspase-3.

Caspase-3-like activity was assessed in cell extracts according to a previously described protocol [196] with slight modifications. The cells were seeded in 6-cm dishes at a density of $6*10^5$ cells/4 ml/dish. Cells were allowed to grow for 24-72 hours. For mitotane time-response experiments, the mitotane treatment (10 μM) was applied at specified time-points (between 0.5 and 48 hours) prior to harvesting the cells. For mitotane dose-response, the cells were treated with increasing concentrations of mitotane (5-25 μM) for 5 hours. For other compounds, the following experimental conditions were established. The cells were treated with everolimus (RAD001) (0.06 μM), NVP-BEZ235 (0.01 μM), LY294002 (1 μM) and their combinations. The treatment was repeated every 24 hours with total treatment time of 72 hours.

In the next step, following the indicated treatment time, detached and attached cells were harvested and centrifuged for 2 min at 4,500 × g to obtain cell pellets, which were washed with ice-cold PBS (0.01 M phosphate buffer, 2.7 mM KCl, 137 mM NaCl, pH 7.4), again centrifuged for 1 min at 17,000 × g and resuspended in 100 μl of lysis buffer (130 mM NaCl, 10 mM Tris-HCl, 10 mM phosphate buffer, 10 mM Na-pyrophosphate and 1% Triton-X 100, pH 7.5). After 30 min on ice, cell extracts

were centrifuged for 2 min at 17,000 × g. The supernatants were collected, frozen immediately and kept at −20°C until the assay of enzyme activity. The reaction buffer contained 2 mM dithiothreitol (DTT) and 10% glycerol in 20 mM HEPES buffer (pH 7.5). The fluorogenic substrate, ac-DEVD-AMC, was added just before the reaction to a final concentration of 100 μM. The reaction was started by addition of the reaction buffer (100 μl) to the extract (30 μl containing approximately 20-75 μg of protein) and monitored for 2 hours using a fluorescence plate reader (POLARstar Galaxy, BMG LabTechnologies) at excitation wavelength 390 nm and emission wavelength 460 nm. Caspase-3-like activity was expressed as a ratio between the reaction rate (increase in fluorescence over time) and protein content (in mg) as determined by the BCA Protein Assay Kit (Thermo Scientific Pierce), which enables the quantification of protein concentration in the presence of detergents. Each experimental group consisted of triplicates and was repeated in at least three independent experiments.

3.6. Western Blot

Evaluation of the protein expression profile was performed using Western Blot technique. The cell extracts were obtained according to previously described protocol [197] with slight modifications. The cells were seeded in 6-cm dishes, allowed to grow for 2-3 days and then serum starved for 24 hours. Subsequently, the cells were treated with inhibitors for 1/24 hour; 0.5/1 hour after that treatment, the EGF (100 ng/ml) was applied. After the specific time of treatment, the cells were washed with ice-cold PBS and harvested in 60-100 μl of SDS buffer (100 mmol/L Tris-HCl (pH 6.8), 20% glycerol, 4% SDS), boiled for 15 minutes in 96°C and placed on ice. Samples were kept at −20°C until the next step. Following the protein content determination using the BCA Protein Assay Kit (Thermo Scientific Pierce), the protein concentration was unified in the samples with SDS buffer. Each sample was complemented with 5 μl of 0.2% bromophenol blue (BPB) and dithiothreitol (DTT) to final concentration of 50 mM. Equal amounts of protein for each sample were

separated by SDS polyacrylamide gel electrophoresis and transferred onto nitrocellulose Hybond ECL membranes (GE Healthcare). The primary antibodies to pEGFR-Y1173 (53A5), tEGFR (D38B1), pAkt-T308 (C31E5E), tAkt (9272), p-mTOR-S2448 (D9C2), t-mTOR (7C10), pERK-T202/Y204 (E10), tERK (9102), p-p70S6K-T389 (108D2), and t-p70S6K (49D7) were obtained from Cell Signaling Technology. Antibody to GAPDH (GT239) was obtained from GeneTex, to tubulin (6-11B-1) from Sigma, and to mono- and polyubiquitinylated conjugates, mAb (FK2) from Enzo Life Sciences. The secondary anti-rabbit (P0448) and anti-mouse (P0447) antibodies were obtained from Dako. Bound antibodies were visualized using ECL reagents (Advansta), acquired with G:BOX Chemi (Syngene) and analyzed on a chemiluminescent image analysis software (Imaging and Analysis Software by Bio-Rad, Quantity-One). Each experimental group was repeated in at least three independent experiments.

3.7. Statistical analysis

The data were analysed with GraphPad Prism v6.02 (King's College London licence). The dose-response data are presented as semi-logarithmic curves (true scale indicated to simplify the presentation), plotted using appropriate non-linear regression curve fitting model. The dose-response curves for mitotane, NVP-BEZ235, LY294002, and U0126 were fitted using Variable slope model (compound concentration expressed in logarithmic scale vs. normalized cytotoxic response in percentage), based on the equation:

$$Y = \frac{100}{1 + 10^{(\log EC_{50} - X) * HillSlope}}$$

where X - log of dose or concentration and Y - normalized response, 0 to 100%, increasing as X increases.

The dose-response curve for everolimus (RAD001) was fitted using Asymmetric Sigmoidal 5PL model (also called Richard's five-parameter dose-response curve), based on the equation:

$$Y = min + \frac{max - min}{[1 + 10^{(\log Xb - X) * HillSlope}]^S}$$

where $$\log Xb = \log EC_{50} + \frac{1}{HillSlope} * \log(2^{\frac{1}{S}} - 1) \ ,$$

X - log of dose or concentration, and Y - normalized response, 0 to 100%.

These methods allow determining EC_{50} (half maximal effective concentration) value, which signifies the concentration of a tested compound, which causes a response halfway between the baseline and maximum response (e.g. when a compound is potent enough to exert a total 100% cell cytotoxicity at some dose, EC_{50} will represent its concentration causing 50% decrease in cell viability).

Cell-density response curves were fitted using second order polynomial (quadratic) model, based on the equation:

$$Y = B0 + B1 * X + B2 * X * X$$

The R square (R^2, the coefficient of determination) value quantifies goodness of fit and indicates the correlation with "0" signifying no correlation and "1" – complete correlation.

To compare each experimental group with the control, the One-Way analysis of variance (abbreviated as One-Way ANOVA) was performed, followed by appropriate *post hoc* testing (Bonferroni correction for comparison between control and treatment groups; Tukey test for multiple comparisons between each experimental group with every other one). The data are expressed as mean ± standard error of the mean (SEM). Results were considered significant when $p<0.05$ and the following gradation was applied: ***$p<0.001$, **$p<0.01$, *$p<0.05$.

4. Results

4.1. Growth rate of H295R cells

The observed rate of growth of the H295R cells in applied conditions (as described in **3.2.1 Cell culture conditions**) is presented in **Fig. 7**. Calculated doubling time equals 93.68 hours.
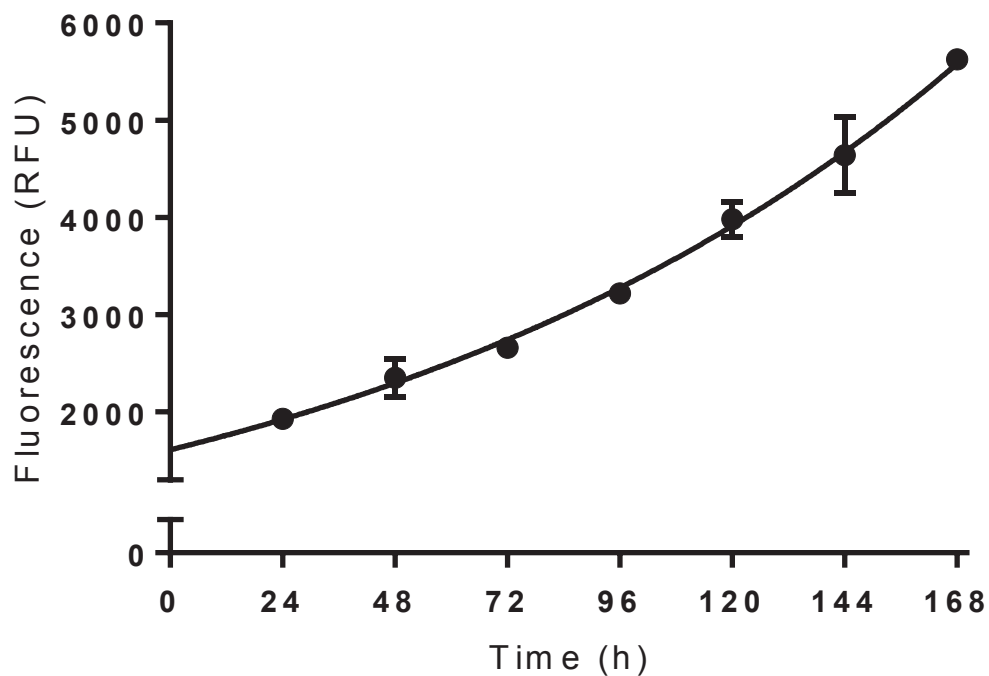
Fig. 7 The growth rate of H295R cells.
Measurements captured with resazurin assay between 24 and 168 hours from seeding. Cells were seeded in quintuplicates in 96-well plates at the density of $5*10^3$/well/100µl (n=3). Fluorescence is presented in relative fluorescence units (RFU). Data expressed as mean±SEM.

4.2. Dose-response and cell density-dependent response of selected PI3K/mTOR and MEK inhibitors in H295R cells

The main aim of the initial experiments was to establish the dose-response and cell density-dependent response of the H295R adrenocortical carcinoma cells to mitotane, everolimus (RAD001), NVP-BEZ235, LY294002, and U0126. These results were the basis for further evaluation of synergistic combinations and selection of optimal doses for short- and long-term treatment regime in experiments employing caspase-3-like activity assay and Western Blot technique.

To assess the dose-response of the H295R cell line to mitotane, the cells were treated for 24 hours with increasing concentrations of mitotane and then the cell viability was assessed by the Resazurin assay. Mitotane proved to be a very potent proliferation inhibitor in H295R cells, reaching total cytotoxic effect already at a dose of 20 μM (**Fig. 8A**). Treatment with 10 μM mitotane resulted in significant cytotoxic effect of 21.0±0.98% and with 15 μM – 72.18±3.87%. The calculated EC_{50} value for mitotane in these experiments was 12.57 μM. Cell density-dependent response, presented in **Fig. 8B**, indicate that the response of H295R cells to mitotane slightly depends on the cell number (R^2=0.23). Upon treatment with 10 μM mitotane, adrenocortical H295R cells presented 48.69±7.95% cytotoxicity at the lowest number of seeded cells ($1.25*10^3$/well) and 17.93±3.43% at the highest one ($15*10^3$/well), responses being significantly different from each other (p≤0.0001).

Everolimus (RAD001) proved to decrease the cell viability of H295R to a limited extent. The highest cytotoxicity values observed were 16.87±1.91% and 15.1±1.12% at the dose of 0.5 and 1 μM, respectively (**Fig. 9A**). At the lowest applied dose of everolimus, 0.01 μM, the significant cytotoxicity of 4.57±1.03% was obtained (n=3, p<0.05). The calculated EC_{50} for everolimus (RAD001) in these experiments was 15.95 nM. Cell density-dependent response experiments indicated that the response of H295R cells to everolimus was independent of the cell number (R^2=0.05), reaching between 9.5±0.54% and 14.03±1.18% for $15*10^3$ and $2.5*10^3$ seeded cells per well, respectively (**Fig. 9B**).

A Mitotane decreases cell viability of the H295R cells in a dose-dependent manner. Cells were seeded at the density of $5*10^3$/well/100 µl in 96-well plates. The effect was captured 24 hours after mitotane treatment (n=6, *p*<0.001). **B** Mitotane effect decreases slightly at a higher cell density. The H295R cells were treated with 10 µM mitotane for 24 hours (n=4). Data expressed as mean±SEM.

Fig. 8 Antiproliferative effect of mitotane in the H295R cells**.**

A

B

Fig. 9 Antiproliferative effect of everolimus in the H295R cells**.**
A Everolimus decreases cell viability of the H295R cells in a dose-dependent manner. Cells were seeded at the density of $5*10^3$/well/100 μl in 96-well plates. The effect was captured 72 hours after first treatment, new dose was administered each 24 hours (n=3, *p*<0.001). **B** Everolimus effect is independent of cell density. The H295R cells were treated with 0.06 mM everolimus for 72 hours, new dose was administered each 24 hours (n=3). Data expressed as mean±SEM.

NVP-BEZ235 (BEZ235) shows significant cytotoxicity in the H295R cells, starting from the dose of 0.1 μM with 7.8±1.3% cytotoxicity (**Fig. 10A**). At the highest applied dose, 5 μM, the significant cytotoxicity of 58.9±1.5% was obtained (n=3, p<0.001). The calculated EC_{50} value for NVP-BEZ235 (BEZ235) in these experiments was 2.42 μM. Cell density-dependent response experiments indicated that the response of the H295R cells to NVP-BEZ235 (BEZ235) was independent of the cell number (R^2=0.13), reaching between 3.25±0.92% and 8.28±0.62% for $15*10^3$ and $5*10^3$ seeded cells per well, respectively (**Fig. 10B**).

LY294002 shows significant cytotoxicity in the H295R cells, starting from the dose of 5 μM with cytotoxicity of 21.98±2.44% (**Fig. 11A**). At the highest applied dose, 40 μM, the significant cytotoxicity of 73.17±1.06% was obtained (n=4, p<0.001). The calculated EC_{50} value for LY294002 in these experiments was 17.23 μM. Cell density-dependent response experiments indicated that the response of the H295R cells to LY294002 was independent of the cell number (R^2=0.14), reaching between 3.08±0.72% and 6.98±0.66% for $15*10^3$ and $10*10^3$ seeded cells per well, respectively (**Fig. 11B**).

U0126 shows significant cytotoxicity in the H295R cells, starting from the dose of 1 μM with cytotoxicity of 7.49±0.51% (**Fig. 12A**). At the highest applied dose, 40 μM, the significant cytotoxicity of 93.26±0.85% was obtained (n=8, p<0.001). The calculated EC_{50} value for U0126 in these experiments was 15.41 μM. Cell density-dependent response, presented in **Fig. 12B**, indicate that the response of the H295R cells to U0126 depends on the cell number (R^2=0.62). Upon treatment with 5 μM U0126, adrenocortical H295R cells presented 27.79±1.38% cytotoxicity at the lowest number of seeded cells ($1.25*10^3$/well) and 12.72±1.19% at the highest one ($15*10^3$/well), responses being significantly different (p≤0.0001).
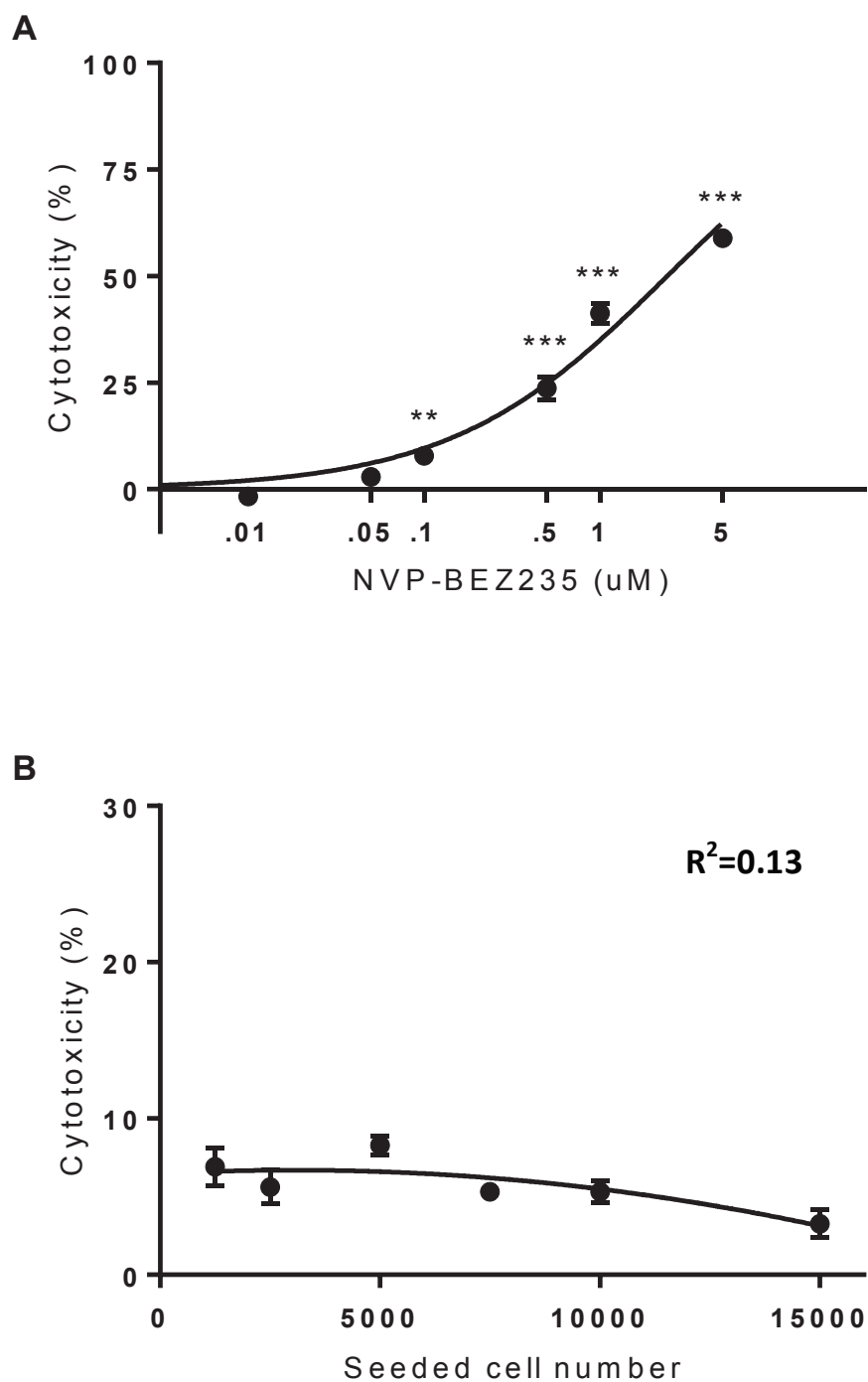
Fig. 10 Antiproliferative effect of NVP-BEZ235 in the H295R cells**.**
A NVP-BEZ235 decreases cell viability of the H295R cells in a dose-dependent manner. Cells were seeded at the density of $5*10^3$/well/100 µl in 96-well plates. The effect was captured 72 hours after first treatment, new dose was administered each 24 hours (n=3, $p<0.001$). **B** NVP-BEZ235 effect is independent of cell density. The H295R cells were treated with 0.01 µM NVP-BEZ235 for 72 hours, new dose was administered each 24 hours (n=3). Data expressed as mean±SEM.

A

B
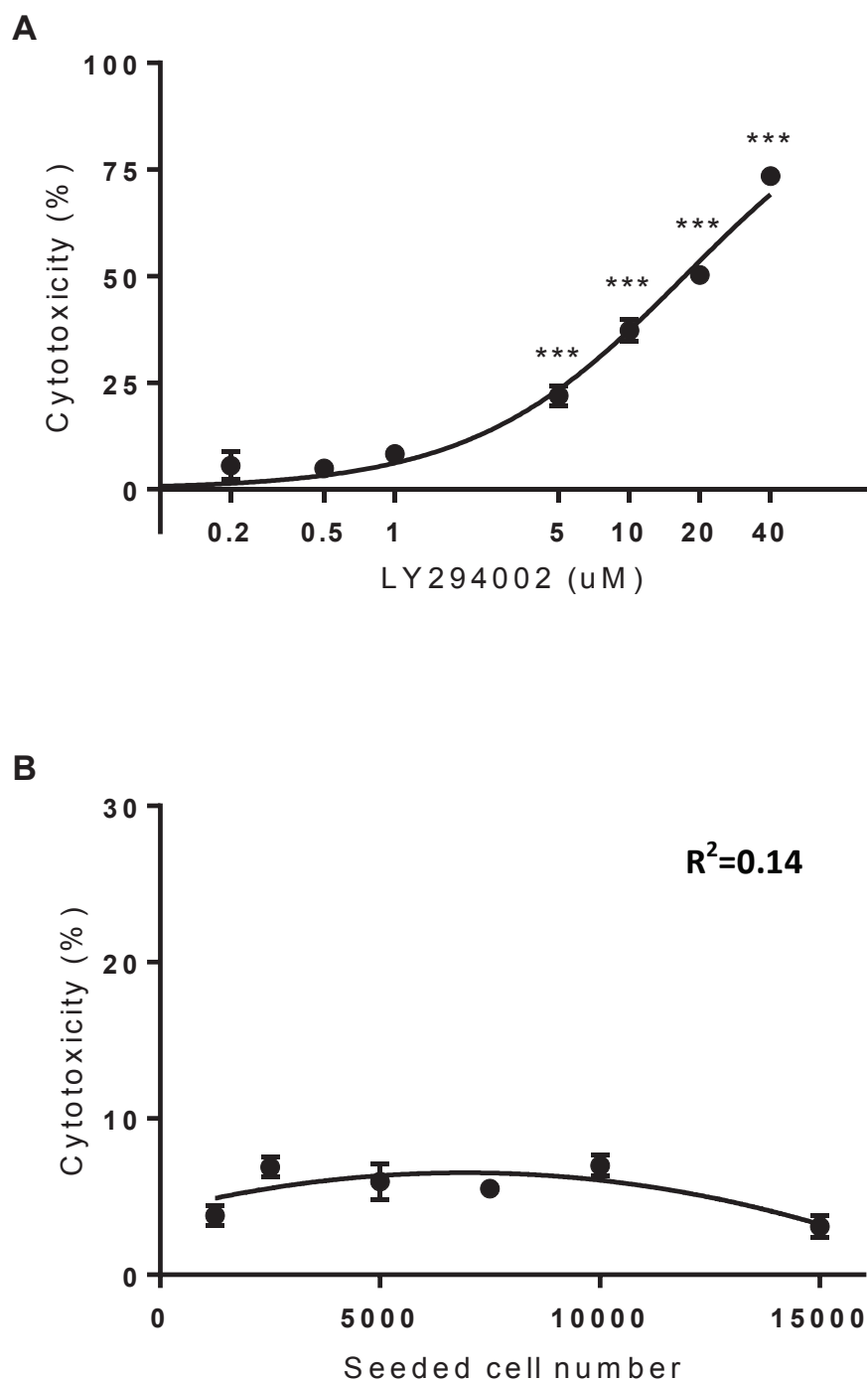
Fig. 11 Antiproliferative effect of LY294002 in the H295R cells**.**
A LY294002 decreases cell viability of the H295R cells in a dose-dependent manner. Cells were seeded at the density of $5*10^3$/well/100 µl in 96-well plates. The effect was captured 72 hours after first treatment, new dose was administered each 24 hours (n=4, $p<0.001$). **B** LY294002 effect is independent of cell density. The H295R cells were treated with 2 µM LY294002 for 72 hours, new dose was administered each 24 hours (n=3). Data expressed as mean±SEM.
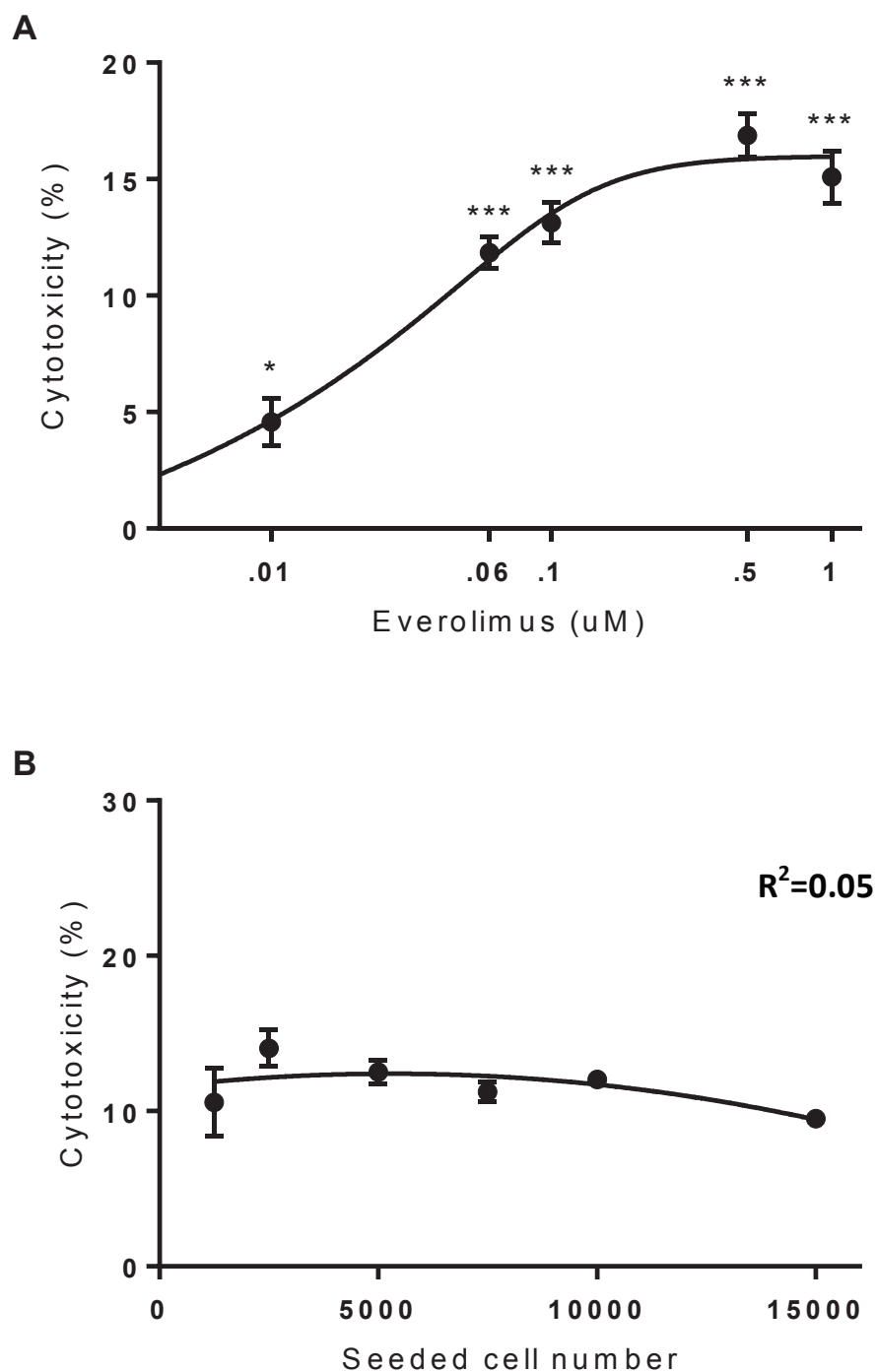
A

B
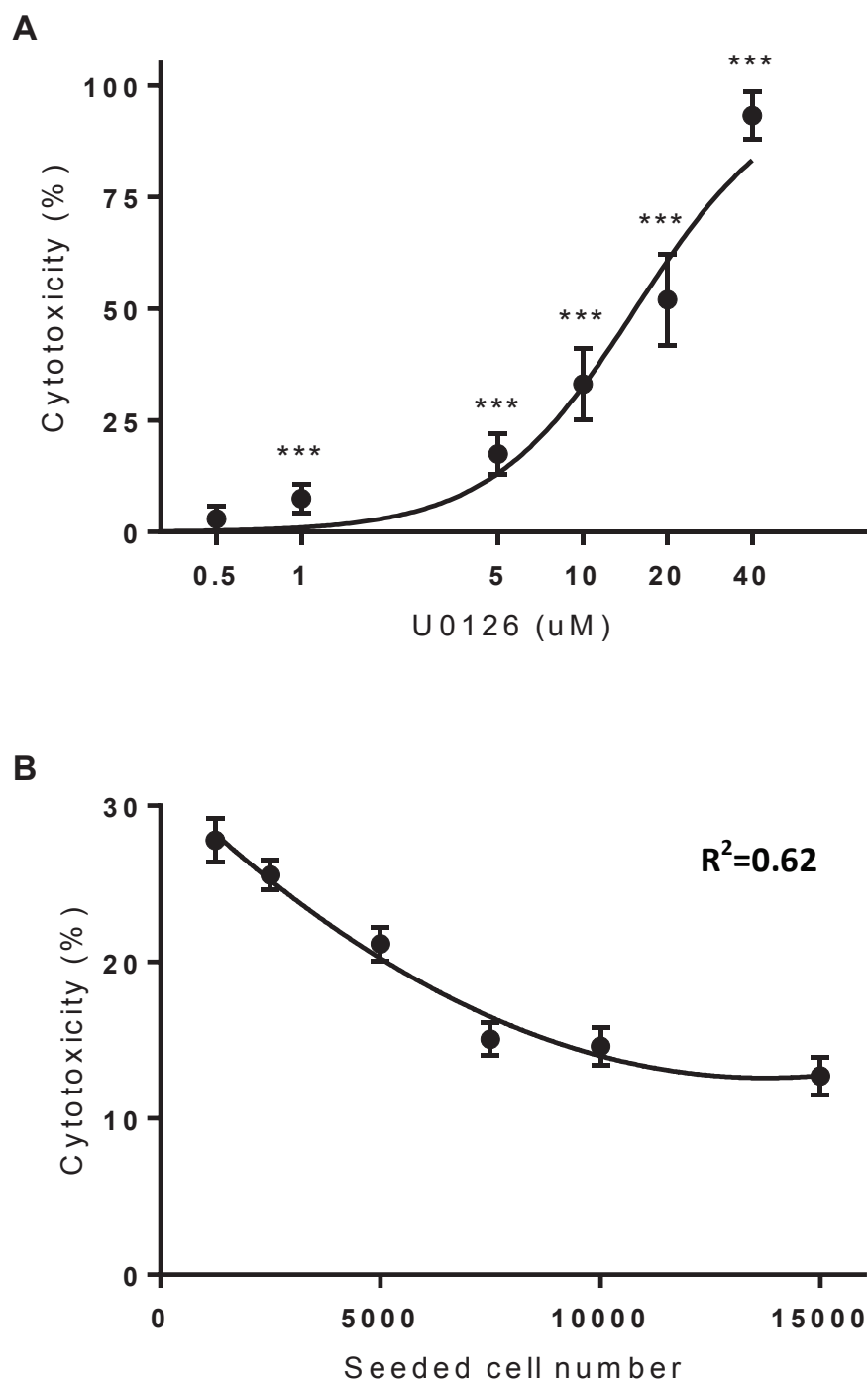
Fig. 12 Antiproliferative effect of U0126 in the H295R cells**.**
A U0126 decreases cell viability of the H295R cells in a dose-dependent manner. Cells were seeded at the density of $5*10^3$/well/100 µl in 96-well plates. The effect was captured 72 hours after treatment (n=8, *p*<0.001). **B** U0126 effect decreases at higher cell density. The H295R cells were treated with 5 µM U0126 for 72 hours (n=3). Data expressed as mean±SEM.

4.3. Combination treatment with PI3K/mTOR and MEK inhibitors and mitotane results in additive effect

Treating with mitotane (10 µM) and one of PI3K, mTOR and MEK1/2 inhibitors: 0.06 µM everolimus (RAD001), 0.01 µM NVP-BEZ235, 1 µM LY294002, or 5 µM U0126 resulted in the additive effect in the tested combinations, meaning that the efficacy of none of these inhibitors was significantly enhanced by addition of mitotane (**Fig. 13**). The results did not indicate a significant synergy in any of those combinations, though the highest efficacy was obtained for combination of mitotane and U0126 with 43.52±5.18% of combined cytotoxic effect (**Fig. 13A**) and 27.43±6.61% cytotoxicity over mitotane (**Fig. 13B**). For everolimus respective combined responses were 35.78±1.94% and 15.66±2.39%; for NVP-BEZ235 – 34.49±2.06% and 11.03±3.02%; for LY294002 – 27.84±1.3% and 4.76±0.87%.

4.4. Combination of everolimus and NVP-BEZ235 results in synergistic effect

Initial experiments have shown that the highest cytotoxicity is obtained with the combination of 0.06 µM everolimus (RAD001), 0.01 µM NVP-BEZ235, and 1 µM LY294002 (**Fig. 14**). These results indicate strong repeatable synergistic effect between everolimus and NVP-BEZ235, meaning that the effect of co-treatment with these drugs is significantly higher than their individual efficacy (added effect). On its own everolimus (RAD001) resulted in 9.54±1.4% cytotoxicity, NVP-BEZ235 – 6.61±1.37%, and LY294002 – 7.44±1.68%. The combination of everolimus and NVP-BEZ235 yielded the cytotoxic rate of 38.43±3.61%, significantly different to calculated added effect of 16.32±2.6% (p=0.012). For the triple combination the cytotoxic rate reached 47.73±4.08%, being significantly different to calculated added effect of 24±5.34% (p=0.019). However, for double combinations with LY294002 such effect was not observed with 20.89±1.9% vs. 17.5±4.61% for co-treatment with everolimus and 19.79±4.14% vs. 14.17±4.42% for NVP-BEZ235.
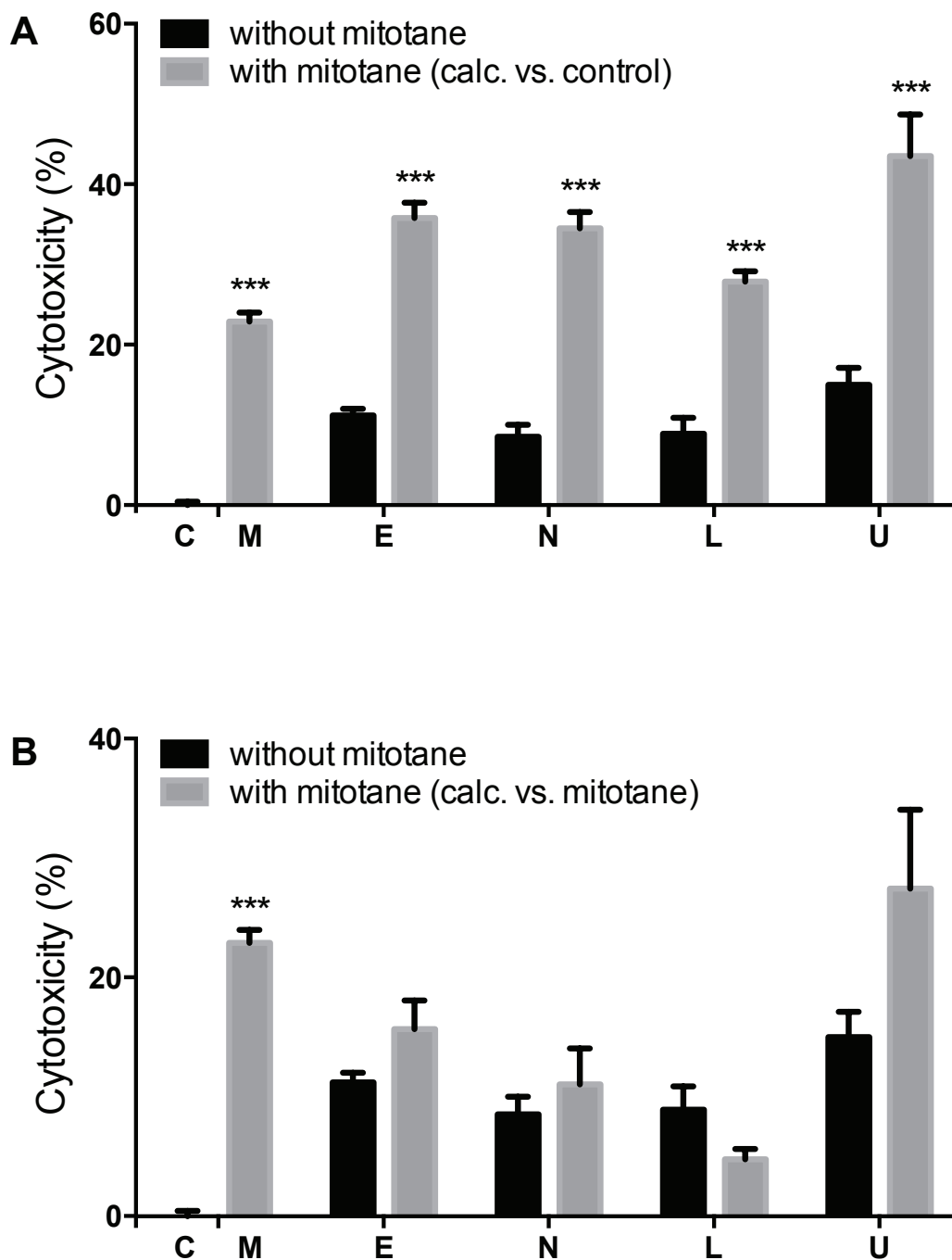
Fig. 13 Combination treatment with mitotane and PI3K, mTOR and MEK1/2 inhibitors.
Treatment with 10 µM mitotane, 0.06 µM everolimus, 0.01 µM NVP-BEZ235, 1 µM LY294002, 5 µM U0126 (n=5). Cells were seeded at the density of $5*10^3$/well/100 µl in 96-well plates. Combination treatment values are normalised to control (**A**) or to mitotane cytotoxicity (**B**). Data expressed as mean±SEM. Abbreviations: **C** - control; **M** - mitotane; **E** - everolimus; **N** - NVP-BEZ235; **L** - LY294002; **U** - U0126.
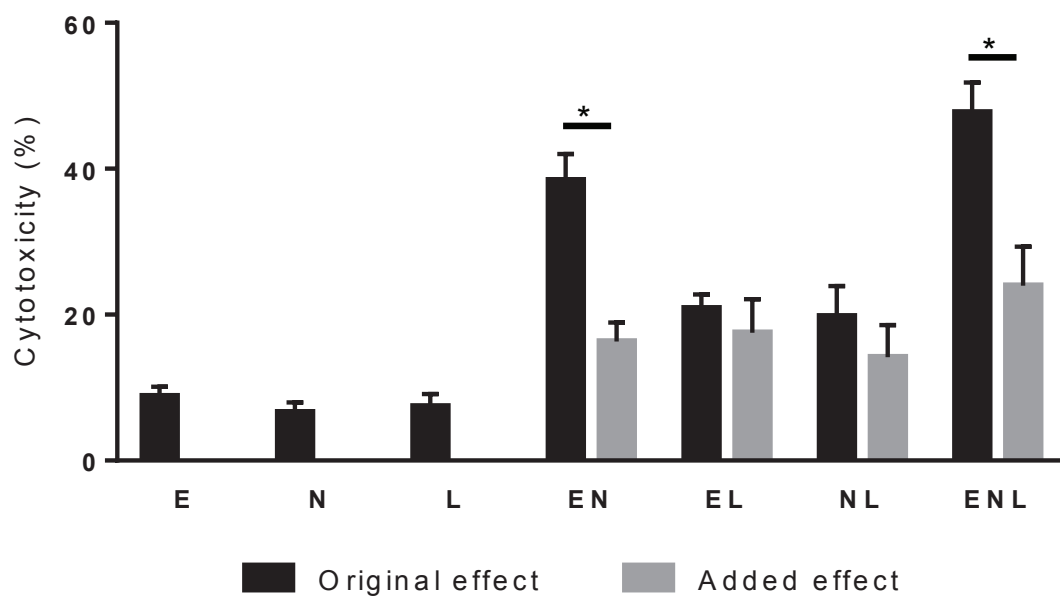
Fig. 14 Combination treatment with everolimus, NVP-BEZ235, and LY294002.

Treatment with combination of 0.06 µM everolimus and 0.01 µM NVP-BEZ235 exerts synergistic effect in the H295R cells 72 hours after treatment (n=4). Triple combination with 1 µM LY294002 does not result in higher synergy, but only additive effect of LY294002. Cells were seeded at the density of $5*10^3$/well/100 µl in 96-well plates. Data expressed as mean±SEM. Abbreviations: **E** - everolimus; **N** - NVP-BEZ235; **L** - LY294002.

4.5. Effect of mitotane and selected PI3K/mTOR inhibitors on caspase-3-like activity in H295R cells

To assess the activation of programmed cell death induced by mitotane and selected PI3K/mTOR inhibitors, the specific caspase-3-like activity was measured in the H295R cells after treatment.

The time- and dose-dependent response to mitotane treatment was assessed. The peak mitotane-induced caspase-3-like activation occurred 1 hour post treatment reaching 3.42±0.25 arbitrary units/mg/min versus control ($p<0.001$) (**Fig. 15 A**), indicating that the majority of caspase-3-like activation occurs very early after mitotane delivery and decreases in time. Standard treatment time used in the cell viability assay was 24 hours and such treatment duration resulted in increase in caspase-3-like activity to 1.6-fold increase over control ($p<0.01$). With regards to protein concentration, it remained roughly the same for all group, being unaffected by duration of treatment with 10 μM mitotane (**Fig. 15 B**).

Mitotane dose-dependent response experiments showed dramatic increase in caspase-3-like activity in H295R cells between the dose of 20 μM and 25 μM with values reaching 2.58±0.3 units/mg/min versus control upon 20 μM mitotane treatment ($p<0.05$) and 8.35±0.29 for 25 μM ($p<0.001$) (**Fig. 16 A**). At the concentration of 10 μM the increase observed reached 1.71±0.03 (**Fig. 16 A**). Protein concentration was unaffected by treatment with 5-20 μM mitotane, dropping significantly only upon treatment with highest dose of 25 μM to 0.73±0.03 mg/ml from control values of 1±0.09 mg/ml ($p<0.01$) (**Fig. 16 B**).

Caspase-3-like activity in response to the individual treatment with 0.06 μM everolimus (RAD001), 0.01 μM NVP-BEZ235, and 1 μM LY294002 was not significantly different from control values, reaching 0.94±0.05, 1.11±0.1, 1.42±0.11 arbitrary units/mg/min versus control, respectively (**Fig. 17A**). For combined treatment, significant increase in caspase-3-like activity was observed for triple combination being 2.22±0.32 ($p<0.001$) and for double combination NVP-BEZ235 with LY294002 - 1.93±0.25 ($p<0.01$). Protein content measurements for samples used in this assay were not significantly affected by any individual treatment, but a

significant decrease was observed for double combination of everolimus with NVP-BEZ235 and for triple combination with addition of LY294002 (**Fig. 17B**).
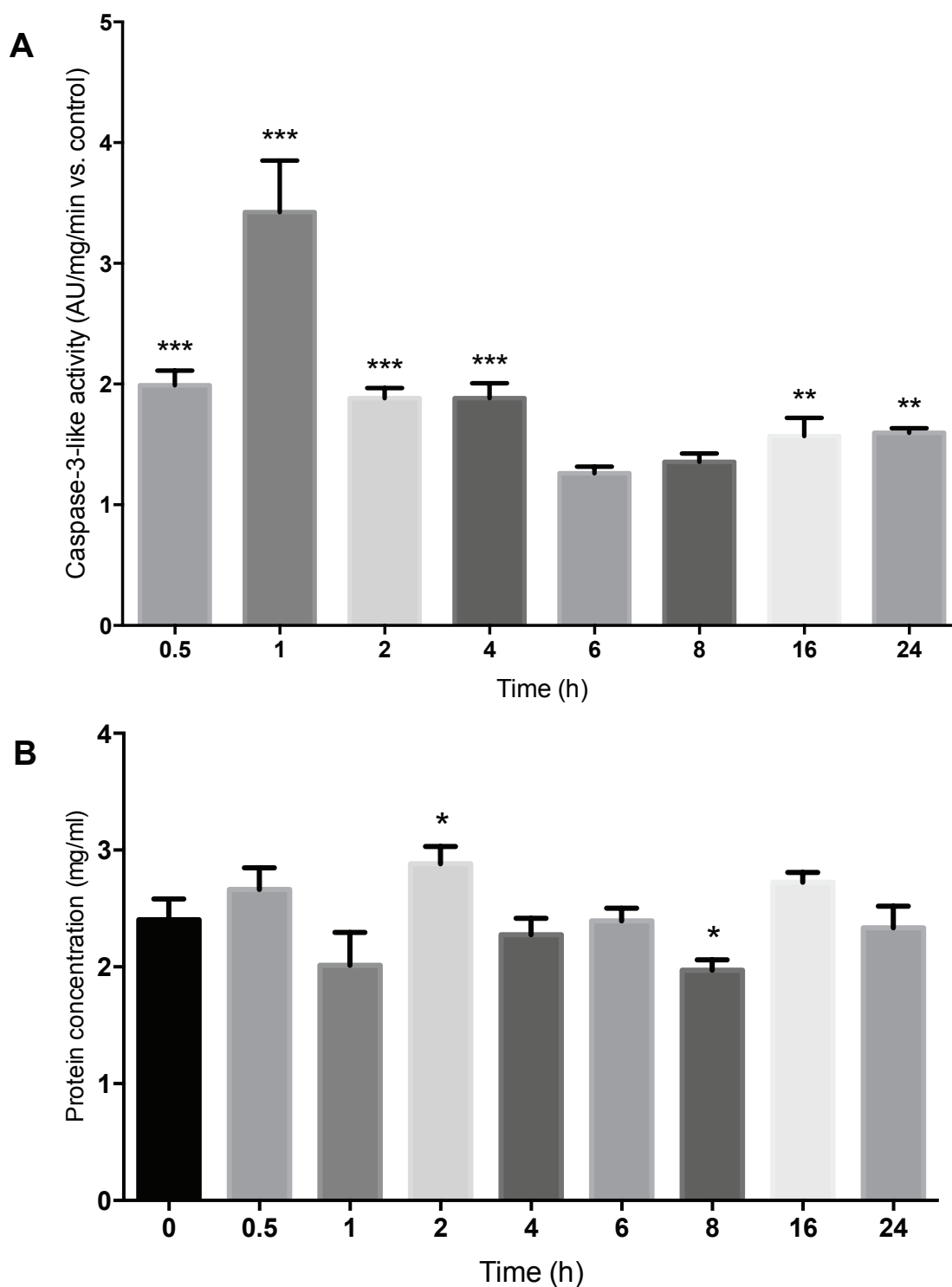
Fig. 15 Caspase-3-like activity - time-dependent response to mitotane.
A Caspase-3-like activity in the H295R cells 0.5-24 hours after treatment with 10 µM mitotane (n=3, representative experiment presented, expressed in arbitrary units (AU)/mg of protein/min). **B** The effect of the mitotane treatment on protein concentration. Data expressed as mean±SEM.
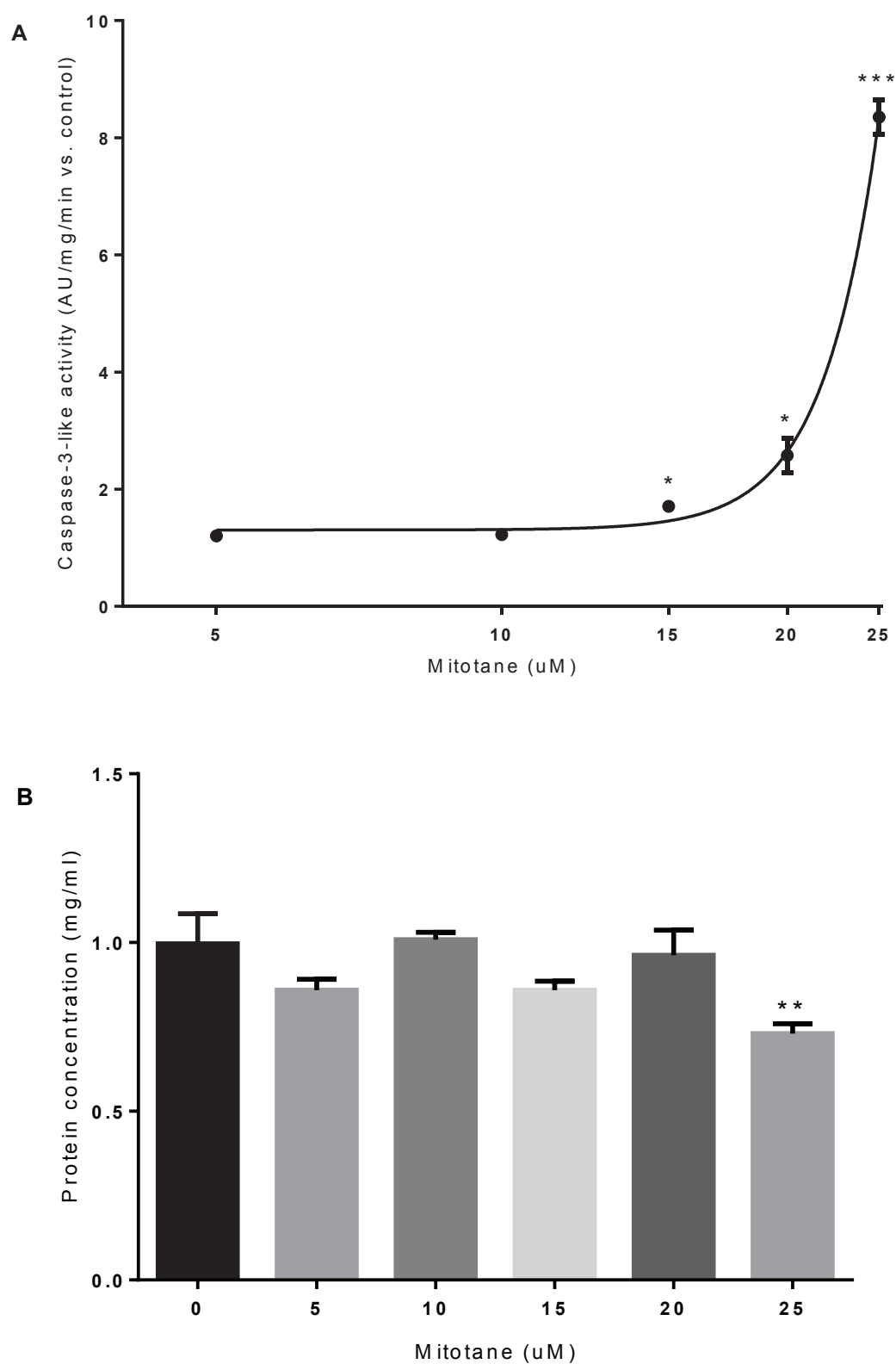
Fig. 16 Caspase-3-like activity - dose-dependent response to mitotane.
A Caspase-3-like activity in the H295R cells 5 hours after treatment with 5-25 µM mitotane (n=3, expressed as a ratio of control in arbitrary units (AU)/mg of protein/min). **B** The effect of the mitotane treatment on protein concentration. Data expressed as mean±SEM.
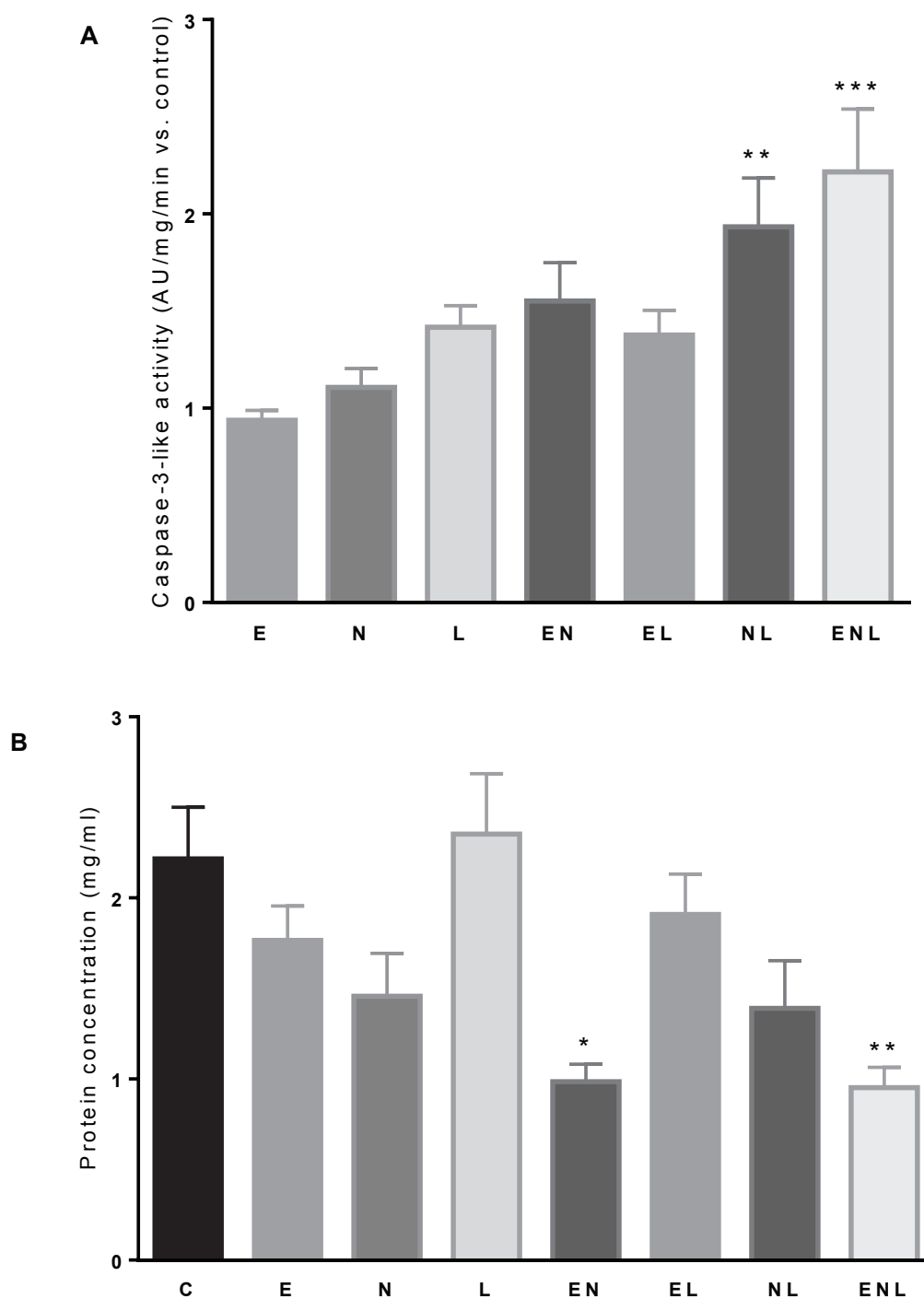
Fig. 17 Caspase-3-like activity in response to combination treatment with everolimus, NVP-BEZ235, and LY294002.

A Caspase-3-like activity in the H295R cells 72 hours after treatment with everolimus (**E**), NVP-BEZ235 (**N**), LY294002 (**L**) and their combinations (n=4, expressed as a ratio of control in arbitrary units (AU)/mg of protein/min). **B** The effect of the treatment on protein concentration. Data expressed as mean±SEM.

4.6. Effect of selected PI3K/mTOR and MEK1/2 inhibitors on protein expression in H295R cells

Western Blot technique was used to assess the effect on protein expression in the H295R cells after the treatment with selected PI3K, mTOR and MEK1/2 inhibitors: everolimus (RAD001), NVP-BEZ235 (BEZ235), LY294002, and U0126. EGF stimulation in H295R cells was more pronounced in a short-term design (0.5 hour), resulting in 11.2-fold EGFR activation, when compared to a long-term one (2.21-fold) (**Fig. 18**). What is interesting, the phospho-specific EGFR^{Y1173} levels were slightly higher, but total EGFR level was significantly decreased after EGF stimulation, indicating increase in degradation processes upon the EGFR activation.
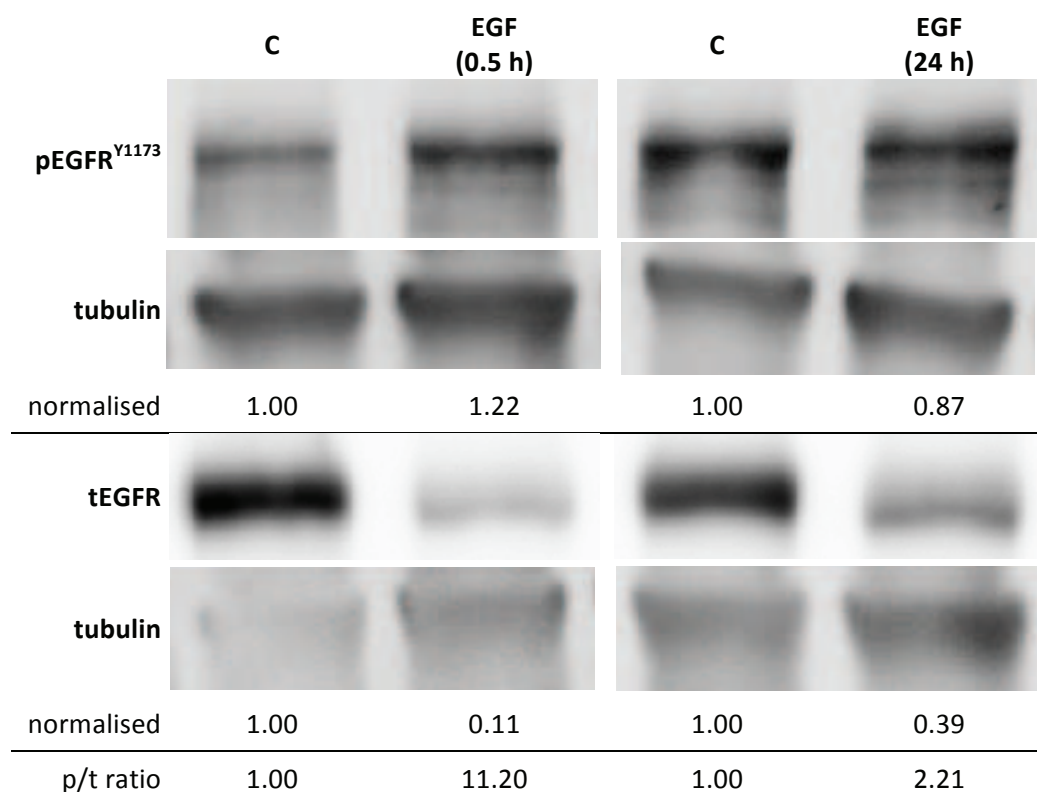
Fig. 18 Protein expression of EGFR after short- and long-term EGF stimulation.
The adrenocortical H295R cells were treated with EGF either for 0.5 hour or for 24 hours. Normalised values represent original results normalised to housekeeping gene and then to control. p/t ratio represents the value for the phospho-specific antibody divided by the value for the total antibody.

Three repeats of Western Blot experiments has been performed to assess the protein expression changes upon the treatment with everolimus (RAD001), NVP-BEZ235 (BEZ235), LY294002, U0126, or selected combinations of these inhibitors. However, high variability was observed; therefore only for some proteins conclusive evidence was obtained.

Both short- (1 hour) and long-term (24 hours) treatment with NVP-BEZ235 resulted in decreased expression of phospho-Akt^{T308} as well as increased levels of phospho-EGFR^{Y1173} in comparison to control with increased levels of total EGFR, contrary to EGFR activation by EGF (**Fig. 19** – short-term, **Fig. 21** – long-term). It may suggest that NVP-BEZ235 blocks degradation processes of activated, phosphorylated EGFR, maintaining increased levels of both phosphorylated and total EGFR.

Both everolimus and NVP-BEZ235 and their combination decreased the expression of phospho-p85S6K^{T412}, phospho-p70S6K^{T389}, and total p70S6K, but increased the phospho-ERK$^{T202/Y204}$ levels (**Fig. 19**). Long-term treatment with NVP-BEZ235 resulted in inverted effect for total p70S6K as well as in pronounced increase in total ERK levels (**Fig. 21**). The everolimus and NVP-BEZ235 combination treatment increased the expression of phospho-EGFR^{Y1173}, but decreased phospho-Akt^{T308} (**Fig. 19**).

The effect of NVP-BEZ235 on the ubiquitin-dependent selective protein degradation was assessed using antibody specific to mono- and polyubiquitinylated conjugated. That exploratory experiment has confirmed that NVP-BEZ235 significantly decreases protein ubiquitination processes (**Fig. 20**).

Treatment with U0126 decreased the expression of phospho-p70S6K^{T389} and phospho-ERK$^{T202/Y204}$, but increased their respective total levels (**Fig. 21**). The combination treatment with U0126 and NVP-BEZ235 resulted in decreased levels of both phospho-EGFR^{Y1173} and total EGFR in a way reverting the effect of NVP-BEZ235 mono-treatment. This co-treatment decreased as well phospho-mTOR^{S2448}, phospho-p85S6K^{T412}, phospho-p70S6K^{T389}, and phospho-Akt^{T308} (**Fig. 21**).

LY294002 decreased the expression of phospho-mTOR^{S2448}, phospho-p85S6K^{T412}, phospho-p70S6K^{T389}, but increased total ERK levels (Fig. X3).

B - #2

C - #3

	C	EGF	EVE	NVP	EVE+NVP	EGF+ EVE+NVP
tubulin (m1)						
tubulin (m2)						
pEGFR						
tEGFR						
p-mTOR						
t-mTOR						
p-p85S6K						
t-p85S6K						
p-p70S6K						
t-p70S6K						
pAkt						
tAkt						
pERK						
tERK						
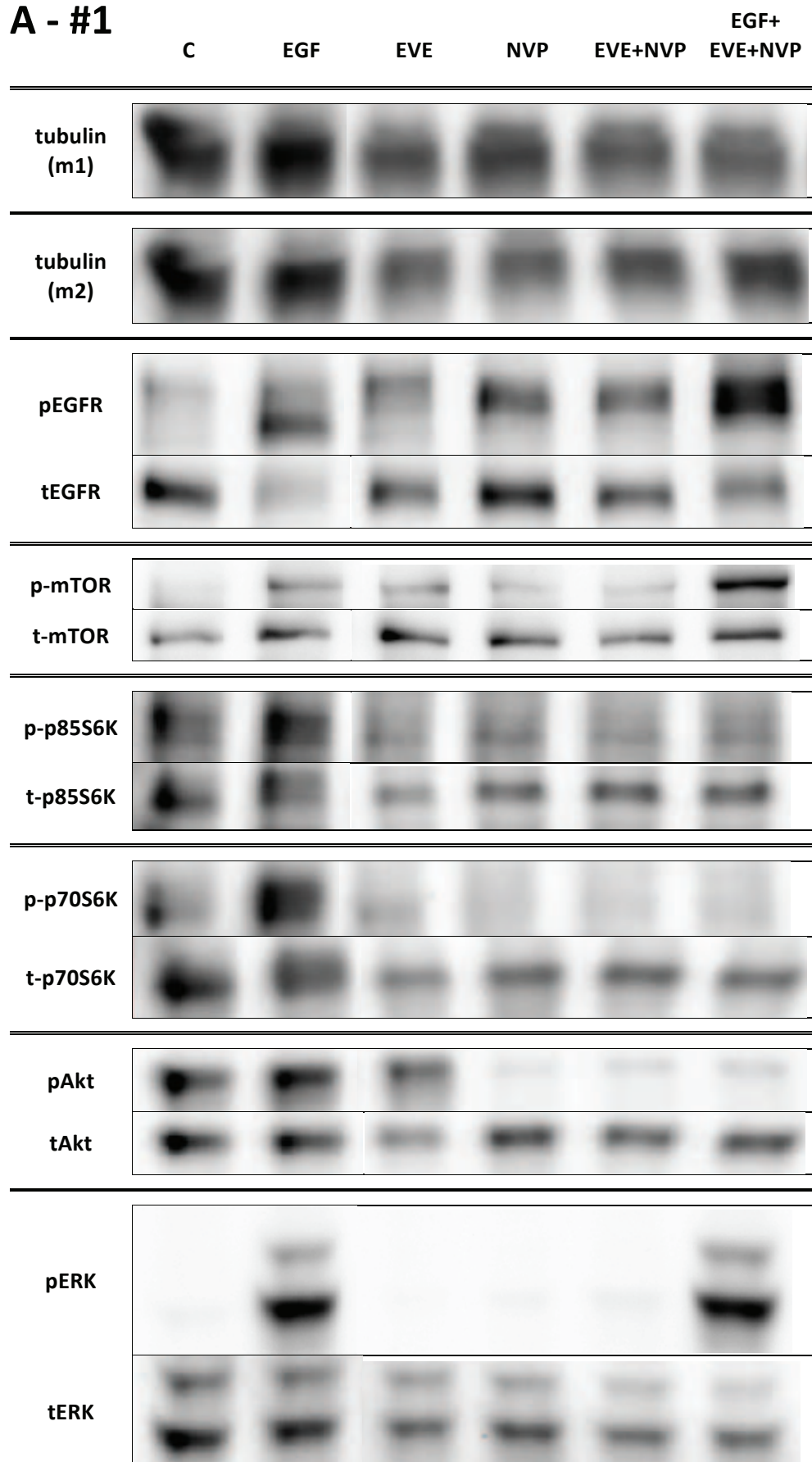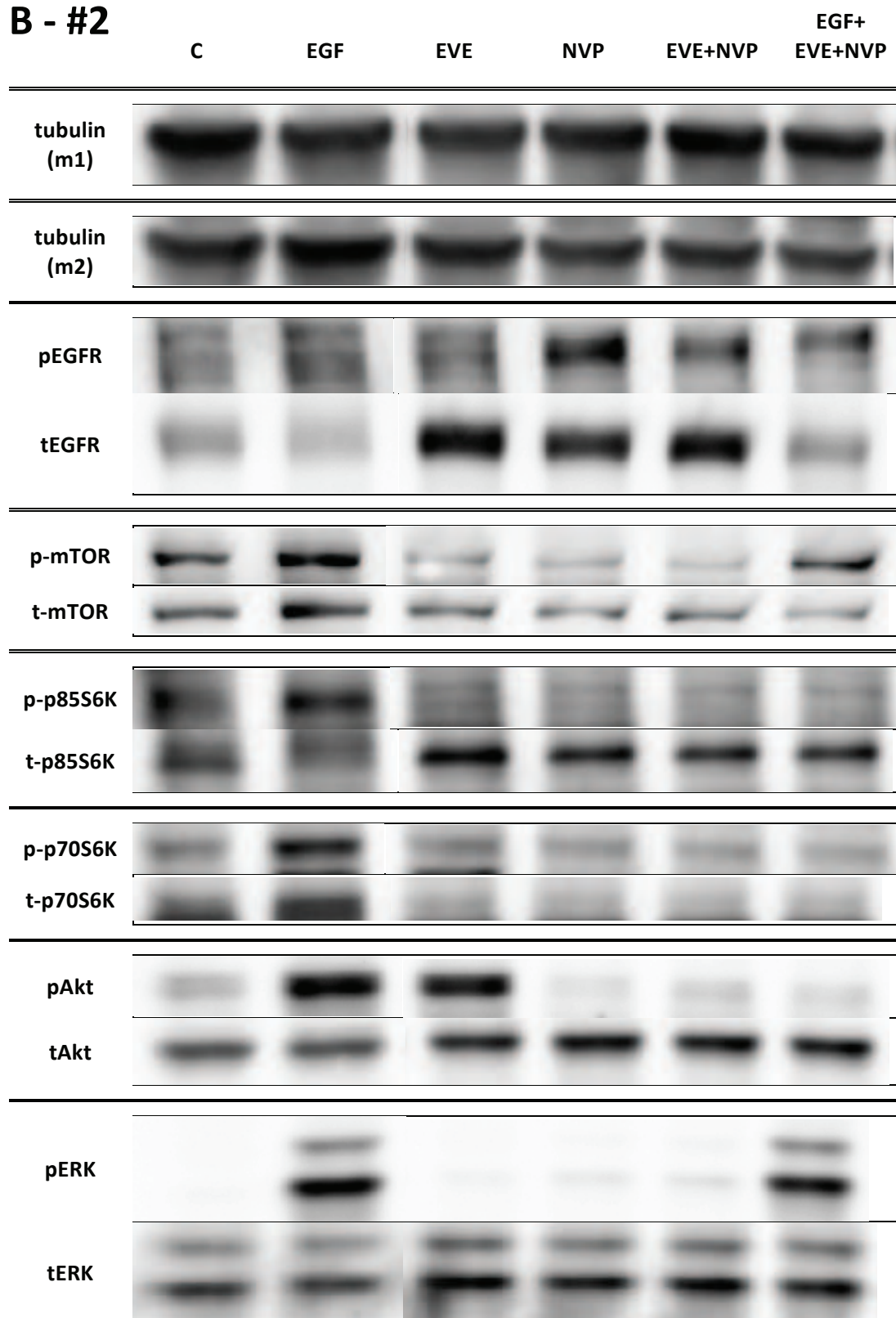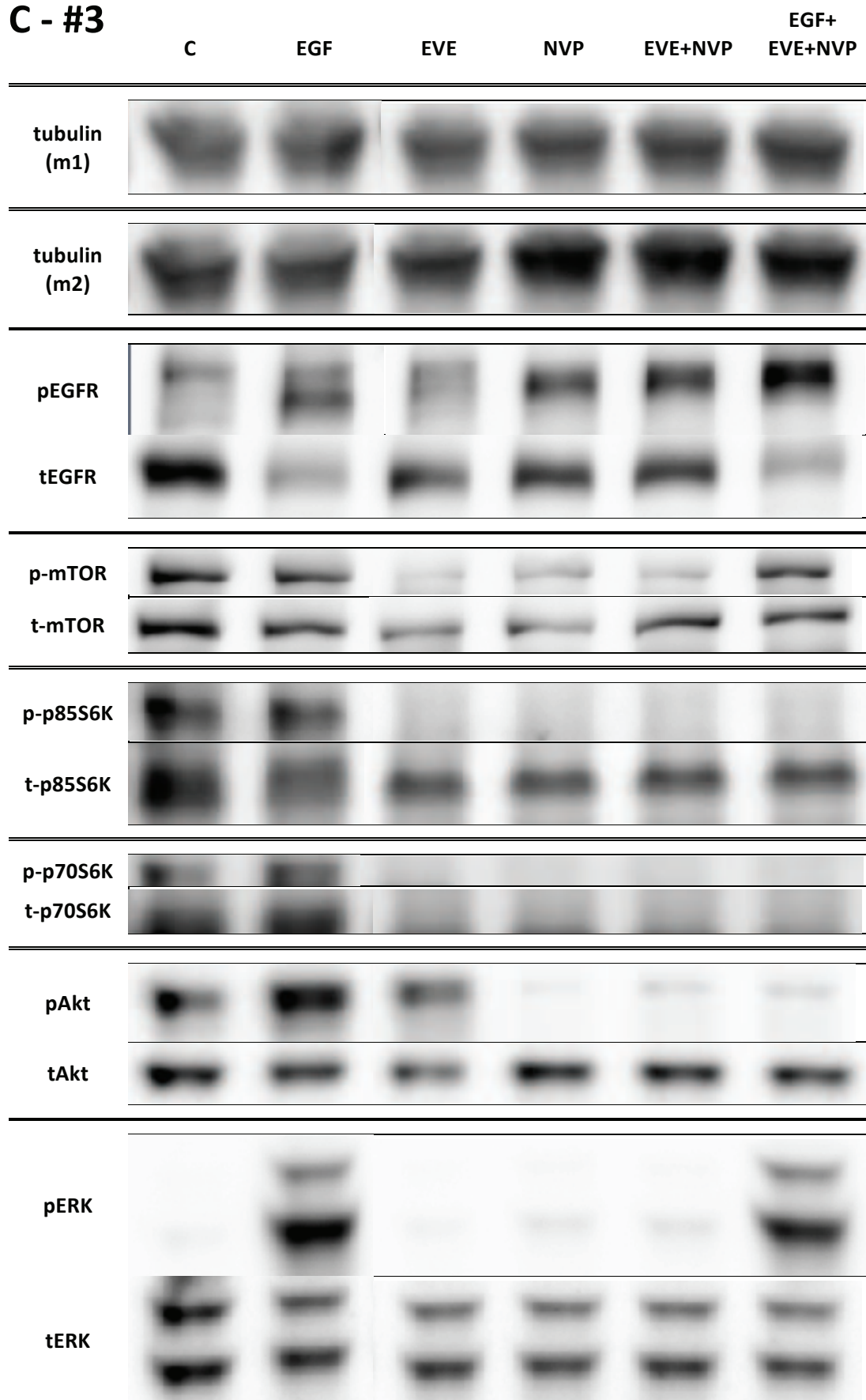
D	**C**	**EGF**	**EVE**	**NVP**	**EVE+NVP**	**EGF+ EVE+NVP**	
pEGFR	1.00	2.55	2.51	2.33	2.24	4.93	#1
	1.00	1.30	1.43	1.51	1.12	1.25	#2
	1.00	1.43	0.95	1.18	1.20	1.47	#3
tEGFR	1.00	0.40	1.10	1.62	1.00	0.76	#1
	1.00	0.59	2.20	2.26	2.41	1.32	#2
	1.00	0.39	0.67	0.57	0.58	0.29	#3
p/t	**1.00**	**6.33**	**2.27**	**1.43**	**2.24**	**6.45**	**#1**
	1.00	**2.20**	**0.65**	**0.67**	**0.46**	**0.95**	**#2**
	1.00	**3.69**	**1.42**	**2.06**	**2.07**	**5.06**	**#3**
p-mTOR	1.00	15.69	15.73	6.93	6.80	64.72	#1
	1.00	1.58	0.44	0.34	0.26	1.31	#2
	1.00	0.75	0.09	0.29	0.18	0.66	#3
t-mTOR	1.00	1.50	2.54	2.27	1.49	1.79	#1
	1.00	1.20	0.93	0.86	0.92	0.78	#2
	1.00	0.79	0.44	0.34	0.55	0.62	#3
p/t	**1.00**	**10.45**	**6.20**	**3.05**	**4.56**	**36.22**	**#1**
	1.00	**1.31**	**0.47**	**0.39**	**0.28**	**1.69**	**#2**
	1.00	**0.95**	**0.21**	**0.86**	**0.34**	**1.07**	**#3**
p-p85S6K	1.00	1.31	0.84	0.78	0.70	0.95	#1
	1.00	1.48	0.91	0.61	0.55	0.60	#2
	1.00	0.92	0.21	0.17	0.14	0.17	#3
t-p85S6K	1.00	1.08	0.80	1.18	1.09	0.91	#1
	1.00	0.75	1.22	1.44	1.25	1.42	#2
	1.00	0.90	0.78	0.59	0.61	0.62	#3
p/t	**1.00**	**1.21**	**1.05**	**0.66**	**0.64**	**1.04**	**#1**
	1.00	**1.98**	**0.75**	**0.42**	**0.44**	**0.43**	**#2**
	1.00	**1.02**	**0.27**	**0.30**	**0.23**	**0.27**	**#3**
p-p70S6K	1.00	1.96	0.72	0.44	0.36	0.52	#1
	1.00	2.00	0.94	0.82	0.67	0.69	#2
	1.00	1.08	0.25	0.16	0.16	0.16	#3
t-p70S6K	1.00	0.91	0.66	0.90	0.80	0.61	#1
	1.00	1.16	0.19	0.19	0.16	0.18	#2
	1.00	1.03	0.48	0.35	0.32	0.33	#3
p/t	**1.00**	**2.15**	**1.09**	**0.49**	**0.45**	**0.86**	**#1**
	1.00	**1.72**	**4.94**	**4.24**	**4.17**	**3.76**	**#2**
	1.00	**1.04**	**0.52**	**0.45**	**0.52**	**0.48**	**#3**
pAkt	1.00	1.14	1.06	0.10	0.16	0.21	#1
	1.00	4.10	4.01	0.48	0.73	0.64	#2
	1.00	1.49	0.93	0.06	0.13	0.12	#3
tAkt	1.00	0.92	0.68	1.24	0.91	0.85	#1
	1.00	0.88	1.19	1.64	1.45	1.67	#2
	1.00	0.88	0.65	0.73	0.69	0.68	#3
p/t	**1.00**	**1.24**	**1.56**	**0.08**	**0.17**	**0.24**	**#1**
	1.00	**4.65**	**3.37**	**0.29**	**0.50**	**0.38**	**#2**
	1.00	**1.69**	**1.41**	**0.08**	**0.19**	**0.17**	**#3**

pERK	1.00	64.05	2.22	2.70	4.14	95.96	#1
	1.00	162.26	4.45	6.98	5.90	145.90	#2
	1.00	72.63	1.78	3.70	3.16	49.66	#3
tERK	1.00	0.87	0.90	0.96	0.59	0.48	#1
	1.00	0.76	1.15	1.34	1.39	1.65	#2
	1.00	0.92	0.80	0.58	0.60	0.60	#3
p/t	**1.00**	**73.58**	**2.48**	**2.82**	**7.01**	**199.87**	**#1**
	1.00	**213.90**	**3.86**	**5.20**	**4.25**	**88.18**	**#2**
	1.00	**79.29**	**2.23**	**6.34**	**5.26**	**82.54**	**#3**
	C	**EGF**	**EVE**	**NVP**	**EVE+NVP**	**EGF+ EVE+NVP**	

Fig. 19 Protein expression after everolimus and NVP-BEZ235 treatment.

The adrenocortical H295R cells were treated with everolimus (0.1 µM) or NVP-BEZ235 (1 µM) for 1 hour; EGF (100 ng/ml) was added 0.5 hour after the treatment with these inhibitors. Protein expression was assessed in cell lysates using Western Blot. Tubulin was used as a house-keeping gene – **m1** refers to first membrane probed for phospho-specific antibodies, **m2** refers to second membrane probed for total antibodies. The experiment was repeated three times (**A**, **B**, **C**). Summary table includes collective data for those three repeats, expressed as normalised values (original results normalised to housekeeping gene and then to control) and p/t ratio (the value for the phospho-specific antibody divided by the value for the total antibody) (**D**).
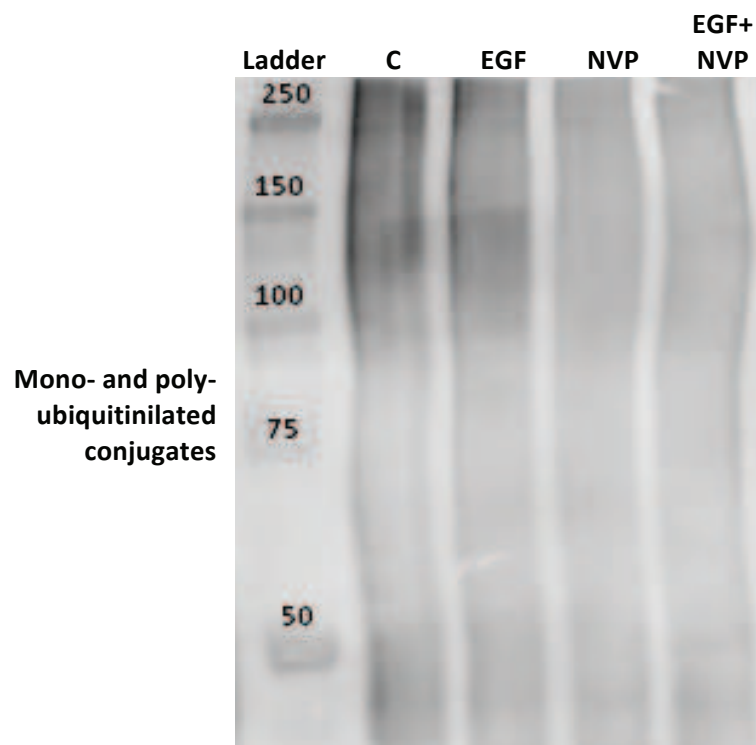
Fig. 20 The effect of NVP-BEZ235 on protein ubiquitinylation.

The adrenocortical H295R cells were treated with NVP-BEZ235 (1 µM) for 24 hour; EGF (100 ng/ml) was added 1 hour after the treatment with this inhibitor.

A - #1

| | C | EGF | U0126 | EGF+ U0126 | NVP | EGF+ NVP | NVP+ U0126 | EGF+ NVP+ U0126 | LY | EGF+ LY |

B - #2

C - #3

	C	EGF	U0126	EGF+ U0126	NVP	EGF+ NVP	NVP+ U0126	EGF+ NVP+ U0126	LY	EGF+ LY

GAPDH (m1)

GAPDH (m2)

pEGFR

tEGFR

p-mTOR

t-mTOR

p-p85S6K

t-p85S6K

p-p70S6K

t-p70S6K

pAkt

tAkt — *non-detectable*

pERK

tERK
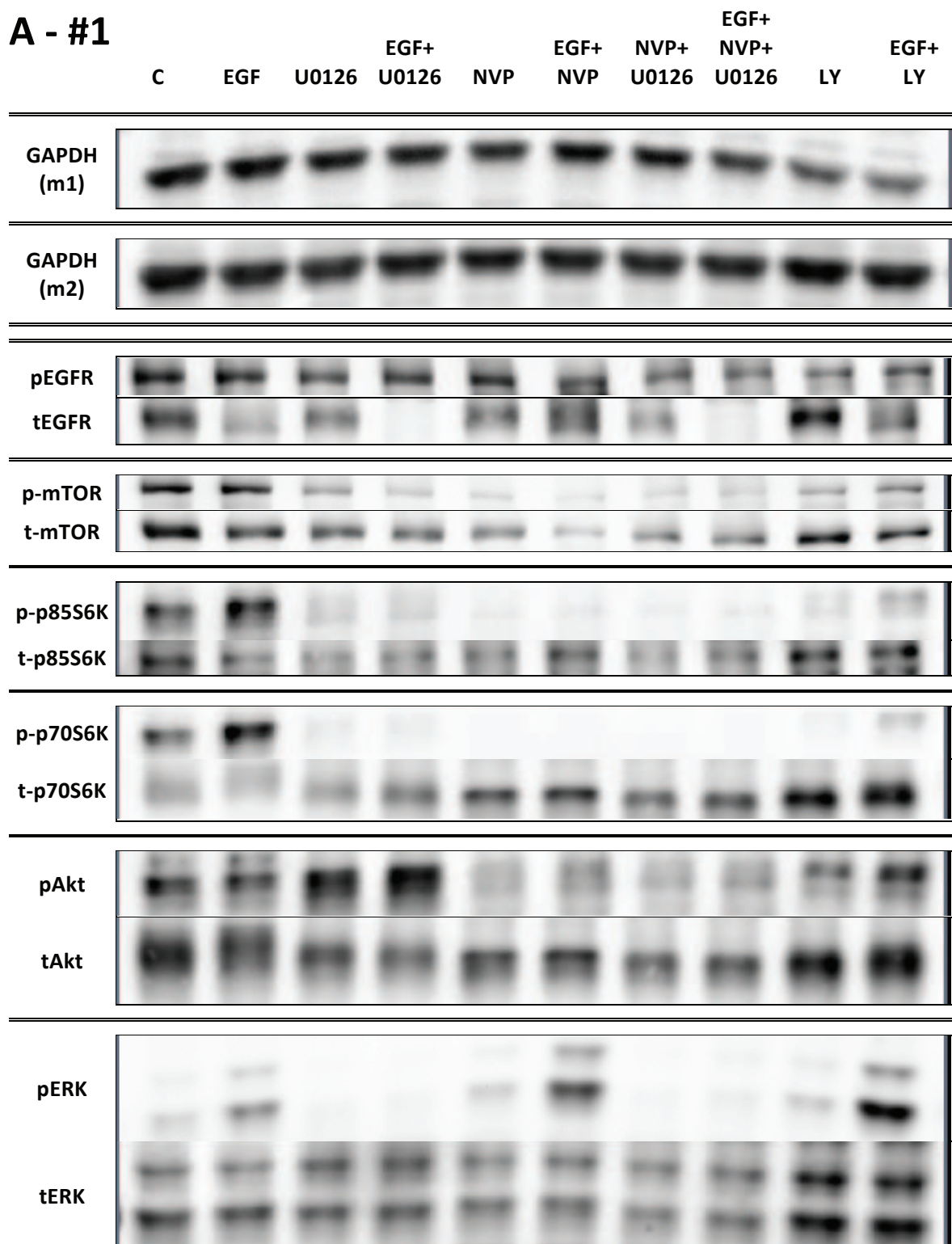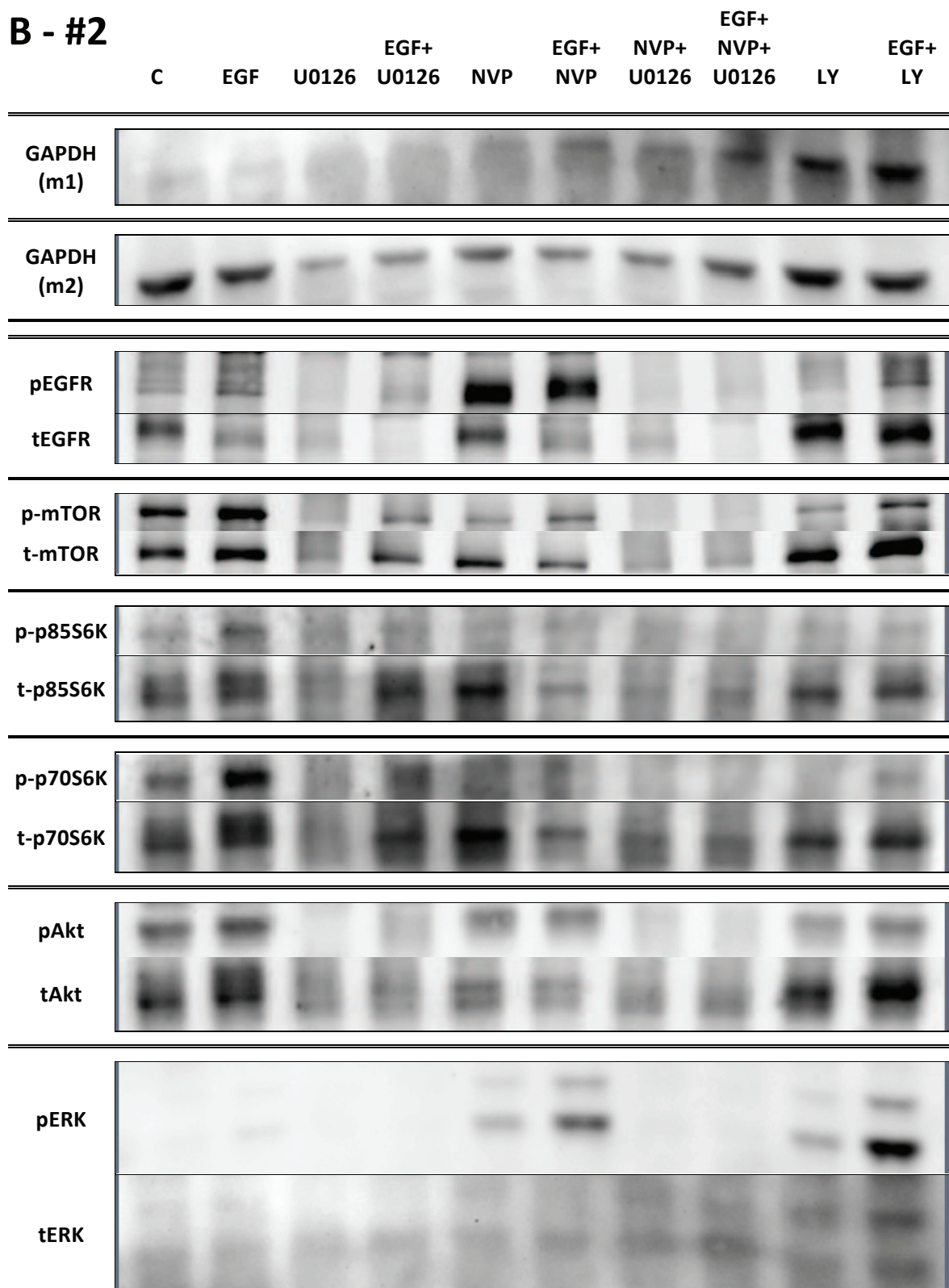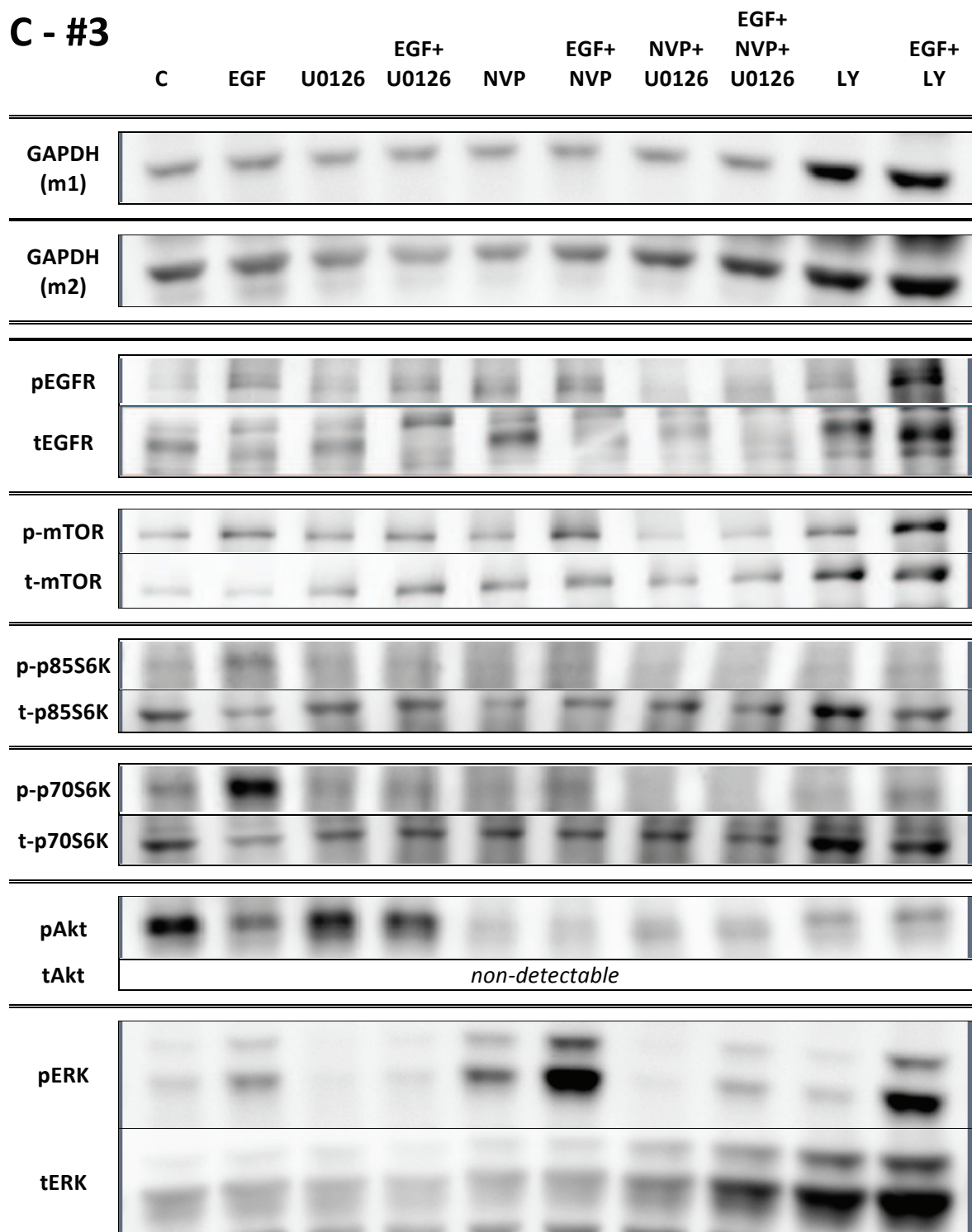
D

	C	EGF	U0126	EGF+U0126	NVP	EGF+NVP	NVP+U0126	EGF+NVP+U0126	LY	EGF+LY	
pEGFR	1.00	0.89	0.86	1.01	1.07	0.50	0.86	0.99	1.07	1.42	#1
	1.00	2.16	0.34	0.91	3.06	2.00	0.22	0.22	0.25	0.38	#2
	1.00	2.53	1.65	2.62	2.96	3.24	0.63	1.19	0.69	1.92	#3
tEGFR	1.00	0.44	0.80	0.01	0.86	0.99	0.53	0.06	1.04	0.73	#1
	1.00	0.80	1.25	0.25	1.78	1.42	0.81	0.11	1.42	1.57	#2
	1.00	0.70	1.36	0.43	2.47	0.31	0.50	0.20	0.95	0.96	#3
p/t	1.00	2.03	1.08	99.32	1.24	0.51	1.63	17.66	1.03	1.94	#1
	1.00	2.68	0.28	3.70	1.72	1.41	0.27	1.93	0.17	0.24	#2
	1.00	3.61	1.21	6.10	1.20	10.54	1.27	5.96	0.73	1.99	#3
p-mTOR	1.00	0.85	0.41	0.22	0.14	0.08	0.16	0.23	0.50	0.92	#1
	1.00	2.00	0.25	0.50	0.23	0.26	0.09	0.06	0.11	0.14	#2
	1.00	1.96	1.63	1.99	1.43	2.99	0.59	0.77	0.65	1.38	#3
t-mTOR	1.00	0.77	0.69	0.59	0.47	0.17	0.43	0.54	0.74	0.60	#1
	1.00	1.62	1.47	1.91	1.58	1.50	0.84	0.54	1.31	2.32	#2
	1.00	0.85	3.29	6.36	5.02	4.29	1.83	2.01	3.57	3.44	#3
p/t	1.00	1.10	0.59	0.38	0.31	0.45	0.38	0.43	0.68	1.53	#1
	1.00	1.23	0.17	0.26	0.14	0.17	0.10	0.12	0.08	0.06	#2
	1.00	2.31	0.50	0.31	0.28	0.70	0.32	0.38	0.18	0.40	#3
p-p85S6K	1.00	1.35	0.31	0.28	0.09	0.09	0.10	0.13	0.38	0.90	#1
	1.00	2.10	0.82	0.69	0.42	0.35	0.34	0.18	0.18	0.15	#2
	1.00	1.54	1.23	1.09	0.95	1.08	0.61	0.46	0.20	0.26	#3
t-p85S6K	1.00	0.78	0.53	0.64	0.76	1.13	0.54	0.70	1.09	1.24	#1
	1.00	1.47	2.25	2.48	1.75	1.07	1.12	0.84	0.81	1.01	#2
	1.00	0.52	1.33	1.45	0.81	0.87	0.74	0.55	0.84	0.44	#3
p/t	1.00	1.72	0.58	0.44	0.12	0.08	0.19	0.19	0.35	0.72	#1
	1.00	1.43	0.36	0.28	0.24	0.33	0.30	0.22	0.23	0.15	#2
	1.00	2.97	0.92	0.75	1.17	1.25	0.83	0.85	0.24	0.58	#3
p-p70S6K	1.00	1.65	0.17	0.17	0.03	0.02	0.01	0.02	0.18	0.68	#1
	1.00	2.50	0.44	0.83	0.35	0.23	0.14	0.10	0.07	0.11	#2
	1.00	2.57	1.00	0.90	0.76	0.97	0.41	0.29	0.15	0.25	#3
t-p70S6K	1.00	0.87	1.19	1.65	1.86	2.14	1.37	1.40	2.22	2.65	#1
	1.00	1.64	1.78	1.71	1.38	1.24	1.21	0.78	0.78	1.07	#2
	1.00	0.57	1.11	1.37	1.41	0.96	0.72	0.45	0.74	0.52	#3
p/t	1.00	1.89	0.15	0.10	0.02	0.01	0.01	0.01	0.08	0.26	#1
	1.00	1.52	0.25	0.49	0.25	0.18	0.12	0.13	0.08	0.11	#2
	1.00	4.50	0.90	0.65	0.54	1.00	0.57	0.65	0.20	0.49	#3
pAkt	1.00	0.80	1.59	1.89	0.57	0.63	0.56	0.90	1.41	2.24	#1
	1.00	1.55	0.05	0.34	0.55	0.42	0.14	0.09	0.20	0.19	#2
	1.00	0.47	1.14	0.97	0.22	0.21	0.30	0.26	0.10	0.11	#3
tAkt	1.00	0.98	0.93	0.76	0.90	1.00	0.79	0.82	1.03	1.15	#1
	1.00	1.54	2.27	1.45	1.26	1.24	1.29	1.00	1.14	1.37	#2
	1.00	N/A	N/A	N/A	N/A	N/A	N/A	N/A	N/A	N/A	#3
p/t	1.00	0.81	1.71	2.47	0.64	0.63	0.71	1.09	1.37	1.95	#1
	1.00	1.01	0.02	0.24	0.44	0.34	0.11	0.09	0.18	0.14	#2
	1.00	N/A	N/A	N/A	N/A	N/A	N/A	N/A	N/A	N/A	#3

		C	EGF	U0126	EGF+ U0126	NVP	EGF+ NVP	NVP+ U0126	EGF+ NVP+ U0126	LY	EGF+ LY	
pERK		1.00	3.07	0.21	0.32	1.56	7.10	0.22	1.05	2.48	18.52	#1
		1.00	4.56	0.72	0.89	8.75	19.21	1.51	0.74	4.51	14.55	#2
		1.00	2.55	0.64	0.86	5.23	15.06	0.43	1.82	0.33	2.91	#3
tERK		1.00	1.06	1.14	1.14	1.03	1.13	0.91	1.03	1.50	1.59	#1
		1.00	1.25	2.55	1.40	1.70	2.72	4.31	3.57	1.78	3.03	#2
		1.00	1.08	1.26	1.21	1.85	1.81	2.00	2.80	2.93	3.51	#3
p/t		1.00	2.91	0.19	0.28	1.52	6.30	0.25	1.02	1.65	11.67	#1
		1.00	3.64	0.28	0.64	5.14	7.08	0.35	0.21	2.53	4.80	#2
		1.00	2.36	0.50	0.71	2.82	8.33	0.21	0.65	0.11	0.83	#3

Fig. 21 Protein expression after U0126, NVP-BEZ235 and LY294002 treatment.

The adrenocortical H295R cells were treated with U0126 (10 µM), NVP-BEZ235 (1 µM) or LY294002 (10 µM) for 24 hours; EGF (100 ng/ml) was added 1 hour after the treatment with these inhibitors. Protein expression was assessed in cell lysates using Western Blot. GAPDH was used as a house-keeping gene – **m1** refers to first membrane probed for phospho-specific antibodies, **m2** refers to second membrane probed for total antibodies. The experiment was repeated three times (**A**, **B**, **C**). Summary table includes collective data for those three repeats, expressed as normalised values (original results normalised to housekeeping gene and then to control) and p/t ratio (the value for the phospho-specific antibody divided by the value for the total antibody) (**D**).

5. Discussion

5.1. Mitotane effects in H295R cells

The present study confirmed the anti-proliferative effect of mitotane in the adrenocortical carcinoma H295R cell line, using the Resazurin cell viability assay. The effect was dose- and cell density-dependent (**Fig. 8**). The clinical therapeutic window (based on mitotane blood levels in patients) lies between 14 and 20 mg/L, corresponding to 43.75–62.5 µM. These doses caused complete cytotoxicity in the H295R cells in the applied conditions.

The EC_{50} values for mitotane observed by other research teams for H295R cells range from as low as 10.6 µM [23], 18 µM [27], 22.8 µM [21], 24 µM [30], to even 30.62 µM [22]. The reason for the described spread probably lies in the differences in experiment conditions, among others: different methods of cytotoxicity assessment, density of seeded cells, growth period prior to the treatment, treatment duration, and cell culture conditions. The mitotane EC_{50} value obtained in this study was 12.57 µM (at 24 hours of treatment), lying in the lower end of the range described in the literature. It may be based on the fact that the established optimal conditions required seeding relatively low amount of cells (at the density of 5,000 cells/100 µl), short pre-treatment growth time (24 hours) and short treatment time (24 hours) in comparison to conditions applied in abovementioned studies. A number of other reports describe mitotane efficiency in reducing H295R cell proliferation without establishing the EC_{50} value [24-26].

The Resazurin cell viability assay measures simply the reducing capacity of the metabolically active living cells, then expressed as viability/cytotoxicity, and does not enable to investigate the underlying mechanisms of cell damage. Hence, the apoptosis (programmed cell death) assay was performed to enhance the picture. The time-response experiments showed that the peak, almost 3.5-fold activation of the caspase-3-like activity was observed an hour after the mitotane treatment and then decreased with time (**Fig. 15**). Though much less pronounced, the 1.6-fold increase was still observed 24 hours after the treatment. The mitotane-induced sharp increase in the caspase-3-like activity occurred promptly after the delivery of

the treatment and then resolved over time. It suggests that cells overcome mitotane effect at the cost of decreased cell viability/reducing capacity (as measured by the Resazurin assay) or a reversible delay in G_2-phase (as observed by Stigliano et al. [25]).

Mitotane increased the caspase-3-like activity in dose-dependent manner with a sharp increment between the concentration of 20 and 25 μM from over 2.5-fold to almost 8.5-fold increase, respectively (**Fig. 16**). Lehmann et al. observed similar mode of response with no detectable changes for lower concentrations (0.6 – 50 μM) and sharp 2- to 2.5-fold increase in caspase-3/7 activity for higher doses (62.5 μM and 100 μM) [24]. It indicates that there is a threshold concentration of mitotane over which the caspase activation is sharply increased. The discrepancy in the effective doses may be related with the fact that Lehmann et al. obtained hardly 20% cytotoxicity with 20 μM mitotane in the cell viability assay (compare with EC_{50} values reported by other groups summarized above), indicating that in conditions they used H295R cells managed to survive higher doses of mitotane.

Interestingly, mitotane did not significantly affect the protein concentration at lower doses, only at the dose of 25 μM upon the short-term 4-hour treatment. It may suggest that short-term treatment with lower doses of mitotane lead to the apoptosis initiation, but do not cause extensive cell death. It is in accordance with the cytofluorimetric analysis of apoptotic events in the H295R cells performed by Poli et al., demonstrating that lower doses of mitotane result in increased number of live apoptotic cells, while higher concentration increases the fraction of dead apoptotic cells [27]. It supports the hypothesis that at specific doses mitotane decreases cell viability/reducing capacity or probably causes cell cycle arrest. Lehmann et al. performed a follow-up experiment, checking for typical apoptotic ladder of DNA bands after DNA electrophoresis; they have not observed this sign of apoptosis, opening speculations that mitotane may lead to cell necrosis [24] or so-called "aponecrosis", characterising with a combination of apoptotic and necrotic features. Poli et al. described a range of mitotane effects, from induction of events related to early (annexin V exposure at plasma membrane, drop in the mitochondrial membrane potential) and late (caspase 3/7 activation) apoptosis. They as well seen that subjecting cells to highly toxic mitotane doses results in

mixed apoptotic/necrotic features (aponecrosis) observed in dead cells (nuclear chromatin condensation, plasma membrane rupture, non-detectable mitochondria) [27]. Further detailed studies on time-dependent mitotane effects and apoptotic/necrotic markers may shed light on exact mechanisms of its action.

5.2. *In vitro* preclinical profiles of everolimus, NVP-BEZ235, LY294002, and U0126

The present study demonstrates that everolimus (RAD001), NVP-BEZ235, LY294002, and U0126 are effective anti-proliferative agents in an adrenocortical carcinoma *in vitro* model, the H295R cell line. For all inhibitors, the dose-dependent effect was observed (**Figs. 9-12**). As indicated in **Tab. 5**, the effect of PI3K/mTOR inhibitors was cell density-independent (**Figs. 9-11**), while the U0126 effect depended on cell density (**Fig. 12**). Within this project, due to limited resources, only the exploratory experiments were performed to see the effect of specific doses of selected inhibitors on the caspase-3-like activity. To evaluate this effect in more detailed way, additional experiments need to be carried out with a few different treatment regimes (e.g. a number of additional doses, treatment duration).

Everolimus (RAD001) proved to decrease the cell viability of the H295R cells only up to 15-16% after 72-hour treatment with treatment repeated every 24 hours. The EC_{50} value was established at the dose of $15.95*10^{-3}$ µM (**Fig. 9A**). The effect was independent of seeded cell density (**Fig. 9B**). Everolimus efficacy in the H295R cells obtained by other teams is very varied (for summary see **Tab. 6**). Pezzani et al. tested it only at one concentration along the study of ouabain (a cardiotonic steroid). They report that everolimus at the dose of 5 µM had virtually no effect on cell viability 72 hours after treatment [155]. On the other hand, other teams report much higher efficacy. Mariniello et al. present the data showing almost complete cytotoxicity at the dose of 2 µM and EC_{50} of approximately 0.4 µM 72 hours after treatment [156]. Other team used very long treatment time of 6 days and consequently obtained even higher efficacy with almost complete cytotoxicity

already at the dose of 0.1 µM and EC_{50} of $7.94*10^{-3}$ µM [154]. In their next paper, they have tested everolimus in another set of experiments, obtaining again almost complete cytotoxicity at the dose of 0.1 µM and EC_{50} of $20.99*10^{-3}$ µM [157]. The reasons behind the differences may be different methods for cell viability/proliferation assessment, experiment conditions and treatment regimes. The established optimal conditions in this project required seeding relatively low amount of cells (at the density of 5,000 cells/100 µl) and short pre-treatment growth time (24 hours). Though the complete cytotoxicity was not obtained, the established EC_{50} value falls in between the ones reported by other teams.

The everolimus dose of 0.06 µM proved to be insufficient to exert a significant effect on the caspase-3-like activity in the H295R cells, though it slightly (non-significantly) decreased protein content (**Fig. 17**). Mariniello et al. investigated as well everolimus effect at the dose of 9 µM on apoptosis, labelling cells for annexin V-FITC and propidium iodide (PI) and seen no increase in apoptosis [156]. In the viability experiments (the Resazurin assay) in this project, the dose of 0.06 µM significantly reduced cell viability by approximately 12%. The conditions (cell density, culture vessels, assay resolution) were different, but it may suggest that, as the everolimus activity was shown to be cell density-independent, the effect of everolimus is more cytostatic than cytotoxic.

Tab. 5 Collective results for dose- and cell density-response.
Everolimus (RAD001), NVP-BEZ235, LY294002, U0126, and mitotane were tested in the adrenocortical carcinoma H295R cell line, using the Resazurin cell viability assay. For dose-response experiments, the **EC_{50}** value (half maximal effective concentration) indicates the concentration of a tested compound, which causes a response halfway between the baseline and maximum response. For cell density-response, the **R^2** value (the coefficient of determination) quantifies goodness of fit and indicates the correlation; the higher the **R^2** value, the stronger the correlation. Based on **Figs. 8-12**.

Compound	Protein(s) directly inhibited	EC_{50} (µM)	R_2
Everolimus (RAD001)	mTOR	$15.95*10^{-3}$	0.05
NVP-BEZ235 (BEZ235)	PI3K, mTOR	2.42	0.13
LY294002	PI3K	17.23	0.14
U0126	MEK1/2	15.41	0.62
Mitotane	N/A	12.57	0.23

Tab. 6 Effects of selected PI3K/mTOR and MEK1/2 inhibitors in H295R cell line.

Reported effects	Ref.
Everolimus (RAD001) **mTOR inhibitor**	
• decreased cell proliferation, • inhibited growth of H295R xenografts.	[154]
• single dose tested (5 µM) – increased cell viability (24 hours), no effect on cell viability (72 hours), • decreased p-p70S6K levels.	[155]
• decreased cell viability, • decreased phospho-p70S6K, slightly reduced phospho-Akt levels, no effect on phospho-ERK levels, • no changes in cell cycle stage, • no significant increase in apoptosis, • no effect on H295R xenografts.	[156]
NVP-BEZ235 **dual PI3K and mTOR inhibitor**	
• decreased cell proliferation, • increased phospho-ERK levels, decreased phospho-Akt and phospho-S6 levels, • increased the percentage of subG$_1$ (apoptotic) cells, reduced the percentage of cells in the G$_0$/G$_1$, S and G$_2$/M phases of the cell cycle, • inhibited growth of H295R xenografts.	[157]
LY294002 **PI3K inhibitor**	
• single dose tested (20 µM) – no effect on cell proliferation, • decreased the TDGF-1-mediated increase in aldosterone secretion.	[158]
• decreased phospho-Akt levels.	[159]
U0126 **MEK1/2 inhibitor**	
• decreased angiotensin II- and BMP-6-induced aldosterone production, no effect on activin-induced aldosterone production.	[187]
• decreased glycoxidized lipoprotein-mediated adrenal steroid secretion.	[188]

• decreased native, glycoxidized and oxidized VLDL-mediated adrenocortical steroid secretion, • decreased *CYP11B2* mRNA levels in response to native, glycoxidized and oxidized VLDL, • inhibit VLDL-induced phosphorylation of ERK1/2.	[189]
• inhibit angiotensin II-induced phosphorylation of ERK, • decreased angiotensin II-induced aldosterone production, no effect on K-induced aldosterone production, • inhibited BMP-6-induced *CYP11B2* transcriptional regulation, no effect on BMP-6-induced Smad1/5/8 signal activation.	[190]

Three above-mentioned groups compared the effect of everolimus also for another adrenocortical cell line SW13, which in all cases proved to be more sensitive to everolimus [154-156]. The next step of everolimus evaluation would be testing its efficacy in inhibiting tumour growth *in vivo* in xenograft mouse models. Two of the above-mentioned reports covered as well these experiments, indicating either effectiveness [154] or no effect on the H295R xenografts [156].

NVP-BEZ235 proved to be a very potent inhibitor of cell proliferation in the adrenocortical H295R cells with low-micromolar EC_{50} of 2.42 μM (**Fig. 10A**). The effect was independent of seeded cell density (**Fig. 10B**). One other report investigated NVP-BEZ235 efficacy in the H295R cells with EC_{50} of $19.9*10^{-3}$ μM upon 6 days (for summary see **Tab 6**) [157]. This group reported as well induction of apoptosis (increase in $subG_1$ (apoptotic) cells) and inhibition of tumour growth in H295R xenografts [157]. NVP-BEZ235 at the dose of 0.01 μM did not significantly affect caspase-3-like activity in the H295R cells, though it slightly (non-significantly) decreased protein content, in accordance with cell viability results (**Fig. 17**).

LY294002 proved to decrease the cell viability of H295R with EC_{50} established at the dose of 17.23 μM after 72-hour treatment (**Fig. 11A**). The effect was independent of seeded cell density (**Fig. 11B**). Up to now, there are no reports describing in detail the effect of LY294002 on the H295R cell proliferation or apoptosis. Two reports concentrating on steroidogenesis described its effect on steroid production and related events in the H295R cell line (for summary see **Tab**

6) [158, 159]. One of them indicates that LY294002 at a single dose of 20 μM does not affect the cell proliferation 72 hours after treatment [158]. LY294002 at the dose of 1 μM did not significantly affect caspase-3-like activity in the H295R cells; though it slightly, non-significantly increased protein content (**Fig. 17**). Similarly to everolimus, comparing this result with viability assay results, it may be concluded that at this dose the effect of LY294002 is more cytostatic, than cytotoxic.

U0126 proved to inhibit the cell viability of H295R in a dose- and cell density-dependent manner with EC_{50} established at the dose of 15.41 μM after 72-hour single treatment (**Fig. 12**). A number of reports show the effect of U0126 in the steroidogenesis-related studies in the H295R cells, but none describes the effect on cell proliferation (for summary see **Tab 6**) [187-190]. U0126 is a promising compound for the ACC treatment of efficacy comparable with LY294002, but acting in a cell density-dependent manner. The direction of further U0126 preclinical trials should probably be investigation of combined treatment with PI3K/mTOR inhibitors, such as everolimus and NVP-BEZ235, as ERK inhibition may synergize with PI3K/mTOR inhibition. Our exploratory experiments showed potential synergism of such combinations in inhibiting cell proliferation (data not shown) and protein expression (**Fig. 21**).

5.3. Combination treatment

This is a first report showing a synergistic effect between suboptimal doses of everolimus (mTOR inhibitor) and NVP-BEZ235 (PI3K/mTOR inhibitor). This combination treatment was highly efficient in decreasing the adrenocortical H295R cells viability, overcoming to a high degree the efficacy of the inhibitors applied as single treatment (**Fig. 14**). This co-treatment significantly decreased as well the amount of protein in cell lysates, but did not have a significant impact on caspase-3-like activity (**Fig. 17**), indicating that its effect is highly cytotoxic and may be based on an apoptotic-independent mechanism. Though the activity of the inhibitors overlaps in a way (they both inhibit mTOR), the source of enhanced efficacy when

combined may be a result of differential mechanism of action on mTOR. Everolimus forms a complex with cyclophilin FKBP-12, which then inhibits mTORC1 and mTORC2 by binding to them, while NVP-BEZ235 is a competitor for ATP-binding site of mTOR (as well affecting both mTORC1 and mTORC2).

Adding another PI3K inhibitor (LY294002) to this double combination resulted in only slightly more decreased cell viability and its addition did not yield the synergistic effect. Neither do any double combination with LY294002 and everolimus or NVP-BEZ235 yielded the synergistic effect (**Fig. 14**). However, when investigated for the effect on caspase-3-like activity, a double combination of LY294002 and NVP-BEZ235 caused a significant increase in the caspase-3 activation, higher than for single treatment with these inhibitors, while presenting merely additive effect in proliferation inhibition. Here, addition of everolimus only slightly increased that effect on caspase-3 activity, indicating that it is powerfully driven from LY294002 and NVP-BEZ235 co-treatment. LY294002 and NVP-BEZ235 act as competitors for the ATP-binding site of PI3K, which activation is important in apoptosis inhibition [198]. As well, PI3K-downstream kinase, Akt was confirmed to play protective role against apoptosis [199]; thus effective inhibition of PI3K may effectively trigger apoptotic events.

The exploration of potential enhancement of mitotane efficacy with PI3K/mTOR or MEK inhibitors unfortunately did not bring any powerful positive results. The highest potential of synergistic effect had the combination of mitotane and U0126, MEK1/2 inhibitor (**Fig. 13**). For our experimental conditions, the effect was slightly higher than additive, but U0126 treatment was not significantly increasing mitotane efficacy. However, as we assessed only single doses of both mitotane and U0126 in combination, further studies involving additional optimisation and establishing different dosing regimes may potentially give positive results.

5.4. Protein expression after PI3K/mTOR or MEK inhibition

The protein expression analysis confirmed to a large extent the expected effects of everolimus (RAD001), NVP-BEZ235, LY294002, and U0126 on the PI3K/Akt/mTOR and Ras/Raf/MEK/ERK pathways (**Tab. 7**, see **Fig. 2** for pathways details).

The mTOR inhibition (everolimus, NVP-BEZ235) effectively blocked the phosphorylation of p70 ribosomal protein S6 kinase 1 (S6K1) and its isoform p85 as well as decreased total levels of p70S6K. The effect proved to be as predicted, because p70S6K is a direct positively regulated target of mTOR. Blocking mTOR led as well to the increased phosphorylated ERK levels. The one of the synergies described between PI3K/Akt/mTOR and Ras/Raf/MEK/ERK pathways is at the level of ERK, which, among others, targets the TSC1/2 complex, leading to its disruption and thus releasing the mTOR activity [175]. However, our results indicate that there is another cross talk between those two pathways working in the other direction, mTOR inhibition (everolimus, NVP-BEZ235) inducing up-regulation of ERK phosphorylation, possibly through compensating mechanism. While Akt/mTOR pathway is blocked, the compensation for cellular processes may come from MEK/ERK side.

Another mechanism involved may be the regulatory cross talk mechanism between PI3K/Akt/mTOR and Ras/Raf/MEK/ERK cascades, based on the Raf phosphorylation by Akt, which leads to the inhibition of the latter pathway [200]. As described below, the Akt inhibition may result is releasing Raf to its active state and activate the downstream ERK. Taken together, it may mean that ERK inhibition may synergize with everolimus and NVP-BEZ235 activity. This cross talk is supported with the results of long-term inhibition (24 hours) of PI3K (NVP-BEZ235, LY294002) that led to increase in total ERK levels. It as well predictably blocks p70S6K and p85S6K phosphorylation. As expected, the inhibition of the PI3K/Akt/mTOR pathway either at the PI3K or mTOR level inevitably causes effective restraint in p70S6K/p85S6K phosphorylation, one of the downstream targets of this pathway.

Tab. 7 Collective results for protein expression.
The effect of everolimus (RAD001), NVP-BEZ235, LY294002, and U0126 on protein expression in the adrenocortical carcinoma H295R cell line was assessed using the Western Blot. Abbreviations: **LT** – long-term; **ST** – short-term treatment. Based on **Figs 19,21**.

Compound	Protein(s) directly inhibited	Effects on protein expression	
		increased	decreased
Everolimus	mTOR	pERK$^{T202/Y204}$	p-p85S6K^{T412} p-p70S6K^{T389} t-p70S6K
NVP-BEZ235	PI3K, mTOR	pEGFR^{Y1173} tEGFR pERK$^{T202/Y204}$ tERK (**LT**) t-p70S6K (**LT**)	pAkt^{T308} p-p85S6K^{T412} p-p70S6K^{T389} t-p70S6K (**ST**)
LY294002	PI3K	tERK	p-mTOR^{S2448} p-p85S6K^{T412} p-p70S6K^{T389}
U0126	MEK1/2	t-p70S6K tERK	p-p70S6K^{T389} pERK$^{T202/Y204}$
Everolimus + NVP-BEZ235	mTOR + PI3K, mTOR	pEGFR^{Y1173} pERK$^{T202/Y204}$	pAkt^{T308} p-p85S6K^{T412} p-p70S6K^{T389} t-p70S6K
U0126 + NVP-BEZ235	MEK1/2 + PI3K, mTOR	-	pEGFR^{Y1173} tEGFR p-mTOR^{S2448} p-p85S6K^{T412} p-p70S6K^{T389} pAkt^{T308}

Simultaneous blocking of PI3K and mTOR (NVP-BEZ235) caused increase in EGFR levels (both phosphorylated and total), indicating that such dual inhibition leads to accumulation of activated EGFR, possibly through constraining the degradation mechanisms. The exploratory data confirmed that NVP-BEZ235 blocked protein ubiquitination, which is a protein alteration, tagging proteins to be

degraded (**Fig. 20**). A dual PI3K and mTOR inhibitor, NVP-BEZ235, predictably decreases as well phosphorylation of Akt, which is downstream of PI3K and mTORC2 and upstream of mTORC1. Such response may as well indicate that inhibiting the signalling downstream to EGFR may turn off the feedback loops that occur in activated pathway.

Co-treatment with mTOR and PI3K/mTOR inhibitors (everolimus, NVP-BEZ235) resulted in similar effects to those of the compounds acting alone. It decreased phosphorylation of Akt, p70S6K and p85S6K and decreased total levels of p70S6K. The positive effects of this co-treatment on EGFR and ERK phosphorylation were observed. It was reported that the H295R cell line presents increased expression of Akt [155], mTOR, and raptor [154], which is in accordance with studies comparing ACTs to ACCs [80, 154, 166] (as summarised in chapter **1.3.2** PI3K/Akt/mTOR pathway alterations in ACC). Taken together with high efficacy of the everolimus and NVP-BEZ235 combination observed in cell viability studies, it may be useful in suggesting plausible explanation for such synergism. As mentioned above, everolimus and NVP-BEZ235 show different modes of mTOR inhibition, plausibly making them more effective when combined. The H295R are more sensitive to this combination treatment due to increase expression of Akt and mTOR, which are effectively directly and indirectly inhibited.

The MEK1/2 inhibition (U0126) exerted an interesting effect on protein expression, decreasing phosphorylation of p70S6K and ERK, but increasing their total levels (**Fig. 21**). It was shown that Ras/Raf/MEK/ERK pathway is over-activated in ACCs [178, 179] (as summarised in chapter **1.4.2** Ras/Raf/MEK/ERK pathway alterations in ACC). As it may be the case of the H295R cells as well, that could be the reason for high efficacy of MEK inhibitor, U0126. Co-treatment with U0126 and PI3K/mTOR inhibitor (NVP-BEZ235) resulted in a robust inhibition of phosphorylation of Akt, mTOR, p70S6K and p85S6K as well as decrease in both phospho- and total EGFR levels. As indicated above, the ERK inhibition may synergize with everolimus and NVP-BEZ235 activity, it may be worth developing further the studies on combined treatment with these PI3K/mTOR inhibitors and MEK/ERK inhibitors, such as U0126.

Comparing to the literature reporting effect of these inhibitors on protein expression in the H295R cells, the observations are similar to a great extent. Everolimus was reported to inhibit phosphorylation of p70S6K [155, 156] and, slightly, of Akt with no effect on phospho-ERK [156]. Doghman et al. described NVP-BEZ235 showing that it blocks p70S6K and Akt phosphorylation, while increasing ERK phosphorylation [157]. LY294002 decreased phospho-Akt levels [159]. U0126 inhibited ERK phosphorylation [189, 190].

5.5. Potential future directions

The presented results established a good basis for further research investigating novel therapeutic options for the adrenocortical carcinoma. Limited options available currently drive an urgent clinical need for different approaches. The customized therapy aiming at the components of PI3K/Akt/mTOR and Ras/Raf/MEK/ERK pathways presents great potential in adrenocortical carcinoma treatment. A number of their components are altered in ACC. Our results indicate that everolimus and NVP-BEZ235 are the most promising combination therapy partners. Further studies in *in vivo* models would be beneficial to prove the synergism observed in *in vitro* studies.

Moreover, these results provide a number of clues on the mechanism of action of tested compounds and their interactions. Additional studies may be necessary to enhance understanding of the precise mechanisms and interactions between PI3K/mTOR and MEK inhibitors.

6. Conclusions

1) This is the first report showing a synergistic effect between suboptimal doses of everolimus (mTOR inhibitor) and NVP-BEZ235 (PI3K/mTOR inhibitor), which is the most promising combination for further studies that was investigated within this project.

2) Everolimus (mTOR inhibitor), NVP-BEZ235 (PI3K/mTOR inhibitor), LY294002 (PI3K inhibitor), and U0126 (MEK inhibitor) are potent anti-proliferative agents in an adrenocortical carcinoma *in vitro* model, the H295R cell line, all acting in a dose-dependent manner. It is the first report of this kind for LY294002 and U0126. All tested compounds show potential for further *in vivo* studies.

3) Apoptotic studies within this project (caspase-3-like activity) shown that co-treatment with dual PI3K/mTOR (NVP-BEZ235) and PI3K (LY294002) inhibitors drives significant increase in caspase-3-like activity, suggesting synergism with regards to this effect, but not on cell viability. Further analyses would be necessary to elucidate the exact mechanism of caspase-3 activation by these compounds.

4) Protein expression analyses indicated that there may be a not yet reported cross talk between PI3K/Akt/mTOR and Ras/Raf/MEK/ERK pathway, based on the up-regulation of ERK phosphorylation upon mTOR inhibition. The co-treatment of U0126 and NVP-BEZ235 was most promising with regards to inhibition of protein expression. As the ERK inhibition may synergize with mTOR inhibition, it may be an interaction worth studying in more detail.

5) Mitotane *in vitro* preclinical profile was confirmed to a large extent with the currently available literature, showing inhibition of H295R cell proliferation in a dose- and cell density-dependent manner. Its effect on caspase-3-like activity peaked shortly after treatment application, indicating its rapid effect, which seems to be resolved to some extent over time.

6) Combination of mitotane and PI3K/mTOR or MEK inhibitors yielded at most the additive effect with U0126 showing highest potential for further studies that may possibly bring synergism with different dosing regime.

References

1. Fassnacht, M. and B. Allolio, *Epidemiology of Adrenocortical Carcinoma*, in *Adrenocortical Carcinoma. Basic Science and Clinical Concepts*, G.D. Hammer and T. Else, Editors. 2011, Springer New York. p. 23-29.
2. Barzon, L., et al., *Prevalence and natural history of adrenal incidentalomas.* Eur J Endocrinol, 2003. **149**(4): p. 273-85.
3. Lafemina, J. and M.F. Brennan, *Adrenocortical carcinoma: past, present, and future.* J Surg Oncol, 2012. **106**(5): p. 586-94.
4. Klein, J.D., et al., *Adrenal cortical tumors in children: factors associated with poor outcome.* Journal of Pediatric Surgery, 2011. **46**(6): p. 1201-1207.
5. Wajchenberg, B.L., et al., *Adrenocortical carcinoma: clinical and laboratory observations.* Cancer, 2000. **88**(4): p. 711-36.
6. Blanes, A. and S.J. Diaz-Cano, *Histologic criteria for adrenocortical proliferative lesions: value of mitotic figure variability.* Am J Clin Pathol, 2007. **127**(3): p. 398-408.
7. Hough, A.J., et al., *Prognostic factors in adrenal cortical tumors. A mathematical analysis of clinical and morphologic data.* Am J Clin Pathol, 1979. **72**(3): p. 390-9.
8. van Slooten, H., et al., *Morphologic characteristics of benign and malignant adrenocortical tumors.* Cancer, 1985. **55**(4): p. 766-73.
9. Weiss, L.M., *Comparative histologic study of 43 metastasizing and nonmetastasizing adrenocortical tumors.* Am J Surg Pathol, 1984. **8**(3): p. 163-9.
10. Lau, S.K. and L.M. Weiss, *The Weiss system for evaluating adrenocortical neoplasms: 25 years later.* Human Pathology, 2009. **40**(6): p. 757-768.
11. Giordano, T.J., *Classification of adrenal cortical tumors: promise of the 'molecular' approach.* Best Pract Res Clin Endocrinol Metab, 2010. **24**(6): p. 887-92.
12. Bertherat, J. and X. Bertagna, *Pathogenesis of adrenocortical cancer.* Best Practice & Research Clinical Endocrinology & Metabolism, 2009. **23**(2): p. 261-271.
13. Glover, A.R., et al., *Current management options for recurrent adrenocortical carcinoma.* Onco Targets Ther, 2013. **6**: p. 635-43.
14. Ronchi, C.L., et al., *EJE prize 2014: current and evolving treatment options in adrenocortical carcinoma: where do we stand and where do we want to go?* Eur J Endocrinol, 2014. **171**(1): p. R1-R11.
15. Maluf, D.F., B.H. de Oliveira, and E. Lalli, *Therapy of adrenocortical cancer: present and future.* Am J Cancer Res, 2011. **1**(2): p. 222-232.
16. Fassnacht, M., M. Kroiss, and B. Allolio, *Update in adrenocortical carcinoma.* J Clin Endocrinol Metab, 2013. **98**(12): p. 4551-64.
17. Else, T., et al., *Adjuvant therapies and patient and tumor characteristics associated with survival of adult patients with adrenocortical carcinoma.* J Clin Endocrinol Metab, 2014. **99**(2): p. 455-61.
18. Terzolo, M., et al., *Mitotane*, in *Adrenocortical Carcinoma*, G.D. Hammer and T. Else, Editors. 2011, Springer New York. p. 369-381.
19. Lindhe, O., B. Skogseid, and I. Brandt, *Cytochrome P450-catalyzed binding of 3-methylsulfonyl-DDE and o,p'-DDD in human adrenal zona fasciculata/reticularis.* J Clin Endocrinol Metab, 2002. **87**(3): p. 1319-26.
20. Chagpar, R., A.E. Siperstein, and E. Berber, *Adrenocortical cancer update.* Surg Clin North Am, 2014. **94**(3): p. 669-87.
21. Doghman, M. and E. Lalli, *Lack of long-lasting effects of mitotane adjuvant therapy in a mouse xenograft model of adrenocortical carcinoma.* Mol Cell Endocrinol, 2013. **381**(1-2): p. 66-9.
22. Germano, A., et al., *Cytotoxic activity of gemcitabine, alone or in combination with mitotane, in adrenocortical carcinoma cell lines.* Mol Cell Endocrinol, 2014. **382**(1): p. 1-7.
23. Asp, V., et al., *Biphasic hormonal responses to the adrenocorticolytic DDT metabolite 3-methylsulfonyl-DDE in human cells.* Toxicol Appl Pharmacol, 2010. **242**(3): p. 281-9.
24. Lehmann, T.P., T. Wrzesinski, and P.P. Jagodzinski, *The effect of mitotane on viability, steroidogenesis and gene expression in NCIH295R adrenocortical cells.* Mol Med Rep, 2013. **7**(3): p. 893-900.
25. Stigliano, A., et al., *Modulation of proteomic profile in H295R adrenocortical cell line induced by mitotane.* Endocr Relat Cancer, 2008. **15**(1): p. 1-10.
26. Zsippai, A., et al., *Effects of mitotane on gene expression in the adrenocortical cell line NCI-H295: a microarray study.* Pharmacogenomics, 2012. **13**(12): p. 1351-61.
27. Poli, G., et al., *Morphofunctional effects of mitotane on mitochondria in human adrenocortical cancer cells.* Endocr Relat Cancer, 2013. **20**(4): p. 537-50.
28. Hescot, S., et al., *Mitotane alters mitochondrial respiratory chain activity by inducing cytochrome c oxidase defect in human adrenocortical cells.* Endocr Relat Cancer, 2013. **20**(3): p. 371-81.
29. Lin, C.W., Y.H. Chang, and H.F. Pu, *Mitotane exhibits dual effects on steroidogenic enzymes gene transcription under basal and cAMP-stimulating microenvironments in NCI-H295 cells.* Toxicology, 2012. **298**(1-3): p. 14-23.
30. Schteingart, D.E., et al., *Comparison of the adrenalytic activity of mitotane and a methylated homolog on normal adrenal cortex and adrenal cortical carcinoma.* Cancer Chemother Pharmacol, 1993. **31**(6): p. 459-66.
31. Gicquel, C., et al., *Molecular markers and long-term recurrences in a large cohort of patients with sporadic adrenocortical tumors.* Cancer Res, 2001. **61**(18): p. 6762-7.
32. Kjellman, M., et al., *Genotyping of adrenocortical tumors: very frequent deletions of the MEN1 locus in 11q13 and of a 1-centimorgan region in 2p16.* J Clin Endocrinol Metab, 1999. **84**(2): p. 730-5.
33. Mateo, E.C., et al., *A study of adrenocortical tumors in children and adolescents by a comparative genomic hybridization technique.* Cancer Genetics, 2011. **204**(6): p. 298-308.
34. Gruschwitz, T., et al., *Improvement of histopathological classification of adrenal gland tumors by genetic differentiation.* World J Urol, 2010. **28**(3): p. 329-34.
35. Sidhu, S., et al., *Comparative genomic hybridization analysis of adrenocortical tumors.* J Clin Endocrinol Metab, 2002. **87**(7): p. 3467-74.
36. Figueiredo, B.C., et al., *Comparative genomic hybridization analysis of adrenocortical tumors of childhood.* J Clin Endocrinol Metab, 1999. **84**(3): p. 1116-21.
37. Zhao, J., et al., *Analysis of genomic alterations in sporadic adrenocortical lesions. Gain of chromosome 17 is an early event in adrenocortical tumorigenesis.* Am J Pathol, 1999. **155**(4): p. 1039-45.

38. Dohna, M., et al., *Adrenocortical carcinoma is characterized by a high frequency of chromosomal gains and high-level amplifications.* Genes Chromosomes Cancer, 2000. **28**(2): p. 145-52.

39. Kjellman, M., et al., *Genetic aberrations in adrenocortical tumors detected using comparative genomic hybridization correlate with tumor size and malignancy.* Cancer Res, 1996. **56**(18): p. 4219-23.

40. Bentz, M., et al., *Minimal sizes of deletions detected by comparative genomic hybridization.* Genes Chromosomes Cancer, 1998. **21**(2): p. 172-5.

41. Barreau, O., et al., *Clinical and pathophysiological implications of chromosomal alterations in adrenocortical tumors: an integrated genomic approach.* J Clin Endocrinol Metab, 2012. **97**(2): p. E301-11.

42. Stephan, E.A., et al., *Adrenocortical carcinoma survival rates correlated to genomic copy number variants.* Mol Cancer Ther, 2008. **7**(2): p. 425-31.

43. De Martino, M.C., et al., *Molecular screening for a personalized treatment approach in advanced adrenocortical cancer.* J Clin Endocrinol Metab, 2013. **98**(10): p. 4080-8.

44. Mateo, E.C., et al., *A study of adrenocortical tumors in children and adolescents by a comparative genomic hybridization technique.* Cancer Genet, 2011. **204**(6): p. 298-308.

45. de Fraipont, F., et al., *Gene expression profiling of human adrenocortical tumors using complementary deoxyribonucleic Acid microarrays identifies several candidate genes as markers of malignancy.* J Clin Endocrinol Metab, 2005. **90**(3): p. 1819-29.

46. Velázquez-Fernández, D., et al., *Expression profiling of adrenocortical neoplasms suggests a molecular signature of malignancy.* Surgery, 2005. **138**(6): p. 1087-1094.

47. Slater, E.P., et al., *Analysis by cDNA microarrays of gene expression patterns of human adrenocortical tumors.* Eur J Endocrinol, 2006. **154**(4): p. 587-98.

48. Laurell, C., et al., *Transcriptional profiling enables molecular classification of adrenocortical tumours.* Eur J Endocrinol, 2009. **161**(1): p. 141-52.

49. Lombardi, C.P., et al., *Gene expression profiling of adrenal cortical tumors by cDNA macroarray analysis. Results of a preliminary study.* Biomed Pharmacother, 2006. **60**(4): p. 186-90.

50. Almeida, M.Q., et al., *Activation of cyclic AMP signaling leads to different pathway alterations in lesions of the adrenal cortex caused by germline PRKAR1A defects versus those due to somatic GNAS mutations.* J Clin Endocrinol Metab, 2012. **97**(4): p. E687-93.

51. Bourdeau, I., et al., *Gene array analysis of macronodular adrenal hyperplasia confirms clinical heterogeneity and identifies several candidate genes as molecular mediators.* Oncogene, 2004. **23**(8): p. 1575-85.

52. Giordano, T.J., et al., *Distinct transcriptional profiles of adrenocortical tumors uncovered by DNA microarray analysis.* Am J Pathol, 2003. **162**(2): p. 521-31.

53. Giordano, T.J., et al., *Molecular classification and prognostication of adrenocortical tumors by transcriptome profiling.* Clin Cancer Res, 2009. **15**(2): p. 668-76.

54. Herbet, M., et al., *Acquisition order of Ras and p53 gene alterations defines distinct adrenocortical tumor phenotypes.* PLoS Genet, 2012. **8**(5): p. e1002700.

55. West, A.N., et al., *Gene expression profiling of childhood adrenocortical tumors.* Cancer Res, 2007. **67**(2): p. 600-8.

56. Ragazzon, B., et al., *Transcriptome analysis reveals that p53 and {beta}-catenin alterations occur in a group of aggressive adrenocortical cancers.* Cancer Res, 2010. **70**(21): p. 8276-81.

57. Fernandez-Ranvier, G.G., et al., *Candidate diagnostic markers and tumor suppressor genes for adrenocortical carcinoma by expression profile of genes on chromosome 11q13.* World J Surg, 2008. **32**(5): p. 873-81.

58. Fernandez-Ranvier, G.G., et al., *Identification of biomarkers of adrenocortical carcinoma using genomewide gene expression profiling.* Arch Surg, 2008. **143**(9): p. 841-6; discussion 846.

59. Soon, P.S., et al., *Microarray gene expression and immunohistochemistry analyses of adrenocortical tumors identify IGF2 and Ki-67 as useful in differentiating carcinomas from adenomas.* Endocr Relat Cancer, 2009. **16**(2): p. 573-83.

60. Ye, P., et al., *G-protein-coupled receptors in aldosterone-producing adenomas: a potential cause of hyperaldosteronism.* J Endocrinol, 2007. **195**(1): p. 39-48.

61. Bassett, M.H., et al., *Expression profiles for steroidogenic enzymes in adrenocortical disease.* J Clin Endocrinol Metab, 2005. **90**(9): p. 5446-55.

62. de Reynies, A., et al., *Gene expression profiling reveals a new classification of adrenocortical tumors and identifies molecular predictors of malignancy and survival.* J Clin Oncol, 2009. **27**(7): p. 1108-15.

63. Ronchi, C.L., et al., *Single nucleotide polymorphism microarray analysis in cortisol-secreting adrenocortical adenomas identifies new candidate genes and pathways.* Neoplasia, 2012. **14**(3): p. 206-18.

64. Keren, B., et al., *SNP arrays in Beckwith-Wiedemann syndrome: An improved diagnostic strategy.* Eur J Med Genet, 2013.

65. Letouze, E., et al., *SNP array profiling of childhood adrenocortical tumors reveals distinct pathways of tumorigenesis and highlights candidate driver genes.* J Clin Endocrinol Metab, 2012. **97**(7): p. E1284-93.

66. Schmitz, K.J., et al., *Differential expression of microRNA-675, microRNA-139-3p and microRNA-335 in benign and malignant adrenocortical tumours.* J Clin Pathol, 2011. **64**(6): p. 529-35.

67. Soon, P.S., et al., *miR-195 and miR-483-5p Identified as Predictors of Poor Prognosis in Adrenocortical Cancer.* Clin Cancer Res, 2009. **15**(24): p. 7684-7692.

68. Patterson, E.E., et al., *MicroRNA profiling of adrenocortical tumors reveals miR-483 as a marker of malignancy.* Cancer, 2011. **117**(8): p. 1630-9.

69. Ozata, D.M., et al., *The role of microRNA deregulation in the pathogenesis of adrenocortical carcinoma.* Endocr Relat Cancer, 2011. **18**(6): p. 643-55.

70. Tombol, Z., et al., *Integrative molecular bioinformatics study of human adrenocortical tumors: microRNA, tissue-specific target prediction, and pathway analysis.* Endocr Relat Cancer, 2009. **16**(3): p. 895-906.

71. Rechache, N.S., et al., *DNA methylation profiling identifies global methylation differences and markers of adrenocortical tumors.* J Clin Endocrinol Metab, 2012. **97**(6): p. E1004-13.

72. Barreau, O., et al., *Identification of a CpG island methylator phenotype in adrenocortical carcinomas.* J Clin Endocrinol Metab, 2013. **98**(1): p. E174-84.

73. Fonseca, A.L., et al., *Comprehensive DNA methylation analysis of benign and malignant adrenocortical tumors.* Genes Chromosomes Cancer, 2012. **51**(10): p. 949-60.

74. Almeida, M.Q., et al., *Integrated genomic analysis of nodular tissue in macronodular adrenocortical hyperplasia: progression of tumorigenesis in a disorder associated with multiple benign lesions.* J Clin Endocrinol Metab, 2011. **96**(4): p. E728-38.

75. Almeida, M.Q., et al., *Mouse Prkar1a haploinsufficiency leads to an increase in tumors in the Trp53+/- or Rb1+/- backgrounds and chemically induced skin papillomas by dysregulation of the cell cycle and Wnt signaling.* Hum Mol Genet, 2010. **19**(8): p. 1387-98.

76. Duregon, E., et al., *Diagnostic and prognostic role of steroidogenic factor 1 in adrenocortical carcinoma: a validation study focusing on clinical and pathologic correlates.* Human Pathology, 2013. **44**(5): p. 822-828.

77. Fenske, W., et al., *Glucose transporter GLUT1 expression is an stage-independent predictor of clinical outcome in adrenocortical carcinoma.* Endocr Relat Cancer, 2009. **16**(3): p. 919-28.

78. Adam, P., et al., *Epidermal growth factor receptor in adrenocortical tumors: analysis of gene sequence, protein expression and correlation with clinical outcome.* Mod Pathol, 2010. **23**(12): p. 1596-604.

79. Almeida, M.Q., et al., *Steroidogenic factor 1 overexpression and gene amplification are more frequent in adrenocortical tumors from children than from adults.* J Clin Endocrinol Metab, 2010. **95**(3): p. 1458-62.

80. Barlaskar, F.M., et al., *Preclinical targeting of the type I insulin-like growth factor receptor in adrenocortical carcinoma.* J Clin Endocrinol Metab, 2009. **94**(1): p. 204-12.

81. Gaujoux, S., et al., *beta-catenin activation is associated with specific clinical and pathologic characteristics and a poor outcome in adrenocortical carcinoma.* Clin Cancer Res, 2011. **17**(2): p. 328-36.

82. Ragazzon, B., G. Assie, and J. Bertherat, *Transcriptome analysis of adrenocortical cancers: from molecular classification to the identification of new treatments.* Endocr Relat Cancer, 2011. **18**(2): p. R15-27.

83. Assie, G., T.J. Giordano, and J. Bertherat, *Gene expression profiling in adrenocortical neoplasia.* Molecular and Cellular Endocrinology, 2012. **351**(1): p. 111-117.

84. Assié, G., et al., *The pathophysiology, diagnosis and prognosis of adrenocortical tumors revisited by transcriptome analyses.* Trends in Endocrinology & Metabolism, 2010. **21**(5): p. 325-334.

85. Heaton, J.H., et al., *Progression to adrenocortical tumorigenesis in mice and humans through insulin-like growth factor 2 and beta-catenin.* Am J Pathol, 2012. **181**(3): p. 1017-33.

86. Drelon, C., et al., *Analysis of the Role of Igf2 in Adrenal Tumour Development in Transgenic Mouse Models.* PLoS ONE, 2012. **7**(8): p. e44171.

87. Easton, J.B., R.T. Kurmasheva, and P.J. Houghton, *IRS-1: auditing the effectiveness of mTOR inhibitors.* Cancer Cell, 2006. **9**(3): p. 153-5.

88. Wilkin, F., et al., *Pediatric adrenocortical tumors: molecular events leading to insulin-like growth factor II gene overexpression.* J Clin Endocrinol Metab, 2000. **85**(5): p. 2048-56.

89. Soon, P.S., et al., *Molecular markers and the pathogenesis of adrenocortical cancer.* Oncologist, 2008. **13**(5): p. 548-61.

90. Mazzuco, T.L., et al., *Genetic aspects of adrenocortical tumours and hyperplasias.* Clinical Endocrinology, 2012. **77**(1): p. 1-10.

91. Almeida, M.Q., et al., *Expression of insulin-like growth factor-II and its receptor in pediatric and adult adrenocortical tumors.* J Clin Endocrinol Metab, 2008. **93**(9): p. 3524-31.

92. El Wakil, A., et al., *Genetics and genomics of childhood adrenocortical tumors.* Molecular and Cellular Endocrinology, 2011. **336**(1–2): p. 169-173.

93. Olivier, M., et al., *Li-Fraumeni and related syndromes: correlation between tumor type, family structure, and TP53 genotype.* Cancer Res, 2003. **63**(20): p. 6643-50.

94. Petitjean A, M.E., Kato S, Ishioka C, Tavtigian SV, Hainaut P, Olivier M., *Impact of mutant p53 functional properties on TP53 mutation patterns and tumor phenotype: lessons from recent developments in the IARC TP53 database. (Database version: R16, November 2012)*, in *Hum Mutat.* 2007. p. 622-9.

95. Libe, R., et al., *Somatic TP53 mutations are relatively rare among adrenocortical cancers with the frequent 17p13 loss of heterozygosity.* Clin Cancer Res, 2007. **13**(3): p. 844-50.

96. Wasserman, J.D., G.P. Zambetti, and D. Malkin, *Towards an understanding of the role of p53 in adrenocortical carcinogenesis.* Mol Cell Endocrinol, 2012. **351**(1): p. 101-10.

97. Barzon, L., et al., *Molecular analysis of CDKN1C and TP53 in sporadic adrenal tumors.* Eur J Endocrinol, 2001. **145**(2): p. 207-12.

98. Sidhu, S., et al., *Mutation and methylation analysis of TP53 in adrenal carcinogenesis.* European Journal of Surgical Oncology (EJSO), 2005. **31**(5): p. 549-554.

99. Berthon, A., et al., *Wnt/β-catenin signalling in adrenal physiology and tumour development.* Molecular and Cellular Endocrinology, 2012. **351**(1): p. 87-95.

100. El Wakil, A. and E. Lalli, *The Wnt/beta-catenin pathway in adrenocortical development and cancer.* Molecular and Cellular Endocrinology, 2011. **332**(1–2): p. 32-37.

101. Tissier, F., et al., *Mutations of beta-catenin in adrenocortical tumors: activation of the Wnt signaling pathway is a frequent event in both benign and malignant adrenocortical tumors.* Cancer Res, 2005. **65**(17): p. 7622-7.

102. Chapman, A., et al., *Identification of genetic alterations of AXIN2 gene in adrenocortical tumors.* J Clin Endocrinol Metab, 2011. **96**(9): p. E1477-81.

103. Bertherat, J., et al., *Molecular and functional analysis of PRKAR1A and its locus (17q22-24) in sporadic adrenocortical tumors: 17q losses, somatic mutations, and protein kinase A expression and activity.* Cancer Res, 2003. **63**(17): p. 5308-19.

104. Mantovani, G., et al., *Different expression of protein kinase A (PKA) regulatory subunits in cortisol-secreting adrenocortical tumors: Relationship with cell proliferation.* Experimental Cell Research, 2008. **314**(1): p. 123-130.

105. de Joussineau, C., et al., *The cAMP pathway and the control of adrenocortical development and growth.* Molecular and Cellular Endocrinology, 2012. **351**(1): p. 28-36.

106. Reincke, M., et al., *Deletion of the adrenocorticotropin receptor gene in human adrenocortical tumors: implications for tumorigenesis.* J Clin Endocrinol Metab, 1997. **82**(9): p. 3054-8.

107. Rothenbuhler, A., et al., *Identification of novel genetic variants in phosphodiesterase 8B (PDE8B), a cAMP-specific phosphodiesterase highly expressed in the adrenal cortex, in a cohort of patients with adrenal tumours.* Clinical Endocrinology, 2012. **77**(2): p. 195-199.

108. Rosenberg, D., et al., *Transcription factor 3',5'-cyclic adenosine 5'-monophosphate-responsive element-binding protein (CREB) is decreased during human adrenal cortex tumorigenesis and fetal development.* J Clin Endocrinol Metab, 2003. **88**(8): p. 3958-65.

109. Peri, A., et al., *Variable expression of the transcription factors cAMP response element-binding protein and inducible cAMP early repressor in the normal adrenal cortex and in adrenocortical adenomas and carcinomas.* J Clin Endocrinol Metab, 2001. **86**(11): p. 5443-9.

110. Val, P., et al., *SF-1 a key player in the development and differentiation of steroidogenic tissues.* Nucl Recept, 2003. **1**(1): p. 8.

111. Lalli, E., et al., *Beyond steroidogenesis: Novel target genes for SF-1 discovered by genomics.* Molecular and Cellular Endocrinology, 2013. **371**(1–2): p. 154-159.

112. Doghman, M., et al., *Increased steroidogenic factor-1 dosage triggers adrenocortical cell proliferation and cancer.* Mol Endocrinol, 2007. **21**(12): p. 2968-87.

113. França, M.M., et al., *POD-1 binding to the E-box sequence inhibits SF-1 and StAR expression in human adrenocortical tumor cells.* Molecular and Cellular Endocrinology, 2013. **371**(1–2): p. 140-147.

114. Pianovski, M.A.D., et al., *SF-1 overexpression in childhood adrenocortical tumours.* European Journal of Cancer, 2006. **42**(8): p. 1040-1043.

115. Figueiredo, B.C., et al., *Amplification of the steroidogenic factor 1 gene in childhood adrenocortical tumors.* J Clin Endocrinol Metab, 2005. **90**(2): p. 615-9.

116. Sbiera, S., et al., *High diagnostic and prognostic value of steroidogenic factor-1 expression in adrenal tumors.* J Clin Endocrinol Metab, 2010. **95**(10): p. E161-71.

117. Payne, A.H. and D.B. Hales, *Overview of steroidogenic enzymes in the pathway from cholesterol to active steroid hormones.* Endocr Rev, 2004. **25**(6): p. 947-70.

118. Beuschlein, F., et al., *ACTH-receptor expression, regulation and role in adrenocortial tumor formation.* Eur J Endocrinol, 2001. **144**(3): p. 199-206.

119. Ehrlund, A., et al., *Knockdown of SF-1 and RNF31 affects components of steroidogenesis, TGFbeta, and Wnt/beta-catenin signaling in adrenocortical carcinoma cells.* PLoS One, 2012. **7**(3): p. e32080.

120. Else, T., *Association of adrenocortical carcinoma with familial cancer susceptibility syndromes.* Mol Cell Endocrinol, 2012. **351**(1): p. 66-70.

121. *Online Mendelian Inheritance in Man, OMIM®.* McKusick-Nathans Institute of Genetic Medicine, Johns Hopkins University: Baltimore, MD.

122. Flicek, P., et al., *Ensembl 2013.* Nucleic Acids Res, 2013. **41**(Database issue): p. D48-55.

123. Hunt, J.L., *Syndromes associated with abnormalities in the adrenal cortex.* Diagnostic Histopathology, 2009. **15**(2): p. 69-78.

124. Faria, A.M. and M.Q. Almeida, *Differences in the molecular mechanisms of adrenocortical tumorigenesis between children and adults.* Molecular and Cellular Endocrinology, 2012. **351**(1): p. 52-57.

125. Li, F.P. and J.F. Fraumeni, Jr., *Soft-tissue sarcomas, breast cancer, and other neoplasms. A familial syndrome?* Ann Intern Med, 1969. **71**(4): p. 747-52.

126. Schneider, K., et al., *Li-Fraumeni Syndrome.*, in *GeneReviews™ [Internet].* R.A. Pagon, M.P. Adam, and T.D. Bird, et al., Editors. 1999 Jan 19 [Updated 2013 Apr 11]: Seattle (WA): University of Washington, Seattle, 1993-2013.

127. Gonzalez, K.D., et al., *Beyond Li Fraumeni Syndrome: clinical characteristics of families with p53 germline mutations.* J Clin Oncol, 2009. **27**(8): p. 1250-6.

128. Lodish, H., et al., *Mutations Affecting Genome Stability.*, in *Molecular Cell Biology*, W.H. Freeman, Editor. 2000: New York.

129. Varley, J.M., *Germline TP53 mutations and Li-Fraumeni syndrome.* Hum Mutat, 2003. **21**(3): p. 313-20.

130. Achatz, M.I., et al., *The TP53 mutation, R337H, is associated with Li-Fraumeni and Li-Fraumeni-like syndromes in Brazilian families.* Cancer Lett, 2007. **245**(1-2): p. 96-102.

131. Herrmann, L.J., et al., *TP53 germline mutations in adult patients with adrenocortical carcinoma.* J Clin Endocrinol Metab, 2012. **97**(3): p. E476-85.

132. Olivier, M., M. Hollstein, and P. Hainaut, *TP53 mutations in human cancers: origins, consequences, and clinical use.* Cold Spring Harb Perspect Biol, 2010. **2**(1): p. a001008.

133. Garritano, S., et al., *Detailed haplotype analysis at the TP53 locus in p.R337H mutation carriers in the population of Southern Brazil: evidence for a founder effect.* Hum Mutat, 2010. **31**(2): p. 143-50.

134. Giacomazzi, J., et al., *TP53 p.R337H is a conditional cancer-predisposing mutation: further evidence from a homozygous patient.* BMC Cancer, 2013. **13**(1): p. 187.

135. Ribeiro, R.C. and B. Figueiredo, *Childhood adrenocortical tumours.* European Journal of Cancer, 2004. **40**(8): p. 1117-1126.

136. Bachinski, L.L., et al., *Genetic mapping of a third Li-Fraumeni syndrome predisposition locus to human chromosome 1q23.* Cancer Res, 2005. **65**(2): p. 427-31.

137. Choufani, S., C. Shuman, and R. Weksberg, *Beckwith-Wiedemann syndrome.* Am J Med Genet C Semin Med Genet, 2010. **154C**(3): p. 343-54.

138. Libe, R. and J. Bertherat, *Molecular genetics of adrenocortical tumours, from familial to sporadic diseases.* Eur J Endocrinol, 2005. **153**(4): p. 477-87.

139. Mazzuco, T.L., et al., *Aberrant GPCR expression is a sufficient genetic event to trigger adrenocortical tumorigenesis.* Molecular and Cellular Endocrinology, 2007. **265–266**(0): p. 23-28.

140. Baujat, G., et al., *Paradoxical NSD1 mutations in Beckwith-Wiedemann syndrome and 11p15 anomalies in Sotos syndrome.* Am J Hum Genet, 2004. **74**(4): p. 715-20.

141. Schulte, K.M., et al., *Complete sequencing and messenger ribonucleic acid expression analysis of the MEN I gene in adrenal cancer.* J Clin Endocrinol Metab, 2000. **85**(1): p. 441-8.

142. Wu, X. and X. Hua, *Menin, histone h3 methyltransferases, and regulation of cell proliferation: current knowledge and perspective.* Curr Mol Med, 2008. **8**(8): p. 805-15.

143. Piecha, G., J. Chudek, and A. Wiecek, *Multiple Endocrine Neoplasia type 1.* Eur J Intern Med, 2008. **19**(2): p. 99-103.

144. Kerr, S.E., et al., *APC germline mutations in individuals being evaluated for familial adenomatous polyposis: a review of the Mayo Clinic experience with 1591 consecutive tests.* J Mol Diagn, 2013. **15**(1): p. 31-43.

145. Juhn, E. and A. Khachemoune, *Gardner syndrome: skin manifestations, differential diagnosis and management.* Am J Clin Dermatol, 2010. **11**(2): p. 117-22.

146. Barlaskar, F.M. and G.D. Hammer, *The molecular genetics of adrenocortical carcinoma.* Rev Endocr Metab Disord, 2007. **8**(4): p. 343-8.

147. Wang, T. and W.E. Rainey, *Human adrenocortical carcinoma cell lines.* Mol Cell Endocrinol, 2012. **351**(1): p. 58-65.

148. Rainey, W.E., K. Saner, and B.P. Schimmer, *Adrenocortical cell lines.* Mol Cell Endocrinol, 2004. **228**(1-2): p. 23-38.

149. Vuorenoja, S., et al., *Adrenocortical tumorigenesis, luteinizing hormone receptor and transcription factors GATA-4 and GATA-6.* Molecular and Cellular Endocrinology, 2007. **269**(1–2): p. 38-45.

150. Beuschlein, F., S. Galac, and D.B. Wilson, *Animal models of adrenocortical tumorigenesis.* Molecular and Cellular Endocrinology, 2012. **351**(1): p. 78-86.

151. Luconi, M. and M. Mannelli, *Xenograft models for preclinical drug testing: implications for adrenocortical cancer.* Mol Cell Endocrinol, 2012. **351**(1): p. 71-7.

152. Fruman, D.A. and C. Rommel, *PI3K and cancer: lessons, challenges and opportunities.* Nat Rev Drug Discov, 2014. **13**(2): p. 140-56.

153. De Martino, M.C., et al., *The role of mTOR inhibitors in the inhibition of growth and cortisol secretion in human adrenocortical carcinoma cells.* Endocr Relat Cancer, 2012. **19**(3): p. 351-64.

154. Doghman, M., et al., *Regulation of insulin-like growth factor-mammalian target of rapamycin signaling by microRNA in childhood adrenocortical tumors.* Cancer Res, 2010. **70**(11): p. 4666-75.

155. Pezzani, R., et al., *The antiproliferative effects of ouabain and everolimus on adrenocortical tumor cells.* Endocr J, 2014. **61**(1): p. 41-53.

156. Mariniello, B., et al., *Combination of sorafenib and everolimus impacts therapeutically on adrenocortical tumor models.* Endocr Relat Cancer, 2012. **19**(4): p. 527-39.

157. Doghman, M. and E. Lalli, *Efficacy of the novel dual PI3-kinase/mTOR inhibitor NVP-BEZ235 in a preclinical model of adrenocortical carcinoma.* Mol Cell Endocrinol, 2012. **364**(1-2): p. 101-4.

158. Williams, T.A., et al., *Teratocarcinoma-derived growth factor-1 is upregulated in aldosterone-producing adenomas and increases aldosterone secretion and inhibits apoptosis in vitro.* Hypertension, 2010. **55**(6): p. 1468-75.

159. Zheng, X. and W.B. Bollag, *AngII induces transient phospholipase D activity in the H295R glomerulosa cell model.* Mol Cell Endocrinol, 2003. **206**(1-2): p. 113-22.

160. De Martino, M.C., et al., *Role of the mTOR pathway in normal and tumoral adrenal cells.* Neuroendocrinology, 2010. **92 Suppl 1**: p. 28-34.

161. Kanehisa, M., et al., *KEGG for integration and interpretation of large-scale molecular data sets.* Nucleic Acids Res, 2012. **40**(Database issue): p. D109-14.

162. Guertin, D.A. and D.M. Sabatini, *Defining the role of mTOR in cancer.* Cancer Cell, 2007. **12**(1): p. 9-22.

163. Laplante, M. and D.M. Sabatini, *mTOR signaling in growth control and disease.* Cell, 2012. **149**(2): p. 274-93.

164. Liu, P., et al., *Targeting the phosphoinositide 3-kinase pathway in cancer.* Nat Rev Drug Discov, 2009. **8**(8): p. 627-44.

165. Wullschleger, S., R. Loewith, and M.N. Hall, *TOR signaling in growth and metabolism.* Cell, 2006. **124**(3): p. 471-84.

166. Fassnacht, M., et al., *AKT is highly phosphorylated in pheochromocytomas but not in benign adrenocortical tumors.* J Clin Endocrinol Metab, 2005. **90**(7): p. 4366-70.

167. Houghton, P.J., *Everolimus.* Clin Cancer Res, 2010. **16**(5): p. 1368-72.

168. Motzer, R.J., et al., *Efficacy of everolimus in advanced renal cell carcinoma: a double-blind, randomised, placebo-controlled phase III trial.* Lancet, 2008. **372**(9637): p. 449-56.

169. Maira, S.M., et al., *Identification and characterization of NVP-BEZ235, a new orally available dual phosphatidylinositol 3-kinase/mammalian target of rapamycin inhibitor with potent in vivo antitumor activity.* Mol Cancer Ther, 2008. **7**(7): p. 1851-63.

170. Semba, S., et al., *The in vitro and in vivo effects of 2-(4-morpholinyl)-8-phenyl-chromone (LY294002), a specific inhibitor of phosphatidylinositol 3'-kinase, in human colon cancer cells.* Clin Cancer Res, 2002. **8**(6): p. 1957-63.

171. Vlahos, C.J., et al., *A specific inhibitor of phosphatidylinositol 3-kinase, 2-(4-morpholinyl)-8-phenyl-4H-1-benzopyran-4-one (LY294002).* J Biol Chem, 1994. **269**(7): p. 5241-8.

172. van der Weyden, L. and D.J. Adams, *The Ras-association domain family (RASSF) members and their role in human tumourigenesis.* Biochimica et Biophysica Acta (BBA) - Reviews on Cancer, 2007. **1776**(1): p. 58-85.

173. Roskoski, R., Jr., *RAF protein-serine/threonine kinases: structure and regulation.* Biochem Biophys Res Commun, 2010. **399**(3): p. 313-7.

174. McCubrey, J.A., et al., *Roles of the Raf/MEK/ERK pathway in cell growth, malignant transformation and drug resistance.* Biochim Biophys Acta, 2007. **1773**(8): p. 1263-84.

175. Chambard, J.C., et al., *ERK implication in cell cycle regulation.* Biochim Biophys Acta, 2007. **1773**(8): p. 1299-310.

176. Shaul, Y.D. and R. Seger, *The MEK/ERK cascade: from signaling specificity to diverse functions.* Biochim Biophys Acta, 2007. **1773**(8): p. 1213-26.

177. Lin, S.R., et al., *Mutations of K-ras oncogene in human adrenal tumours in Taiwan.* Br J Cancer, 1998. **77**(7): p. 1060-5.

178. Kotoula, V., et al., *Mutational analysis of the BRAF, RAS and EGFR genes in human adrenocortical carcinomas.* Endocr Relat Cancer, 2009. **16**(2): p. 565-72.

179. Yashiro, T., et al., *Point mutations of ras genes in human adrenal cortical tumors: absence in adrenocortical hyperplasia.* World J Surg, 1994. **18**(4): p. 455-60; discussion 460-1.

180. Moul, J.W., et al., *Absent ras gene mutations in human adrenal cortical neoplasms and pheochromocytomas.* J Urol, 1993. **149**(6): p. 1389-94.

181. Ocker, M., et al., *PCR-SSCP analysis of human adrenocortical adenomas: absence of K-ras gene mutations.* Exp Clin Endocrinol Diabetes, 2000. **108**(8): p. 513-4.

182. Duncia, J.V., et al., *MEK inhibitors: the chemistry and biological activity of U0126, its analogs, and cyclization products.* Bioorg Med Chem Lett, 1998. **8**(20): p. 2839-44.

183. Favata, M.F., et al., *Identification of a novel inhibitor of mitogen-activated protein kinase kinase.* J Biol Chem, 1998. **273**(29): p. 18623-32.

184. Packer, L.M., et al., *Nilotinib and MEK inhibitors induce synthetic lethality through paradoxical activation of RAF in drug-resistant chronic myeloid leukemia.* Cancer Cell, 2011. **20**(6): p. 715-27.

185. Guenther, M.K., U. Graab, and S. Fulda, *Synthetic lethal interaction between PI3K/Akt/mTOR and Ras/MEK/ERK pathway inhibition in rhabdomyosarcoma.* Cancer Lett, 2013. **337**(2): p. 200-9.

186. Bozic, I., et al., *Evolutionary dynamics of cancer in response to targeted combination therapy.* Elife, 2013. **2**: p. e00747.

187. Suzuki, J., et al., *Novel action of activin and bone morphogenetic protein in regulating aldosterone production by human adrenocortical cells.* Endocrinology, 2004. **145**(2): p. 639-49.

188. Saha, S., et al., *Diabetic lipoproteins and adrenal aldosterone synthesis--a possible pathophysiological link?* Horm Metab Res, 2012. **44**(3): p. 239-44.

189. Saha, S., et al., *Very-low-density lipoprotein mediates transcriptional regulation of aldosterone synthase in human adrenocortical cells through multiple signaling pathways.* Cell Tissue Res, 2012. **348**(1): p. 71-80.

190. Inagaki, K., et al., *Involvement of bone morphogenetic protein-6 in differential regulation of aldosterone production by angiotensin II and potassium in human adrenocortical cells.* Endocrinology, 2006. **147**(6): p. 2681-9.

191. Gazdar, A.F., et al., *Establishment and characterization of a human adrenocortical carcinoma cell line that expresses multiple pathways of steroid biosynthesis.* Cancer Res, 1990. **50**(17): p. 5488-96.

192. Rainey, W.E., I.M. Bird, and J.I. Mason, *The NCI-H295 cell line: a pluripotent model for human adrenocortical studies.* Mol Cell Endocrinol, 1994. **100**(1-2): p. 45-50.

193. Barber, P.R., et al., *The Gray Institute open microscopes applied to radiobiology and protein interaction studies*, in *Three-dimensional and multidimensional microscopy*, T. Wilson and T. Wilson, Editors. 2014, S P I E - International Society for Optical Engineering: Bellingham, Washington.

194. Rampersad, S.N., *Multiple applications of Alamar Blue as an indicator of metabolic function and cellular health in cell viability bioassays.* Sensors (Basel), 2012. **12**(9): p. 12347-60.

195. Riss TL, M.R., Niles ALet al., *Cell Viability Assays*, in *Assay Guidance Manual [Internet]*, C.N. Sittampalam GS, Nelson H, et al., Editor. 2013 Eli Lilly & Company and the National Center for Advancing Translational Sciences: Bethesda (MD).

196. Weitsman, G.E., et al., *Vitamin D enhances caspase-dependent and -independent TNFalpha-induced breast cancer cell death: The role of reactive oxygen species and mitochondria.* Int J Cancer, 2003. **106**(2): p. 178-86.

197. Weitsman, G.E., et al., *Estrogen receptor-alpha phosphorylated at Ser118 is present at the promoters of estrogen-regulated genes and is not altered due to HER-2 overexpression.* Cancer Res, 2006. **66**(20): p. 10162-70.

198. Yao, R. and G.M. Cooper, *Requirement for phosphatidylinositol-3 kinase in the prevention of apoptosis by nerve growth factor.* Science, 1995. **267**(5206): p. 2003-6.

199. Franke, T.F., et al., *PI3K/Akt and apoptosis: size matters.* Oncogene, 2003. **22**(56): p. 8983-98.

200. Zimmermann, S. and K. Moelling, *Phosphorylation and regulation of Raf by Akt (protein kinase B).* Science, 1999. **286**(5445): p. 1741-4.